Université des Sciences et Technologies de Lille

Habilitation à Diriger des Recherches

en Sciences Mathématiques

Par

Abdelkader Hachemi

Institut für Allgemeine Mechanik, RWTH Aachen

Sur les méthodes directes et leurs applications

Date de soutenance : 13 *Décembre* 2005. *Jury composé de* :

Président	Pr. O. Mahrenholtz	Technische Universität Hamburg-Harburg
Rapporteurs	Pr. O. Débordes	Ecole Généraliste d'Ingénieurs de Marseille
	Pr. G. de Saxcé	Université des Sciences et Technologies de Lille
	Pr. A.R.S. Ponter	University of Leicester
Examinateurs	Pr. S. Degallaix	Ecole Centrale de Lille
	Pr. I. Shahrour	Ecole Polytechnique Universitaire de Lille
	Pr. D. Weichert	RWTH Aachen

À ma femme, Iman
et à tout membre de ma famille.

Sommaire

Organisation du document

1. Préambule

Ce document constitue une synthèse de mes travaux de recherche effectués depuis ma thèse de doctorat, obtenue en octobre 1994, jusqu'à ce jour. Ces travaux se sont effectués respectivement, au Département Informatique de l'Ecole des Mines de Douai, au Laboratoire de Mécanique de Lille (axe Fiabilité des Matériaux et des Structures) de l'Université des Sciences et Technologies de Lille et à l'Institut de Mécanique Générale (Institut für Allgemeine Mechanik) de l'Université Technologique d'Aix-la-Chapelle (RWTH Aachen) (cf. curriculum vitae en annexes). Ce rapport est rédigé comme un document de travail pour des recherches à venir. Il correspond à la volonté de présenter de manière synthétique la démarche, les outils, les résultats principaux obtenus, les travaux en cours et les perspectives proposées. Le détail des développements est renvoyé aux différentes publications, dont certaines copies sont données en annexes, et aux travaux co-encadrés.

2. Cadre général

Les structures mécaniques conçues, sont généralement destinées à remplir leur fonction sans dommage notable durant le temps d'exploitation escompté, en étant soumis à un ensemble de sollicitations défini préalablement. Lors de sa conception, une structure doit remplir certains critères sur sa résistance et sa fiabilité vis-à-vis des charges qu'elle aura à supporter. Prédire l'effondrement et avoir connaissance de la charge limite d'une structure a toujours été l'une des préoccupations principales des ingénieurs mécaniciens. La détermination de la charge limite est importante et cruciale en ce qui concerne la capacité de résistance et la sécurité de la structure. Selon les conditions spécifiques de service d'une structure ou d'un élément structural, l'effondrement peut être causé par différents effets physiques. On cite comme exemple, la déformation excessive, le flambage et la perte de résistance par endommagement ou fissuration. Du point de vue de la mécanique, ces effets ont été classifiés selon leur nature physique et des méthodes d'analyse spécifiques ont été développées, formant un ensemble d'outils pour la conception des structures.

Dans notre travail de recherche, nous nous sommes intéressés à l'extension et à l'application des "méthodes directes", selon la définition du groupe de travail de la communauté européenne "Codes and Standards" cité par Maier et al. [116]. Ces méthodes permettent d'étudier le comportement inélastique des structures sans connaître l'historique des charges avec exactitude. On s'est focalisé principalement sur le cas général de l'histoire du chargement variable, en opposition au chargement monotone ou proportionnel. Il est intéressant de noter qu'historiquement ces deux scénarios de chargement ont été traités séparément par les ingénieurs et les chercheurs, respectivement désignés sous le nom de "l'analyse d'adaptation ou shakedown" et de "l'analyse limite", bien qu'ils constituent un seul groupe. On convient maintenant que l'analyse limite peut être considérée comme un cas particulier de l'analyse d'adaptation ou que l'analyse d'adaptation est une généralisation de l'analyse limite, comme il a été montré par exemple par Kamenjarzh [86] et Kamenjarzh et al. [84, 85]. Le lecteur intéressé à ces méthodes est renvoyé aux ouvrages de König [95], Gokhfeld et Cherniavsky [54], Kamenjarzh [86], Save et al. [155] et Maier et al. [115, 117] ainsi qu'aux collections d'articles édités par Polizzotto et Sawczuk [135], Mróz et al. [126] et Weichert et Maier [185, 186].

Motivé par des problèmes d'ouvrages en génie civil, les premières ébauches de l'analyse limite ont été anticipées en mécanique au 18ème siècle (cf. [116]). Les fondements théoriques des méthodes directes ont commencé à connaître un véritable développement que vers la fin des années trente, quand la communauté scientifique a commencé à assimiler la première vague des développements de la théorie de plasticité. Si on veut marquer un point de départ, on peut prendre l'année 1938 où Gvozdev [63] a prouvé les théorèmes fondamentaux de l'analyse limite et, indépendamment, le théorème statique d'adaptation de Melan [122]. On devrait, cependant, mentionner que ce dernier avait été en partie anticipé par Grüning [61], Bleich [14] et Melan [121] lui-même vers la fin des années vingt et au début des années trente.

On doit se rappeler que les possibilités pour une analyse numérique étaient très limitées à cette période et il était difficile de construire une solution complète pour des systèmes mécaniques à géométrie quelconque, même en élasticité. Dans ces conditions, les méthodes directes ont été développées dans un esprit pratique en engineering afin d'obtenir rapidement et simplement des informations sur l'état ultime sans avoir recours à l'évolution des déformations et des propriétés mécaniques comme fonction de l'histoire du chargement. Seulement des solutions analytiques ont pu être obtenues pour des structures

spécifiques, telles que les poutres, portiques, plaques et coques sous des hypothèses restrictives sur la géométrie et les conditions d'équilibre pour la capacité du chargement. Il semble que jusqu'à la fin des années quarante, l'analyse d'adaptation était complètement ignorée et que l'analyse limite a trouvé peu d'intérêt. C'est seulement dans les années cinquante qu'on a observé un développement intense dans la formulation théorique et l'application des méthodes directes, suite entre autres aux travaux de Koiter [97], Symonds [166], Hodge [76], Prager [148] et Neal [128]. Le développement des moyens de calcul puissants, dans les années 60 et 70, a changé considérablement la situation. Les méthodes numériques en général et, en particulier les "méthodes incrémentales" ou "méthodes pas-à-pas", ont permis la discrétisation dans l'espace temps des conditions d'équilibre pour l'analyse des processus physiquement non-linéaires et irréversibles. Ceci a donné accès à la modélisation du processus total de déformations comprenant l'évolution des propriétés mécaniques. A la lumière de telles possibilités pour simuler le processus total de déformations d'une structure, l'intérêt pour les méthodes directes a diminué pendant cette période, bien qu'un certain nombre de travaux les plus remarquables aient été développés, donnant le fondement de la recherche actuelle.

Un intérêt croissant pour les méthodes directes a été observé depuis les deux ou trois dernières décennies. Il est devenu claire maintenant que les méthodes pas-à-pas montrent quelques insuffisances en comparaison aux méthodes directes et ne peuvent être considérées comme solution unique à n'importe quel problème :

(i) les méthodes pas-à-pas exigent comme donnée la connaissance exacte de l'histoire du chargement, ce qui est difficile à réaliser dans la réalité. Ceci conduit, dans la conception optimale des structures, à un nombre très coûteux de paramètres à étudier si l'information sur le chargement est exigée.

(ii) en opposition aux méthodes directes, les états ultimes et les charges critiques ne peuvent être obtenues d'une façon constructive ; ils sont définis par des instabilités numériques. Une telle insuffisance, cependant, peut avoir d'autres raisons que l'effondrement physique de la structure et ce genre d'analyse peut s'avérer dangereux. Par conséquent on convient aujourd'hui, que les méthodes directes et les méthodes pas-à-pas doivent être considérées plutôt comme complémentaires que concurrentes, non seulement du point de vue méthodologique, mais également par rapport aux réponses que peuvent être données par l'une ou l'autre méthode d'analyse.

3. Les faiblesses des méthodes directes classiques et leurs remèdes

Dans ce qui suit, on donne une revue historique des travaux de recherche développés dans le domaine des méthodes directes, en particulier les problèmes de la non-linéarité géométrique et les modèles de matériaux à comportement complexe. Un choix des travaux fut nécessaire dû à la littérature très riche dans ce domaine de recherche, on cite par exemple le livre de Życzkowski sur le chargement combiné dans la théorie de plasticité [190], dont une grande partie est consacrée aux méthodes directes, qui contient plus de trois mille références. Dans cette brève revue historique, les développements récents concernant les problèmes de dualité entre les approches statique et cinématique, le chargement dynamique et le fluage ne sont pas inclus. Pour une revue des travaux développés dans ce domaine, on renvoie le lecteur aux articles cités par Maier et al. [115, 117] et aux ouvrages cités plus-haut.

Les énoncés des théorèmes classiques de méthodes directes sont loin d'être atteints. En particulier pour le théorème statique, qui va être le centre de notre intérêt (le cas de l'analyse limite est considéré, tel qu'il a été spécifié précédemment, comme un cas particulier de l'analyse d'adaptation). Ainsi le théorème statique de l'adaptation [121], stipule que si certaines conditions sur l'état de contraintes sont satisfaites, alors pour n'importe quelle combinaison possible de charges à l'intérieur des limites prescrites, la structure peut être considérée comme fiable à chaque instant. L'énoncé du théorème complémentaire, le théorème cinématique [98], stipule par contre que l'effondrement aura lieu s'il existe un champ de déformations plastiques et une histoire du chargement pour lesquels le travail des contraintes élastiques soit strictement supérieur au travail dissipé plastiquement par la structure au cours de ce chargement. Ces théorèmes fondamentaux d'adaptation utilisent la propriété de convexité du domaine élastique et introduisent la fonction d'énergie totale résiduelle de déformations élastiques qui joue le rôle de norme énergétique. Ils sont basés sur les hypothèses suivantes :

- transformations infiniment petites, isothermes,
- évolution quasi-statique,
- comportement élastoplastique parfait, ou à écrouissage cinématique linéaire illimité,
- loi d'écoulement associée,
- milieu continu isotrope.

Il est bien connu maintenant que ces hypothèses restrictives réduisent considérablement les possibilités d'application de ces théorèmes aux problèmes technologique modernes. En effet, une structure peut s'effondrer à long-terme, même si les conditions (de sécurité) du théorème fondamental statique d'adaptation sont satisfaites. Il est donc important de comprendre la signification de ces hypothèses restrictives, pas seulement du point de vue théorique mais aussi de leur implication pratique et technique dans l'interprétation physique des résultats de l'analyse d'adaptation et de l'analyse limite.

3.1. Le problème géométrique

Les théorèmes fondamentaux de l'adaptation et de l'analyse limite ont été développés sous l'hypothèse de la linéarité géométrique dans le cadre de la mécanique des milieux continus. Néanmoins, une structure peut avoir des changements considérables dans sa géométrie avec une influence sur l'état de contraintes et sur les conditions d'équilibre. Ces changements peuvent stabiliser ou accélérer le processus de déformations inélastiques et sont donc étroitement liés au problème de la stabilité inélastique. La formulation incomplète du problème de conditions aux limites et la construction des solutions dans l'espace des contraintes statiquement admissibles ou des déformations cinématiquement admissibles fausse considérablement la relation entre les champs de déplacements et de contraintes. Ce problème avait été traité pour la première fois par Maier [112]. Il présenta une approche, tenant compte des effets géométriques du second ordre, appliquée aux structures discrètes, en utilisant une formulation matricielle simplifiée. L'idée de cette approche est de linéariser les termes géométriques dans les équations d'équilibre qui décrivent le changement géométrique de la structure durant le processus de déformations. Couplée à la linéarisation du critère d'écoulement, cette approche est simple à implémenter dans des codes de calcul et préserve les avantages de la théorie géométriquement linéaire classique. Cette idée a été développée avec succès par la suite [113] pour la détermination des bornes des déformations. Maier et Novati [114] et König et Maier [90] ont inclus les effets de la température. En appliquant les deux théorèmes, statique et cinématique, de l'adaptation, Weichert [178] introduit l'influence des non-linéarités géométriques en utilisant l'approche tensorielle dans le cadre de la mécanique des milieux continus sous l'hypothèse d'une décomposition additive des déformations totales en une partie élastique et une partie inélastique. Pour des raisons pratiques, il étudie les petites évolutions au voisinage d'une configuration déformée de référence, en mentionnant l'intérêt des

approximations cinématiques proposées par Casey [23]. L'approche proposée a été développée par la suite théoriquement et numériquement [57, 138, 149, 154, 163, 182] pour une analyse en élément finis de problèmes types de plaques et coques (cf. [56]). L'avantage de ces investigations est le couplage entre la méthode pas-à-pas et l'analyse d'adaptation [174]. Cette combinaison conduit à l'utilisation des problèmes géométriquement non-linéaires d'une manière simple et efficace. König [94], Siemaszko et König [159] et Siemaszko [160] ont présenté une méthode pratique pour l'étude de la stabilité des portiques on se basant sur le théorème cinématique.

Il est intéressant de noter que les effets géométriques en analyse limite avaient été étudiés dans les années 60 et 70 par Duszek et Sawczuk [156], Duszek et al. [43, 44] et récemment, dans un cadre mathématique, par Gao [50, 51]. Bien que loin d'être complète, cette synthèse des contributions au problème de la non-linéarité géométrique, dans le contexte des méthodes directes, permet les conclusions suivantes : le découplage des équations cinématique et statique ne tient pas compte du calcul exact des configurations déformées et des conséquences sur les états de contraintes et de déformations. Néanmoins, on peut observer un progrès considérable dans la prise en compte des effets géométriques durant le processus de déformations.

3.2. Les lois constitutives

En dehors de l'hypothèse de la linéarité géométrique, les méthodes directes classiques ne prennent pas en compte, ou seulement de façon très simplifiée, l'évolution du matériau durant le processus de déformations inélastiques. Un comportement rigide-parfaitement plastique est supposé dans l'analyse limite classique et linéaire parfaitement plastique ou à écrouissage cinématique illimité dans le théorème fondamental d'adaptation avec l'hypothèse de la loi d'écoulement associée. Ces hypothèses sont la base des démonstrations des théorèmes fondamentaux. Cependant, le scénario de rupture est plus compliqué et diffère d'un matériau à l'autre, même si on se limite aux matériaux métalliques utilisés dans des applications techniques. Ces matériaux ont un comportement à écrouissage cinématique, en général non-linéaire et limité, et peuvent avoir des défauts sous forme de microvides et de microfissures qui évoluent pendant le processus du chargement et finalement les macro-fissures apparaissent conduisant à la rupture totale de la structure ou d'un élément structural. Dépendant des conditions de service, l'effondrement peut se produire même avant l'étape finale de ce scénario. A ces

événements purement mécaniques s'ajoutent les effets thermiques supplémentaires tels que les changements des propriétés élastiques, de la limite d'écoulement et des paramètres décrivant l'écrouissage. De plus, aux températures élevées, les propriétés visqueuses d'un métal jouent un rôle très important dans le processus réel, aussi bien que les transformations de phases et les réactions chimiques. Pour les sols, les roches, le béton et les matériaux utilisés dans les chaussés, d'autres effets physiques sont importants comme les règles d'écoulement non-associées, la fraction volumique de porosité avec le mélange solide-fluide et la perte de résistance à la traction. Comme pour les effets géométriques, les lois constitutives très primitives adoptées dans les théorèmes fondamentaux sont insuffisantes pour étudier le comportement réel à long-terme. Par conséquent, l'extension de la gamme de validité des théorèmes de méthodes directes est depuis plusieurs années un thème central de recherche.

3.2.1. Effets thermiques

En dehors des charges mécaniques, les sollicitations thermiques contribuent considérablement à l'effondrement des systèmes mécaniques. Si l'interaction entre la température et les propriétés mécaniques du matériau est faible, des changements de température peuvent générer des extra-déformations ou extra-contraintes, s'ajoutant à celles résultants du chargement mécanique. En outre, la réduction de la limite d'élasticité par l'effet de la température, est indépendante de l'évolution des déformations inélastiques et des paramètres internes durant le processus du chargement [92, 93, 148]. Les modules d'élasticité dépendants de la température ont une influence directe sur la solution élastique de référence dans l'analyse d'adaptation et diffèrent des effets thermiques mentionnés ci-dessus. Des contributions intéressantes sur l'effet de la température dans le cadre des méthodes directes peuvent être trouvées par exemple dans König [89], Kleiber et König [87], Ponter et Karadeniz [145], Cazzani et al. [24] et Giambanco et Palizzolo [52].

Le phénomène du comportement inélastique dépendant du temps explicite, désigné sous le nom de la viscoplasticité et du fluage, est la plupart du temps associé aux problèmes à hautes températures en mécanique, tels que les réacteurs nucléaires et thermiques. Déjà, au début des années 70, une contribution très importante a été proposée dans ce cadre par Leckie et Martin [100], Leckie [101], Ponter et al. [141, 143-144], Ainsworth [1, 2], et par la suite par Polizzotto [134, 136], Cocks et Leckie [28], Dorosz [39] et Hjiaj et al. [75].

La demande urgente pour une grande sécurité thermique de combustions, actuellement liée aux questions de l'environnement et de l'utilisation économique des ressources énergétiques, a réanimé la discussion sur cette question qui est considérée comme un sujet de recherche de grande importance.

3.2.2. Ecrouissage cinématique

Pour l'application des méthodes directes, le postulat de stabilité de Drucker est un critère majeur pour la classification des lois de comportement [116]. Si les matériaux sont stables au sens de Drucker, en se limitant à la plasticité classique, au critère d'écoulement convexe et à la règle d'écoulement associée, alors le potentiel plastique, définissant la direction de l'écoulement plastique, est identique à la surface de charge. N'importe quel changement des propriétés du matériau durcit alors la réaction de la structure en ce qui concerne les contraintes locales, appelé "écrouissage". Le comportement parfaitement plastique est inclus comme un cas spécial dégénéré. Ce type de comportement du matériau a fait l'objet depuis longtemps de recherche intense. L'effet de l'écrouissage a été étudié en premier par Melan [122], dans un article original par l'introduction de l'écrouissage cinématique linéaire. Neal [128] utilise le critère d'écoulement linéaire pour des considérations numériques ; Maier [112] présenta un modèle généralisé pour les structures discrètes, tenant compte des effets géométriques du second ordre ; Mandel et al. [119] mirent en évidence une condition nécessaire de l'adaptation pour des structures élastoplastiques à écrouissage isotrope et cinématique combinés. König et Siemaszko [96] développèrent une méthode d'analyse de stabilité du processus d'adaptation ; Mandel [118] étendit le théorème au comportement du matériau écroui, en utilisant le "Modèle du Matériau Standard Généralisé" développé par Halphen et Quoc Son [72]. Tous ces auteurs ont traité le cas de l'écrouissage cinématique linéaire illimité.

Ponter [142], Zarka et Casier [189] et König [95] constatèrent que l'hypothèse de l'écrouissage illimité conduit à l'impossibilité de prédire l'inadaptation par déformations plastiques progressives, et que seul l'effondrement de la structure par plasticité alternée peut être modélisé. Utilisant le Modèle du Matériau Standard Généralisé, Weichert et Gross-Weege [179] proposèrent une limite d'évolution du paramètre d'écrouissage cinématique linéaire, au moyen d'une condition simplifiée de deux surfaces d'écoulement, où la surface de charge peut se déplacer à l'intérieur d'une surface limite fixe, définie par les paramètres d'écrouissage limité (cf. [137]). Stein et al. [161, 162] proposèrent un

modèle micro-mécanique ”Overlay model” avec écrouissage cinématique non-linéaire limité, similaire au modèle micro-mécanique proposé par Neal [128] pour les états de contraintes unidimensionnelles. Bodovillé et de Saxcé [15] ont proposé une analyse d'adaptation par l'approche du bi-potentiel en considérant l'écrouissage cinématique non-linéaire.

La littérature très riche sur le comportement stable du matériau avec écrouissage, en particulier dans le contexte de l'adaptation, prouve que les phénomènes physiques observés du durcissement peuvent être modélisés par l'agrandissement de l'espace des variables sans changer la structure mathématique des théorèmes fondamentaux. Cette catégorie de problèmes semble être plutôt bien assimilée à l'heure actuelle pour être prise en considération dans le contexte des méthodes directes.

3.2.3. Règle d'écoulement non-associée

L'étude des matériaux instables dans le sens de Drucker [40] a attiré l'attention de plusieurs chercheurs en relation avec les méthodes directes. Il est connu que pour les matériaux à friction interne, tels que les sols, les règles d'écoulement associées ne décrivent pas fidèlement l'évolution des déformations plastiques. Une possibilité pour résoudre ce problème, est de faire la distinction entre la surface d'écoulement et le potentiel plastique, défini implicitement par la règle de normalité. En se basant sur ce concept, Radenkovic [152] et Palmer [131] ont obtenu les théorèmes correspondants pour l'analyse limite. C'est Maier [111], en 1969, qui a montré que ce concept peut être introduit dans l'analyse d'adaptation en employant le potentiel plastique au lieu du critère d'écoulement. Pour des lois spéciales des géomatériaux, Boulbibane et Weichert [17] sont arrivés à la même conclusion, évitant une linéarisation du potentiel plastique et du critère d'écoulement. Corigliano et al. [30, 31] ont traité, dans la même ligne de conduite, le problème d'adaptation en dynamique. Une grande classe de règles d'écoulement non-associées a été considérée par Pycko et Maier [150], de Saxcé et Bousshine [36] et Bousshine et al. [18]. Nayroles et Weichert [127] ont montré que l'existence d'un domaine sûr ”sanctuaire d'élasticité” dans l'espace des contraintes, satisfaisant le principe généralisé du travail maximal de Hill, est suffisant pour la validité du théorème généralisé d'adaptation. Les approches proposées semblent être prometteuses pour l'étude des matériaux instables.

3.2.4. Matériaux endommagés

Une des raisons de perte de stabilité des matériaux est l'endommagement. Par ce terme, il faut entendre la détérioration progressive de la cohésion de la matière sous l'action de sollicitations monotones ou répétées, conduisant à la formation et à la croissance de microfissures et microvides, pouvant aller jusqu'à la rupture de l'élément de volume. Ce phénomène peut être traduit par une variable interne cachée au sens de la thermodynamique des processus irréversibles, qui fournit les équations d'évolution correspondantes, couplées aux lois de comportement. Ce formalisme est appliqué à la modélisation des endommagements de plasticité, de fluage et de fatigue qui constituent les trois mécanismes de naissance des macrofissures dans les structures métalliques [105]. Une tentative d'introduire l'endommagement des matériaux dans le cadre des méthodes directes a été faite pour la première fois par Hachemi et Weichert [64]. Ils ont montré, par analogie avec l'utilisation d'un espace agrandi des contraintes généralisées dans le cas de l'écrouissage, comment le raisonnement classique de Melan peut être étendu aux matériaux endommagés, si des différences cruciales sont respectées :

(i) par définition et en opposition aux déformations plastiques en plasticité classique, la variable d'endommagement est limitée par une valeur critique, inférieure à un dans le cas d'un paramètre d'endommagement isotrope. Par conséquent, la valeur de la variable d'endommagement doit être contrôlée localement pendant le processus du chargement,

(ii) en opposition à l'écrouissage, l'endommagement du matériau joue un rôle déstabilisant. Ceci est reflété dans la formulation du problème par l'utilisation du concept des contraintes effectives où la variable d'endommagement est introduite. Ces effets d'instabilité, dus à la perte de rigidité apparente et de la limite d'élasticité, doivent être considérés dans la modélisation, comme il a été montré par les mêmes auteurs [66, 67].

D'autres contributions à ce sujet, en suivant le même raisonnement, ont été élaborées par Feng et Yu [46, 47], Polizzotto et al. [139, 140] et Druyanov et Romain [41, 42]. Siemaszko [160] présenta une méthode pas-à-pas d'analyse de l'inadaptation pour des structures discrètes élastoplastiques. Cette méthode tient compte de l'effet géométrique non-linéaire, de l'endommagement progressif et de l'écrouissage non-linéaire.

L'endommagement est pris en compte par un paramètre de porosité qui est interprété comme une fraction de volume des vides. L'évolution de ce paramètre décrit le changement des imperfections internes, utilisant la fonction d'adoucissement du matériau développé par Perzyna [132], combiné avec l'écrouissage isotrope. Le domaine d'application de ces développements est limité du point de vue numérique et expérimentale.

3.2.5. Propagation des fissures

La détérioration finale des structures est le plus souvent précédée par l'apparition et la propagation de fissures. Ce phénomène a été en général, exclu de l'analyse d'adaptation. Ce manque d'investigations s'explique par le fait que, suivant les théorèmes fondamentaux d'adaptation, la charge limite que peut supporter une structure fissurée devra être nulle. Ceci est dû à la singularité du champ de contraintes élastiques à la pointe de la fissure. D'un autre coté, l'expérience montre qu'il existe une certaine valeur limite de l'intensité de la charge, qui si le chargement appliqué n'excède pas cette valeur, la structure fissurée sera dans un état de sécurité et une propagation de fissure ne se produit pas. La première tentative de combiner la théorie d'adaptation et la propagation stable de la fissure est due à Weichert [181]. Par la suite, Huang et Stein [79] ont utilisé une méthode analytique d'adaptation de ces même auteurs [78], pour tirer un facteur d'intensité de contraintes à l'adaptation pour une plaque sollicitée en tension. La fissure est assimilée à une entaille aiguë suivant le concept du bloc de matériau de Neuber [129]. Belouchrani et al. [11, 12] proposèrent une extension du théorème statique d'adaptation aux structures fissurées, en utilisant une analyse de la rupture développée par Quoc Son [151] dans le cadre général des matériaux standards généralisés et la théorie de croissance des fissures donnée par Griffith [60]. Ces travaux ont été utilisés par la suite par Feng et Gross [48].

3.3. Matériaux hétérogènes

Récemment, deux thèmes additionnels de recherche ont émergé concernant l'application des méthodes directes aux classes de matériaux non-classiques. Le premier thème est la poroplasticité, appliquée plus particulièrement à la géotechnique, en considérant les géomatériaux comme étant des solides plastiques poreux remplis par un liquide visqueux.

L'extension de la théorie d'adaptation à ce type de matériaux a été développée par Cochetti et Maier [26, 27]. Cette extension a été appliquée avec succès à l'étude des barrages [116] et est un sujet de recherche continue.

Le deuxième thème est le problème de fatigue des matériaux composites, où au moins une composante présente des propriétés ductiles. Une classe particulièrement intéressante de ces matériaux est celle des composites à matrice métallique. En considérant le composite comme une structure mécanique, les méthodes directes ont été appliquées sur une cellule de base représentative (VER) à l'échelle microscopique (plus grande que l'échelle atomique et plus petite que l'échelle macroscopique de la structure considérée) avec des hypothèses appropriées sur les conditions de bords et de périodicité. Avec l'aide de la technique d'homogénéisation [164], il est possible d'avoir des informations sur "le domaine de contraintes macroscopique admissible" pour le composite considéré. Les premières applications de l'analyse d'adaptation aux matériaux composites sont dues aux Tarn et al. [168] et Dvorak et al. [45], pour la détermination de domaines de résistance des composites unidirectionnels sollicités par des chargements axisymétriques. Récemment, la stratégie, citée plus-haut, qui consiste à combiner la théorie d'adaptation et la technique d'homogénéisation a été appliquée avec succès par Carvelli et al. [21], Ponter et Leckie [146, 147], Tirosh [171], Weichert et al. [183, 184, 187], Hachemi et al. [68, 70, 71] et Magoariec et al. [108, 110], basée sur les premiers concepts utilisant l'analyse limite [20, 22, 165, 167, 170]. Les progrès dans les techniques de fabrication des matériaux composites et leur utilisation dans des applications relevant des technologies de pointe, provoquent un intérêt croissant dans les techniques de simulation afin de prédire le comportement réel de ces matériaux. L'application des méthodes directes semble être une perspective très prometteuse définissant un champ intéressant pour la recherche actuelle et future.

4. Synthèse des travaux

La synthèse de mes travaux de recherche a été subdivisée en quatre chapitres. L'ordre des chapitres ne correspond pas forcément à la chronologie des travaux mais ils sont présentés de façon qu'ils soient exploitables séparément. Le détail des travaux est renvoyé aux différentes publications citées dans le curriculum vitae en annexes.

Chaque chapitre est structuré comme suit :

- la description du thème scientifique traité et les objectifs visés sous forme d'introduction,
- les développements scientifiques proposés, à partir d'une étude bibliographique sur les modèles et les théories utilisées,
- une synthèse des propositions avec un accent particulier sur les perspectives de recherche.

En début de chaque chapitre figure les noms des personnes ayant contribuées aux travaux présentés. Il s'agit de doctorants et ingénieurs que j'ai pu co-encadrer et des personnalités avec lesquelles des collaborations ont été mis en place.

5. Description des chapitres

Le **premier chapitre** de ce rapport est consacré à la formulation non-classique des théorèmes statique et cinématique d'adaptation dans le domaine de petites transformations. Plus précisément, les thèmes suivants ont été abordés : l'application du concept du matériau standard généralisé (M.M.S.G.), l'introduction de l'endommagement ductile et du facteur d'intensité de contraintes et la notion du sanctuaire d'élasticité. L'approche adoptée est celle de la thermodynamique des phénomènes irréversibles, qui constitue l'un des fondements indispensables de la théorie de plasticité. Nous commençons par définir la variable d'endommagement introduite par Kachanov [83] ainsi que la contrainte effective en utilisant le concept d'équivalence en déformation [104]. Pour tenir compte de l'écrouissage cinématique linéaire, nous utilisons le concept du matériau standard généralisé [72]. Par la définition du potentiel thermodynamique, et à partir du principe de la thermodynamique, nous déduisons les inégalités dissipatives. Deux modèles tridimensionnels d'endommagement plastique ductile établis par Lemaitre [103] et Shichun et Hua [158] ont été utilisés. Ces modèles sont fondés sur la notion de variable continue d'endommagement et sur le concept de contraintes effectives. Ils expriment la vitesse d'endommagement en fonction de sa variable associée et de la vitesse de déformation plastique cumulée. Ce sont ces deux modèles qui seront utilisés au chapitre 2

afin de cerner l'influence de chacun. Des facteurs d'intensité de contraintes correspondants à l'état d'adaptation de la structure fissurée, sollicitée en mode I, ont été calculés. La comparaison de ces facteurs aux seuils de fatigue de certains matériaux sera faite, et quelques propriétés de ces facteurs seront tirées.

Le **deuxième chapitre** présente une extension du théorème statique d'adaptation aux matériaux endommagés en tenant compte des effets géométriques non-linéaires. Cette extension est une combinaison des formulations proposées par Hachemi et Weichert [64] et Tritsch et Weichert [173]. Pour modéliser les effets géométriques dus aux déformations, la décomposition multiplicative du gradient total de déformation en une partie élastique et une partie plastique, telle qu'elle a été proposée par Lee [102], est utilisée dans le développement théorique. Pour cela, une configuration intermédiaire globale est introduite dans le processus de déformations correspondant à un état de déformation satisfaisant les conditions de compatibilité. Cette configuration contient les déformations résiduelles élastiques et plastiques. Pour des raisons pratiques, cette formulation a été restreinte à un cas de chargement simple [178], où la structure est soumise à des charges initiales, induisant des grands déplacements et un endommagement initial, telle qu'elle se trouve dans une configuration de référence en équilibre. Par la suite, la structure est soumise aux charges additionnelles variables ou cycliques, induisant des petits déplacements et un endommagement additionnel. Cette approche a été appliquée aux structures axisymétriques, où la théorie classique des coques de Donnell-Mushtari-Vlasov est utilisée. Les résultats numériques obtenus dans le cas de petites transformations ont été comparés à ceux existants dans la littérature en considérant l'effet de la température sur le seuil limite d'élasticité. L'influence de l'écrouissage cinématique linéaire, de l'endommagement ductile et de la géométrie non-linéaire sont considérés dans différents exemples numériques.

Dans le **troisième chapitre**, une méthode de prédiction de défaillance des matériaux composites périodiques est proposée. En utilisant la technique d'homogénéisation des milieux périodiques développée par Suquet [164], le domaine admissible de contraintes macroscopiques est déterminé par la résolution d'un problème de l'analyse d'adaptation à l'échelle microscopique sur une cellule de base représentative. On commence dans ce chapitre par définir le cadre théorique et les conditions générales à satisfaire afin de traiter

ce genre de problème, en mettant l'accent sur le modèle utilisé pour considérer l'effet de la décohésion qui peut se produire durant le chargement. Pour cela, le processus de décohésion est modélisé dans le cadre de la mécanique d'endommagement d'interface, où les déplacements relatifs créés par la décohésion progressive sont liés aux lois constitutives étendus par un modèle d'endommagement anisotrope [37]. La démonstration du théorème statique permet de déterminer une borne des déplacements relatifs résiduels afin de prédire l'effondrement dû à la décohésion. L'implémentation numérique est basée sur la méthode d'éléments finis et sur la méthode de programmation mathématique. Cette dernière consiste à déterminer le facteur de charge qui garantit l'adaptation et la sécurité vis-à-vis de l'effondrement par plasticité accumulée. Quelques simulations numériques permettant d'une part de valider les développements réalisés, grâce à des comparaisons avec d'autres résultats de la littérature, et d'autre part de mettre en lumière les possibilités de la méthode proposée.

Nous présentons, dans le **quatrième chapitre**, un nouvel algorithme pour résoudre des problèmes industriels à très grand nombre de variables d'optimisation [5, 69]. En effet, et comme il est montré dans les trois premiers chapitre, les méthodes directes conduisent à un problème d'optimisation non-linéaire. Les logiciels classiques semblent peiner à traiter en des temps raisonnables des problèmes non-linéaires à grandes dimensions. Puisqu'une grande partie des temps de calculs, dans les méthodes directes, est consommée par la partie optimisation. Cet algorithme est basé sur la méthode des points intérieurs combinée à la méthode de différence des fonctions convexes [133]. En utilisant le code Ansys, les résultats obtenus par cet algorithme ont été comparés à ceux obtenus par le logiciel Lancelot [29] en mettant en évidence les temps de calculs.

Chapitre 1

Formulation non-classique des méthodes directes

Non-classical formulation of Direct Methods

Collaborations liées à ce chapitre :

- Dr. M.A. Belouchrani, EMP-Alger
- Dr. M.A. Hamadouche, RWTH Aachen

Table of contents

1. Introduction

To guarantee the integrity of structures or structural elements as a necessary condition for safe functioning has always been one of the most important tasks for mechanical and civil engineers. Shakedown analysis is a powerful method to predict if, under variable loads in a structure, failure occurs or not. Its characteristic feature is that the information, if failure will occur or not, is obtained directly, without solving an evolutionary problem. The statements of the theorems underlying "Direct Methods", in contrast to "step-by-step methods", are very far reaching. This holds in particular for the theorems of shakedown which will be in the centre of the interest (limit analysis will be regarded as particular case). So the static shakedown theorem [121, 122], called also lower bound theorem, in its classical form says that if certain conditions on the state of stresses can be shown to be satisfied, then for any arbitrary loading history within given limits, the considered structure will not fail for any time. The complementary statement of the classical kinematic theorem, namely upper bound theorem [97, 98] says that failure will definitely occur if one can find only one specific inelastic strain cycle, satisfying certain conditions of compatibility. As it is well known, these strong statements are valid only under severe assumptions restricting considerably the applicability of the theory to modern technological problems. Clearly, a structure may suffer breakdown on long term even if the conditions of the classical static "safe" shakedown theorem are satisfied. It is therefore important to understand the meaning of the assumptions underlying the addressed theorems not only from theoretical point of view but also as to their practical and technical implications in order to interpret correctly the results of Direct Methods. In this chapter, some extensions of shakedown theory will be addressed to enlarge the class of material laws, in particular the issues of material hardening, material damage and crack propagation.

2. Assumption on the constitutive relations

We first concentrate on the material effects in the framework of the geometrically linear theory of continuum mechanics. For that, we consider the behaviour of an elastic-plastic body $\mathcal{B}$ of finite volume V with a sufficiently smooth surface ∂V consisting of the disjoint parts ∂V_p and ∂V_u, where statical and kinematical boundary conditions respectively are

prescribed ($\partial V = \partial V_p \cup \partial V_u$, $\partial V_p \cap \partial V_u = \varnothing$). The body $\mathscr{B}$ (Figure 1.1) is subjected to the quasi-statically varying external agencies $\mathbf{a}^*(\mathbf{x}, t) \in \mathcal{L}$ at time t consisting of body forces $\mathbf{f}^*$ in V, surface tractions $\mathbf{p}^*$ on ∂V_p, given displacements $\mathbf{u}^*$ on ∂V_u and prescribed temperature ϑ^* in V and on ∂V.

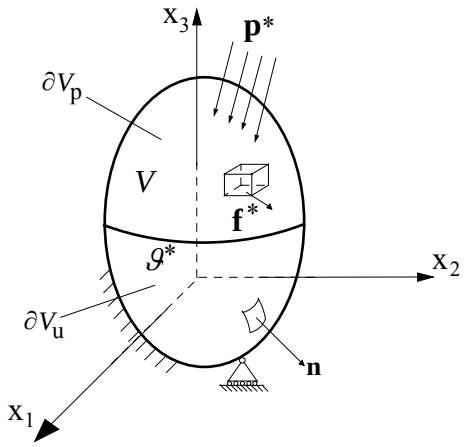

Figure 1.1. Structure or body $\mathscr{B}$.

The assumptions on the constitutive relations in classical shakedown theory are as follows:

1. The additive decomposition of total strains into elastic and an inelastic part is justified

$$\boldsymbol{\varepsilon} = \boldsymbol{\varepsilon}^e + \boldsymbol{\varepsilon}^p \tag{1.1}$$

2. The material is either linear elastic-perfectly plastic or linear elastic-unlimited linear kinematic hardening (Figure 1.2).

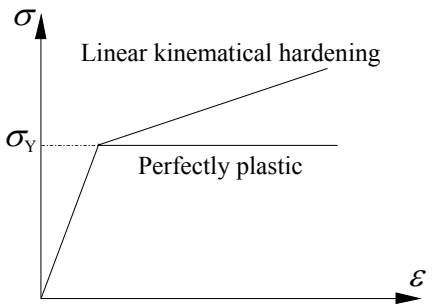

Figure 1.2. Uni-axial representation of linear elastic perfectly plastic respectively unlimited linear kinematical hardening behaviour.

3. For the plastic part it is assumed that there exists a convex yield surface and that the normality rule is valid (Figure 1.3). This can be represented by the maximum plastic work [73]

$$(\boldsymbol{\sigma} - \boldsymbol{\sigma}^{(s)}) : \dot{\boldsymbol{\varepsilon}}^{p} \geq 0 \tag{1.2}$$

where $\boldsymbol{\sigma}^{(s)}$ is a so-called "safe" state of stresses, i.e. from the strict interior of the elastic domain, bounded by the yield surface. The normality rule can be represented by

$$\dot{\boldsymbol{\varepsilon}}^{p} = \dot{\lambda} \frac{\partial \mathscr{F}}{\partial \boldsymbol{\sigma}} \tag{1.3}$$

with $\mathscr{F}(\boldsymbol{\sigma})$ as yield function and $\dot{\lambda}$ as plastic multiplier.

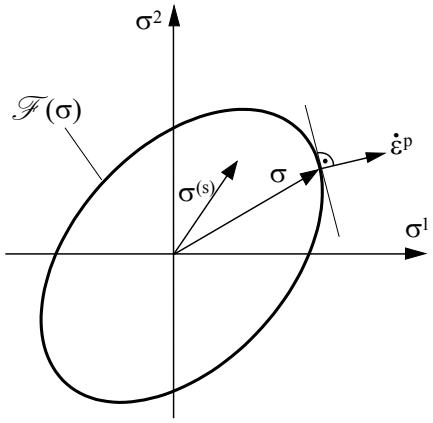

Figure 1.3. Convexity of the yield surface.

3. Structural behaviour

The behaviour of the structure or body $\mathcal{B}$ subjected to variable loads $\mathbf{a}^{*}(\mathbf{x}, t)$ (Figure 1.1), can be classified in the following ways (see Figure 1.4) [95]:

1. If the load intensities remain sufficiently low, the response of the body is "*purely elastic*" (with the exception of stress singularities).

2. If the load intensities become sufficiently high, the instantaneous load-carrying capacity of the body becomes exhausted and unconstrained plastic flow occurs. The body collapses in this case.
3. If the plastic strain increments in each load cycle are of the same sign then, after a sufficient number of cycles, the total strains (and therefore displacements) become so large that the body departs from its original form and becomes unserviceable. This phenomenon is called "*incremental collapse*" or "*ratchetting*".
4. If the strain increment change sign in every cycle, they tend to cancel each other and total deformation remains small leading to "*alternating plasticity*". In this case, however, the material at the most stressed points may fail due to "*low-cycle fatigue*".
5. If, after some time plastic flow cease to develop further and the accumulated dissipated energy in the whole body remains bounded such that the body responds purely elastically to the applied variable loads, one says that the body "*shakes down*".

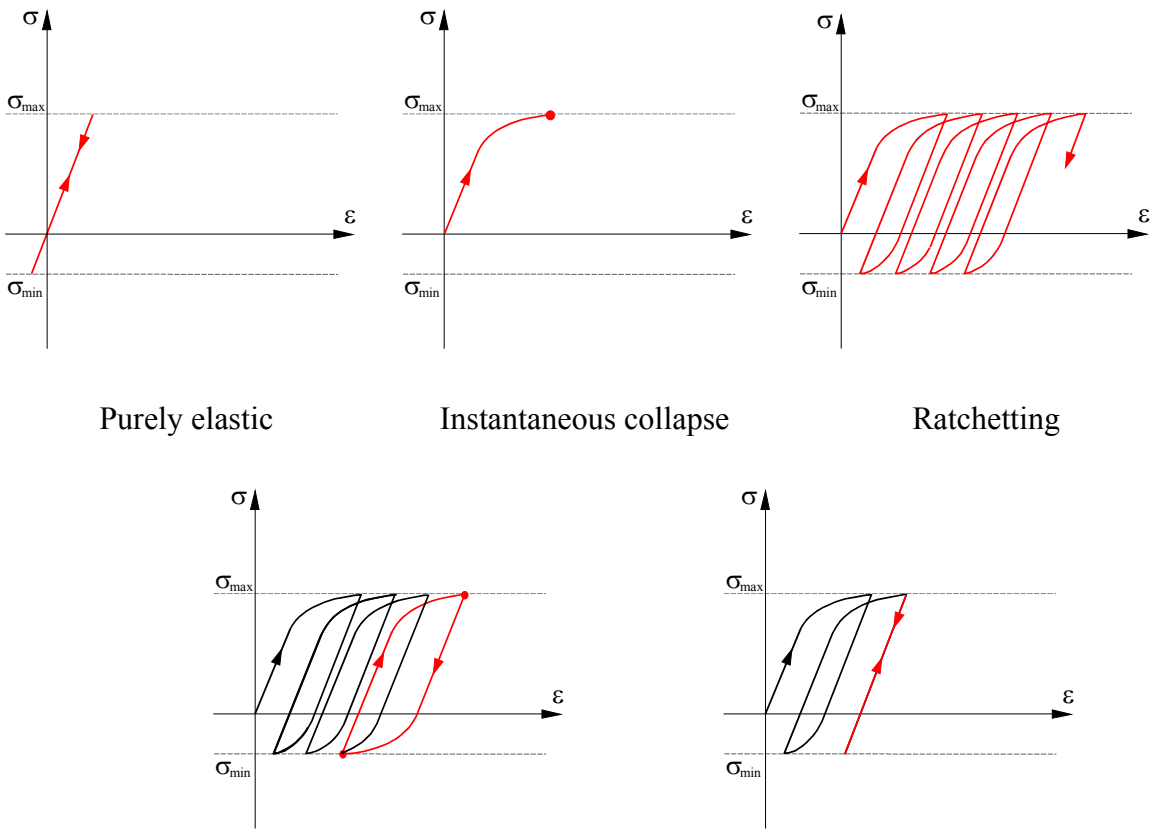

Figure 1.4. Possibilities of local response to cyclic loading.

The behaviour of the body according to the first point is not dangerous, since no plastic deformation occurs. However, the load carrying potential of the body is not fully exploited. The failure of types (2)-(4) are characterised by the fact, that plastic flow does not cease and that related quantities such as plastic flow does not become stationary. Thus, there exist points $\mathbf{x} \in V$ for which the following hold

$$\lim_{t \to \infty} \dot{\boldsymbol{\varepsilon}}^{\mathrm{p}} (\mathbf{x}, t) \neq 0 \tag{1.4}$$

If the case (5) occurs, the body shakes down for the given history of loading $\mathbf{a}^{*}(\mathbf{x}, t)$. It follows that

$$\lim_{t \to \infty} \dot{\boldsymbol{\varepsilon}}^{\mathrm{p}} (\mathbf{x}, t) = 0. \tag{1.5}$$

If one accounts for plastic deformation in the structural design, it seems natural to require that, for any possible loading history, the plastic deformation in the considered body will stabilise, i.e. the body will shakes down. It is worthwhile mentioning that the phenomena of incremental collapse "*ratchetting*" and alternating plasticity "*low-cycle fatigue*" may appear simultaneously.

The question of shakedown could be answered by examining the structural behaviour by means of step-by-step procedure. However, such a procedure is in general very cumbersome and, in many cases, inapplicable. Therefore, direct methods, namely the static method expressed in stress variables and kinematic method expressed in velocities variables, respectively have been developed allowing to find out whether a given body will shake down, without recurring on the evaluation of stresses and strains. Both methods can be related to a mixed formulation and lead to bounds of the shakedown or limit load: a lower bound by the static method and upper bound by the kinematic method.

4. The generalised standard material model

By the introduction of internal parameters representing the change of the materials properties without affecting the equations of equilibrium and compatibility, this concept can be easily extended to a larger class of materials. One particularly attractive way to do so is to use the General Standard Material Model (GSMM) [72]. By introducing additional

dimensions in the space of stresses and strains, limited kinematical hardening can be treated in the same manner as perfectly plastic material (Figures 1.5-6). The generalised stresses and strains are then defined by

$$\mathbf{e} = [\boldsymbol{\varepsilon}, \mathbf{0}]^T, \mathbf{e}^e = [\boldsymbol{\varepsilon}^e, \boldsymbol{\omega}]^T, \mathbf{e}^p = [\boldsymbol{\varepsilon}^p, \boldsymbol{\kappa}]^T, \mathbf{e}^\vartheta = [\boldsymbol{\varepsilon}^\vartheta, \mathbf{0}]^T, \mathbf{s} = [\boldsymbol{\sigma}, \boldsymbol{\pi}]^T \tag{1.6}$$

where $\boldsymbol{\omega}$, $\boldsymbol{\kappa}$ and $\boldsymbol{\pi}$ denote the vectors of internal parameters. Then, the elastic behaviour of the material is represented by

$$\mathbf{s} = \mathbf{M} : \mathbf{e}^e \tag{1.7}$$

where $\mathbf{M}$ is a constant positive definite supermatrix defined by

$$\mathbf{M} = \begin{pmatrix} \mathbf{L} & \mathbf{0} \\ \mathbf{0} & \mathbf{Z} \end{pmatrix}. \tag{1.8}$$

The usual tensor of elastic moduli is represented by $\mathbf{L}$, whereas the elastic relation between internal parameters of stresses and strains according to the illustration of the rheological model is represented by the tensor $\mathbf{Z}$.

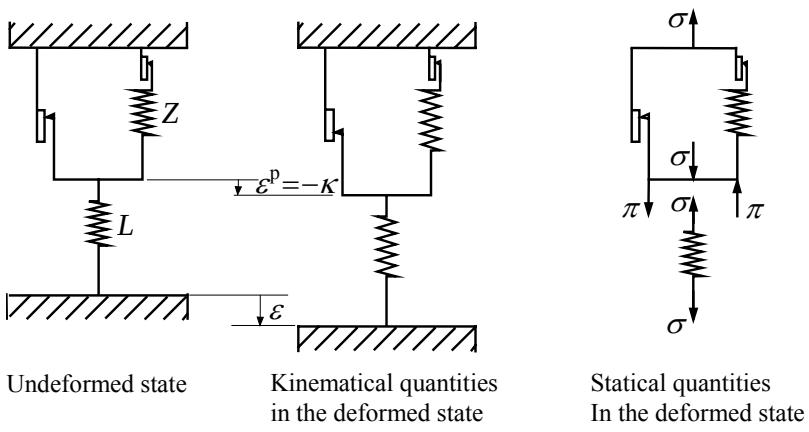

Figure 1.5. Rheological model of linear elastic-limited hardening plastic behaviour.

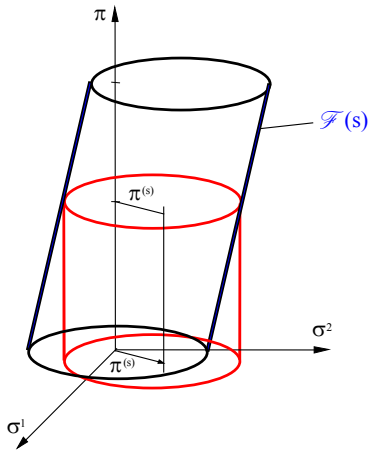

Figure 1.6. Representation of the yield surface in the space of generalised stresses.

5. Material damage

With progressing plastic deformations, ductile materials, in particular metals, exhibit defects on a scale much larger than the scale of dislocations, which are responsible for plastic deformations, and much smaller than the characteristic length of the considered body. These defects will be called “damage” and can be represented in the framework of continuum mechanics by the reduction of the apparent stiffness. In order to find a convenient form for application in shakedown theory, the concept of effective stress is adopted in what follows (Figure 1.7) [83].

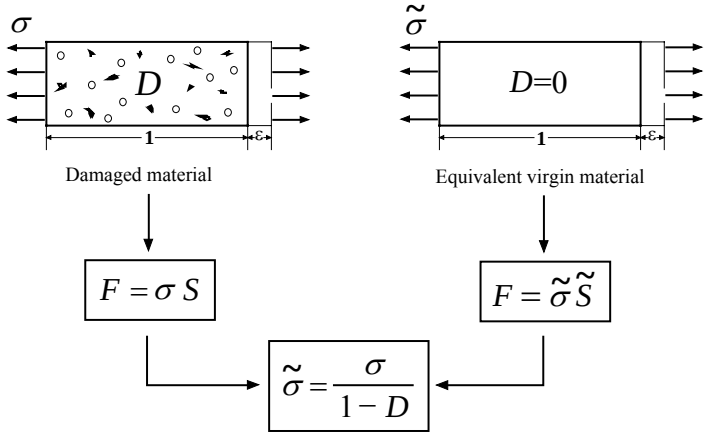

Figure 1.7. Illustration of the concept of effective stress.

Here, $D = 0$ corresponds to the undamaged state, for a damaged state the damage variable D takes a value $D \in (0, D_c)$, where D_c corresponds to a critical value. Local rupture of the material is supposed to occur for $D = D_c$ with $D_c \in [0, 1]$.

6. Thermodynamic framework

The second principle of thermodynamics applied to solid mechanics is used in the form of the dissipation inequality given by Clausius-Duhem

$$\boldsymbol{\sigma}:\dot{\boldsymbol{\varepsilon}} - \rho\,(\dot{\Psi} + s\dot{T}) + \mathbf{g}.\mathbf{q} \geq 0 \tag{1.9}$$

with the free energy Ψ composed of the parts Ψ_e and Ψ_p, related to the immediately recoverable and the stored elastic energy density, respectively and T denotes the absolute temperature

$$\Psi = \Psi_e(\boldsymbol{\varepsilon}^e, T, D) + \Psi_p(\boldsymbol{\kappa}, D) \tag{1.10}$$

where

$$\mathbf{g} = -\,\mathbf{grad}T/T. \tag{1.11}$$

Straightforward application to elastic-plastic hardening material with damage leads to [82, 104, 105]

$$\boldsymbol{\sigma}:\dot{\boldsymbol{\varepsilon}}^p + \boldsymbol{\pi}.\dot{\boldsymbol{\kappa}} + Y\dot{D} + \mathbf{g}.\mathbf{q} \geq 0 \tag{1.12}$$

with the definitions

$$\boldsymbol{\sigma} = \rho\frac{\partial \Psi}{\partial \boldsymbol{\varepsilon}^e} = (1 - D)\mathbf{L}:(\boldsymbol{\varepsilon}^e - \alpha_\vartheta\,\vartheta\mathbf{I}) \tag{1.13}$$

$$\boldsymbol{\pi} = -\,\rho\frac{\partial \Psi}{\partial \boldsymbol{\kappa}} = -\,(1 - D)\,\mathbf{Z}.\boldsymbol{\kappa} \tag{1.14}$$

$$Y = -\,\rho\frac{\partial \Psi}{\partial D} = \frac{1}{2}\mathbf{L}:(\boldsymbol{\varepsilon}^e - \alpha_\vartheta\,\vartheta\mathbf{I}):(\boldsymbol{\varepsilon}^e - \alpha_\vartheta\,\vartheta\mathbf{I}) + \frac{1}{2}\mathbf{Z}.\boldsymbol{\kappa}.\boldsymbol{\kappa}. \tag{1.15}$$

This way, Y can be identified as generalised force associated to the rate of damage $\dot{D}$. For the sequel, the following restrictive assumptions on the dissipation inequality are made:

- mechanical and thermal dissipation fulfill independently the dissipation inequality

$$\phi_1 = \boldsymbol{\sigma}:\dot{\boldsymbol{\varepsilon}}^p + \boldsymbol{\pi}.\dot{\boldsymbol{\kappa}} + Y\dot{D} \geq 0 \tag{1.16}$$

$$\phi_2 = \mathbf{g}.\mathbf{q} \geq 0 \tag{1.17}$$

- plastic and damage dissipation fulfill independently the dissipation inequality

$$\phi_p = \boldsymbol{\sigma}:\dot{\boldsymbol{\varepsilon}}^p + \boldsymbol{\pi}.\dot{\boldsymbol{\kappa}} \geq 0 \tag{1.18}$$

$$\phi_D = Y\dot{D} \geq 0 \tag{1.19}$$

To describe plasticity, the up mentioned GSMM is used. The generalised normality rule for plastic flow is assumed valid, such that

$$\dot{\mathbf{e}}^p \in \delta\varphi(\mathbf{s}) \tag{1.20}$$

where $\delta\varphi(\mathbf{s})$ denotes the sub-gradients of the plastic potential $\varphi(\mathbf{s})$ [72] which is the indicator function of a convex generalised elastic domain $\mathrm{P}(\mathbf{x})$ of all plastically admissible stress states

$$\mathbf{s}(\mathbf{x}) \in \mathrm{P}(\mathbf{x}), \quad \forall \mathbf{x} \in V. \tag{1.21}$$

$\mathrm{P}(\mathbf{x})$ is defined by means of a yield function $\mathscr{F}(\tilde{\mathbf{s}}, \mathbf{x})$

$$\mathrm{P}(\mathbf{x}) = \{\mathbf{s} \,/\, \mathscr{F}(\tilde{\mathbf{s}}, \mathbf{x}) \leq 0, \ \forall \mathbf{x} \in V\}. \tag{1.22}$$

Here, it is assumed that the yield function $\mathscr{F}(\tilde{\mathbf{s}}, \mathbf{x})$ is of von Mises type

$$\mathscr{F}(\tilde{\mathbf{s}}, \mathbf{x}) = \left\{\frac{3}{2}\left(\frac{\boldsymbol{\sigma}^D}{1-D} - \frac{\boldsymbol{\pi}}{1-D}\right):\left(\frac{\boldsymbol{\sigma}^D}{1-D} - \frac{\boldsymbol{\pi}}{1-D}\right)\right\}^{1/2} - \sigma_Y \leq 0 \tag{1.23}$$

where σ_Y denotes the yield stress and $\boldsymbol{\sigma}^D$ the deviatoric part of $\boldsymbol{\sigma}$. The convexity of $\mathscr{F}(\tilde{\mathbf{s}}, \mathbf{x})$ and the validity of the normality rule can be expressed by the generalised maximum plastic work inequality (Figure 1.8)

$$(\mathbf{s} - \mathbf{s}^{(s)}) : \dot{\mathbf{e}}^p > 0, \quad \forall \mathbf{s}^{(s)}(\mathbf{x}) \in \overline{P}(\mathbf{x}) \tag{1.24}$$

in detail

$$(\boldsymbol{\sigma} - \boldsymbol{\sigma}^{(s)}) : \dot{\boldsymbol{\varepsilon}}^p + (\boldsymbol{\pi} - \boldsymbol{\pi}^{(s)}) . \dot{\boldsymbol{\kappa}} > 0 \tag{1.25}$$

where $\mathbf{s}^{(s)} = [\boldsymbol{\sigma}^{(s)}, \boldsymbol{\pi}^{(s)}]^T$ is any safe state of generalised stresses defined by

$$\overline{P}(\mathbf{x}) = \{\mathbf{s}^{(s)} / \mathscr{F}(\tilde{\mathbf{s}}^{(s)}, \mathbf{x}) < 0, \ \forall \mathbf{x} \in V\}. \tag{1.26}$$

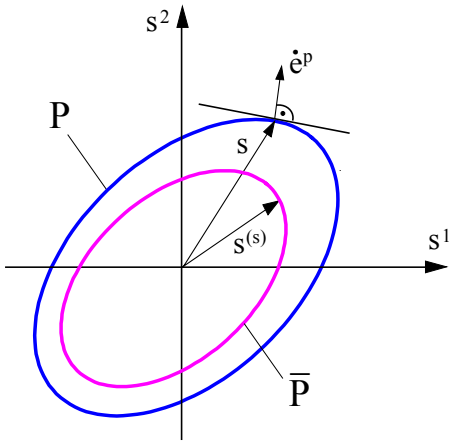

Figure 1.8. Illustration of the principle of maximum plastic work.

To complete this section, two simple models for the determination of the damage variable D are presented. These models are used to establish local bounds for D [65, 66].

(a) *Model of Lemaitre* [103]

$$D = \frac{D_c}{\varepsilon_R - \varepsilon_D} \left\langle \left\{ \frac{2}{3}(1+\nu) + 3(1-2\nu)\left(\frac{\sigma_H}{\sigma_{eq}}\right)^2 \right\} \varepsilon_{eq} - \varepsilon_D \right\rangle \tag{1.27}$$

(b) *Model of Shichun and Hua* [158]

$$D = \frac{D_c}{\varepsilon_R - \varepsilon_D} \left\langle \exp\left\{ \frac{3}{2} \left(\frac{\sigma_H}{\sigma_{eq}} - \frac{1}{3} \right) \right\} \varepsilon_{eq} - \varepsilon_D \right\rangle \tag{1.28}$$

with $\langle x \rangle = x$ if $x > 0$ and $\langle x \rangle = 0$ if $x \leq 0$. The scalars D_c, ε_R and ε_D are characteristic material coefficients and ε_{eq} is the equivalent plastic strain defined by $\varepsilon_{eq} = \int_0^t [2/3\ \dot{\boldsymbol{\varepsilon}}^p : \dot{\boldsymbol{\varepsilon}}^p]^{1/2}\, dt$ (see [103]).

7. Formulation of direct methods

7.1. Assumptions

In the following, we introduce the notion of a "***purely elastic reference body*** $\mathcal{B}^{(c)}$" (Figure 1.9), differing from the real body $\mathcal{B}$ only by the fact that its material reacts purely elastically with the same elastic moduli as for the elastic part of the material law in the real body. All quantities related to this reference representative volume element are indicated by superscript (^{c}). The internal parameters to describe the state of hardening and damage in the material vanish naturally for the reference body $\mathcal{B}^{(c)}$, so that the generalised strains and stresses are given by

$$\mathbf{e}^{(c)} = \mathbf{e}^{e(c)} = [\boldsymbol{\varepsilon}^{(c)}, \mathbf{0}]^T,\ \mathbf{e}^{p(c)} = [\mathbf{0}, \mathbf{0}]^T,\ \mathbf{e}^{\vartheta(c)} = [\boldsymbol{\varepsilon}^{\vartheta}, \mathbf{0}]^T,\ \mathbf{s}^{(c)} = [\boldsymbol{\sigma}^{(c)}, \mathbf{0}]^T. \tag{1.29}$$

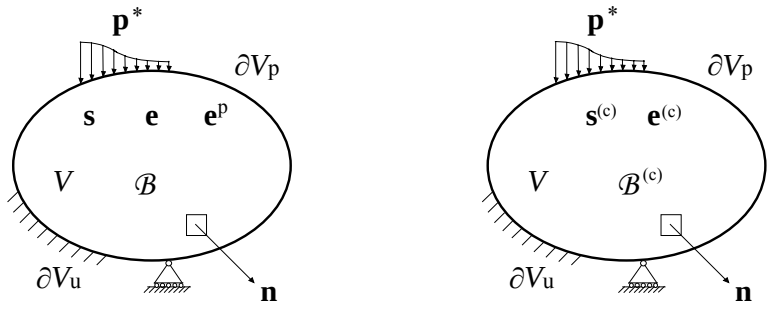

Elastic-plastic body Purely elastic body

Figure 1.9. Purely elastic and elastic-plastic body

7.2. Minimum requirements

Independent from any specific kind of material behaviour, the minimum requirements from mathematical point of view for the occurrence of shakedown can be defined. For this, the notion of the "*Sanctuary of Elasticity*" is introduced [127]:

(*a*). Be $\Gamma(\mathbf{x})$ an open domain in the space of stresses $\mathbf{\Sigma}$ such that if $\boldsymbol{\sigma}(\mathbf{x}) \in \mathbf{\Sigma}$, no additional inelastic deformation occurs.
(*b*). $\forall\ \boldsymbol{\sigma}^{(s)} \in \Gamma(\mathbf{x})$, holds $(\boldsymbol{\sigma} - \boldsymbol{\sigma}^{(s)}) : \dot{\boldsymbol{\varepsilon}}^{p} > 0$.
(*c*). The Sanctuary of Elasticity C is defined by $C = \{\boldsymbol{\sigma}(\mathbf{x}) \in \mathbf{\Sigma} \,/\, \forall \mathbf{x} \in V, \boldsymbol{\sigma} \in \Gamma(\mathbf{x})\}$

7.3. Lower bound direct method

The extended static (Melan's) theorem of shakedown can be expressed as follows:
If there exist a solution $\tilde{\mathbf{s}}^{(c)}(\mathbf{x}, t) = [\tilde{\boldsymbol{\sigma}}^{(c)}(\mathbf{x}, t), \mathbf{0}]^{T}$ of a purely elastic reference problem, a real number $\alpha > 1$ and a field of time-independent generalised stresses $\overset{\sim}{\circ}{\mathbf{s}}(\mathbf{x}) = [\overset{\sim}{\circ}{\boldsymbol{\sigma}}^{(r)}(\mathbf{x}), \overset{\sim}{\circ}{\boldsymbol{\pi}}(\mathbf{x})]^{T}$ such that $\alpha\,(\tilde{\mathbf{s}}^{(c)} + \overset{\sim}{\circ}{\mathbf{s}}) \subset C$, then the inelastic work W is bounded by

$$W \leq \frac{1}{2}\frac{\alpha}{\alpha - 1} \langle \mathbf{L}^{-1} : (\tilde{\mathbf{s}}(0) - \overset{\sim}{\circ}{\mathbf{s}}), (\tilde{\mathbf{s}}(0) - \overset{\sim}{\circ}{\mathbf{s}}) \rangle \tag{1.30}$$

with

$$\langle \mathbf{a}, \mathbf{b} \rangle = \int_{(V)} (\mathbf{a} : \mathbf{b})\, \mathrm{d}V. \tag{1.31}$$

One sees easily that for elastic-perfectly plastic material behaviour with an associated flow rule the "Sanctuary of Elasticity" (*SE*) corresponds to the usual elastic domain in the 6-dimensional space of stresses, bounded by the yield function (Figure 1.10). For the GSMM, the SE corresponds to the elastic domain in the space of generalised stresses of dimension 6+*r*, where *r* denotes the number of independent internal parameters describing the evolution of the internal structure of the material. However, due to the fact that the "*SE*" has not necessarily a specific physical meaning, other kinds of inelastic behaviour are covered by the theorem. The question arises, how such other laws can be put into practice.

Another methodology to prove the boundedness of dissipation due to inelastic effects for specific materials, including or not geometrical effects, is now presented. It follows the pattern of the proof of the theorem by Melan [121] by simply modifying the underlying quadratic form and the choice of generalised variables. The procedure consists of the following steps:

1. Choose an appropriate *positive and bounded* definite form $W = \langle \mathbf{M}^{-1}\mathbf{:v}, \mathbf{v}\rangle$, function of the problems generalised state variables and associated fictitious admissible fields, collected in the field $\mathbf{v}(\mathbf{x}, t)$.
2. Calculate the derivative of W with respect to time, $\dot{W} = \mathrm{d}W/\mathrm{d}t$, show that for *active failure mechanism* one part of $\dot{W}$, say $\dot{W}_{\mathrm{L}}$, is always *negative.*
3. Show that the time integral of the remaining part of $\dot{W}$, $\dot{W}_{\mathrm{NL}} = \dot{W} - \dot{W}_{\mathrm{L}}$ is bounded for the particular application.
4. Then the classical argument is that the considered failure mechanism must cease to be active beyond a certain instant, otherwise there is contradiction with the starting point.

The field of purely elastic stresses satisfies the following system of equations

$$\mathrm{Div}\,\boldsymbol{\sigma}^{(\mathrm{c})} = -\mathbf{f}^* \quad \text{in } V \tag{1.32}$$

$$\mathbf{n}\cdot\boldsymbol{\sigma}^{(\mathrm{c})} = \mathbf{p}^* \quad \text{on } \partial V_{\mathrm{p}} \tag{1.33}$$

$$\mathbf{u}^{(\mathrm{c})} = \mathbf{u}^* \quad \text{on } \partial V_{\mathrm{u}} \tag{1.34}$$

with

$$\boldsymbol{\varepsilon}^{(\mathrm{c})} = \frac{1}{2}\left(\nabla(\mathbf{u}^{(\mathrm{c})}) + \nabla(\mathbf{u}^{(\mathrm{c})})^{\mathrm{T}}\right) \tag{1.35}$$

$$\boldsymbol{\varepsilon}^{(\mathrm{c})} = \mathbf{L}^{-1}\mathbf{:}\boldsymbol{\sigma}^{(\mathrm{c})} + \alpha_\vartheta\,\vartheta\,\mathbf{I} \tag{1.36}$$

and the field of residual stresses satisfies

$$\mathrm{Div}\,\mathring{\boldsymbol{\sigma}}^{(\mathrm{r})} = 0 \quad \text{in } V \tag{1.37}$$

$$\mathbf{n}\cdot\mathring{\boldsymbol{\sigma}}^{(\mathrm{r})} = 0 \quad \text{on } \partial V_{\mathrm{p}} \tag{1.38}$$

where $\mathbf{n}$ is the outward normal vector to ∂V.

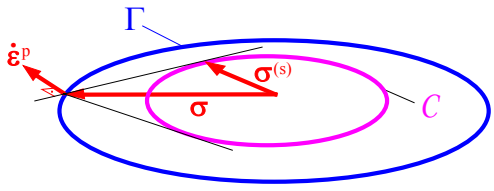

Figure 1.10. Illustration of the Sanctuary of Elasticity.

Then, the static shakedown theorem for the determination of the safety factor against failure due to inadmissible damage or unlimited accumulation of plastic deformations can then be expressed by the following optimisation problem [66]:

$$\alpha_{\mathrm{SD}}^{\mathrm{L}} = \max_{\overset{\circ}{\boldsymbol{\sigma}}^{(\mathrm{r})},\, \overset{\circ}{\boldsymbol{\pi}},\, D} \alpha \tag{1.39}$$

with the subsidiary conditions (1.37-38) and

$$D < D_{\mathrm{c}} \qquad \text{in } V \tag{1.40}$$

$$\mathscr{F}_{\mathrm{I}}\left(\alpha \frac{\boldsymbol{\sigma}^{(\mathrm{c})}}{1-D} + \frac{\overset{\circ}{\boldsymbol{\sigma}}^{(\mathrm{r})}}{1-D} - \frac{\overset{\circ}{\boldsymbol{\pi}}}{1-D},\, \sigma_{\mathrm{Y}}\right) \le 0 \qquad \text{in } V \tag{1.41}$$

$$\mathscr{F}_{\mathrm{L}}\left(\alpha \frac{\boldsymbol{\sigma}^{(\mathrm{c})}}{1-D} + \frac{\overset{\circ}{\boldsymbol{\sigma}}^{(\mathrm{r})}}{1-D},\, \sigma_{\mathrm{S}}\right) \le 0 \qquad \text{in } V \tag{1.42}$$

This is a problem of mathematical programming, with α as objective function to be optimised with respect to $\overset{\circ}{\boldsymbol{\sigma}}^{(\mathrm{r})}$, $\overset{\circ}{\boldsymbol{\pi}}$ and D and with inequalities (1.40-42) as non-linear constraints. Here, $\mathscr{F}_{\mathrm{I}}$ and $\mathscr{F}_{\mathrm{L}}$ denote the initial yield condition and the limit yield condition, respectively, with uniaxial yield stress σ_{Y} and uniaxial limit strength σ_{S}. The condition (1.40) assures structural safety against failure due to material damage and (1.41) assures that safe states of stresses $\boldsymbol{\sigma}^{(\mathrm{s})} = \alpha\, \boldsymbol{\sigma}^{(\mathrm{c})} + \overset{\circ}{\boldsymbol{\sigma}}$ are never outside the loading surface $\mathscr{F}_{\mathrm{L}}$ and so guarantees implicitly the boundedness of the back-stresses. Condition (1.42) controls the shakedown requirement of existence of a time-independent back-stress vector $\overset{\circ}{\boldsymbol{\pi}}$ describing a fixed translation of the yield surface $\mathscr{F}_{\mathrm{I}}$ inside the loading surface $\mathscr{F}_{\mathrm{L}}$ and so assures that safe states of observable stresses $\boldsymbol{\sigma}^{(\mathrm{s})}$ are related to a fixed time independent position of the yield surface $\mathscr{F}_{\mathrm{I}}$ inside the loading surface $\mathscr{F}_{\mathrm{L}}$ [179].

Material damage however by definition cannot grow indefinitely and is limited by local rupture. Therefore, it is necessary to control the degree of material damage by imposing locally bounds on the evolution of the damage parameter D. For the considered approach (eqn. (1.27-28)), damage is basically generated by plastic strains, bounds for damage can be given in this special case by bounding of the equivalent plastic strains (for detail we refer to [65, 66]):

$$\varepsilon_{\mathrm{eq}} = \frac{1}{V}\frac{1}{(1-D_{\mathrm{c}})\sigma_{\mathrm{Y}}}\frac{\alpha}{\alpha-1}\int_{(V)} \frac{1}{2}\, \overset{\circ}{\boldsymbol{\sigma}}^{(\mathrm{r})} : \mathbf{L}^{-1} : \overset{\circ}{\boldsymbol{\sigma}}^{(\mathrm{r})}\, \mathrm{d}V \tag{1.43}$$

where V is an arbitrary sub-domain of the total volume of $\mathscr{B}$.

7.4. Upper bound direct method

To formulate the upper bound theorem, we restrict ourselves to perfectly plastic material with the assumption of small geometrical transformations. Using the associated flow rule (eqn. (1.20)) and the von Mises yield criterion (eqn. (1.23)), the plastic dissipation can be expressed by

$$D^{\mathrm{p}}(\dot{\boldsymbol{\varepsilon}}^{\mathrm{p}}) = \boldsymbol{\sigma}:\dot{\boldsymbol{\varepsilon}}^{\mathrm{p}} = (1-D)\sigma_{\mathrm{Y}}\,(2/3\;\dot{\boldsymbol{\varepsilon}}^{\mathrm{p}}:\dot{\boldsymbol{\varepsilon}}^{\mathrm{p}})^{1/2} \tag{1.44}$$

which is a non-negative scalar convex function. The admissible set of stresses in the static formulation is unbounded: the addition of a scalar function in the diagonal of $\boldsymbol{\sigma}$, corresponding to adding hydrostatic pressure, does not affect the yield condition. This is why one needs in this case so called “incompressible finite elements” to perform the calculation of shakedown loading factor. Then, the shakedown loading factor α_{SD} is the minimum of the following optimisation problem:

$$\alpha_{\mathrm{SD}}^{\mathrm{U}} = \min_{\dot{\boldsymbol{\varepsilon}}^{\mathrm{p}},\,\Delta\mathbf{u}} \sqrt{2/3}\;\sigma_{\mathrm{Y}}\,(1-D)\int_0^T\!\!\int_{(V)} (\dot{\boldsymbol{\varepsilon}}^{\mathrm{p}}:\dot{\boldsymbol{\varepsilon}}^{\mathrm{p}})^{1/2}\,\mathrm{d}V\mathrm{d}t \tag{1.45}$$

with the subsidiary conditions

$$D < D_{\mathrm{c}} \qquad \text{in } V \tag{1.46}$$

$$\int_0^T\!\!\int_{(V)} \boldsymbol{\sigma}^{(\mathrm{c})}:\dot{\boldsymbol{\varepsilon}}^{\mathrm{p}}\,\mathrm{d}V\mathrm{d}t = 1 \qquad \text{in } V \tag{1.47}$$

$$\mathbf{tr}\,\dot{\boldsymbol{\varepsilon}}^{\mathrm{p}} = 0 \qquad \text{in } V \tag{1.48}$$

$$\Delta\boldsymbol{\varepsilon}^{\mathrm{p}} = \int_0^T \dot{\boldsymbol{\varepsilon}}^{\mathrm{p}}\,\mathrm{d}t = \frac{1}{2}\left(\nabla(\Delta\mathbf{u}) + \nabla(\Delta\mathbf{u})^{\mathrm{T}}\right) \qquad \text{in } V \tag{1.49}$$

$$\Delta\mathbf{u} = 0 \qquad \text{on } \partial V_{\mathrm{u}} \tag{1.50}$$

where $\dot{\boldsymbol{\varepsilon}}^{\mathrm{p}}$ and $\Delta\boldsymbol{\varepsilon}^{\mathrm{p}}$ denote plastic strain rate and plastic strain increment, respectively, $\Delta\mathbf{u}$ is the increment of residual displacement and $\boldsymbol{\sigma}^{(\mathrm{c})}$ is the fictitious elastic stresses caused by external loads. The period of cyclic loading programs is denoted by T.

Regularisation by the Norton-Hoff-Friaâ method

The objective function (eqn. (1.45)) is not differentiable at 0. To overcome this difficulty Friaâ proposed a regularised method [49, 62] which consists to replace the plastic

dissipation $D^{\mathrm{p}}(\dot{\boldsymbol{\varepsilon}}^{\mathrm{p}})$ of perfectly plastic material by the regularised and differentiable support function $[D^{\mathrm{p}}(\dot{\boldsymbol{\varepsilon}}^{\mathrm{p}})]^{\mathrm{NH}}$ of Norton-Hoff viscoplastic material:

$$[D^{\mathrm{p}}(\dot{\boldsymbol{\varepsilon}}^{\mathrm{p}})]^{\mathrm{NH}} = \frac{k^{1-m}}{m}[D^{\mathrm{p}}(\dot{\boldsymbol{\varepsilon}}^{\mathrm{p}})]^{m} = \frac{\sigma_{\mathrm{Y}}^{2-m}}{m}[3\,\mu]^{m-1}(1-D)^{m}(2/3\,\dot{\boldsymbol{\varepsilon}}^{\mathrm{p}}\!:\dot{\boldsymbol{\varepsilon}}^{\mathrm{p}})^{m/2} \qquad (1.51)$$

where μ is Lamé's coefficient and m is the viscosity parameter ($1 \le m \le 2$). The viscoplastic dissipation tends to the plastic dissipation when the viscosity parameter tends to one (see, e.g. [176]).

It may be proven that the duality theory of mathematical programming provides a meaningful link between the lower and the upper bound of limit and shakedown loads (see e.g. [33, 85]). The unique exact shakedown load factor occurs when the lower and upper bounds coincide so that $\alpha_{\mathrm{SD}}^{\mathrm{L}} = \alpha_{\mathrm{SD}}^{\mathrm{U}} = \alpha_{\mathrm{SD}}$. For load factors greater than α_{SD}, two types of collapse can occur:

– incremental collapse, corresponding to an unlimited growth of plastic strains,
– low-cycle fatigue, corresponding to alternating plastic strains.

8. Fatigue threshold and influence of the microstructure

It what follows, the propagation of micro-cracks on the level of grains in polycrystalline ductile materials is investigated, leading to what is commonly named "failure by fatigue". Starting point is the assumption of the existence of such micro-cracks in the material. It is then supposed that it undergoes cyclic loading.

The classical concept of existence of a threshold K_{S} for the stress intensity factor K_{I} in opening mode I

$$K_{\mathrm{I}} = \sigma\sqrt{\pi a} \qquad (1.52)$$

is used. Therefore, it is assumed that micro-crack propagation does not occur if

$$K_{\mathrm{I}} < K_{\mathrm{S}} \qquad (1.53)$$

and the material state is safe against failure by fatigue. Among other parameters, the fatigue threshold is influenced by the microstructure of the material. Generally, it is admitted that K_S increases with the size of the grain as has been observed on ferritic steels by Radhakrishna [153] and Wasen et al. [177]. It has been suggested that the dependence between K_S and $\xi^{1/2}$ (ξ is the diameter of the grain) are related by a linear function [153, 169, 177]

$$K_S = a_1 + b_1\ \xi^{1/2} \tag{1.54}$$

where the dimensions of K_S and ξ are, respectively, [MPa·m$^{1/2}$] and [m]. Here, a_1 and b_1 are material constants.

8.1. Formulation of the lower bound for a cracked body

It has been suggested by Belouchrani et al. [10, 11], a cracked body shakes down with respect to a given loading history, if a time-independent state of residual stress $\overset{\circ}{\boldsymbol{\sigma}}^{(r)}$ exists, such that for all times $t > 0$

$$\text{Div}\ \overset{\circ}{\boldsymbol{\sigma}}^{(r)} = 0 \qquad \text{in } V \tag{1.55}$$

$$\mathbf{n}\cdot\ \overset{\circ}{\boldsymbol{\sigma}}^{(r)} = 0 \qquad \text{on } \partial V_p \tag{1.56}$$

$$\mathscr{F}(\alpha\,\boldsymbol{\sigma}^{(c)}(\mathbf{x}, t) + \overset{\circ}{\boldsymbol{\sigma}}^{(r)}(\mathbf{x}),\ \sigma_Y) < 0 \qquad \text{in } V \tag{1.57}$$

with a supplementary condition imposed on the admissible length of a typical micro-crack in the material

$$a_{Lim} < a_c. \tag{1.58}$$

For the Lemaitre-Chaboche model [104] adopted for ductile fracture, a_{Lim} is given by [11]

$$a_{Lim} = a_0 + \left[\frac{m+1}{m}\frac{1}{K}\ \frac{\alpha}{\alpha-1}\int_{(V)}\frac{1}{2}\,\overset{\circ}{\boldsymbol{\sigma}}^{(r)}\!:\mathbf{L}^{-1}\!:\overset{\circ}{\boldsymbol{\sigma}}^{(r)}\,dV\right]^{m/(m+1)} \tag{1.59}$$

Here, a_0 is the initial crack length, m and K are material constants characterizing the R-curve parameters.

As mentioned before, the problem of stress singularity of the elastic stress field deserves special attention for the application of the shakedown theorem to cracked structures. In this case, no time-independent field of residual stresses $\overset{\circ}{\boldsymbol{\sigma}}^{(r)}(\mathbf{x})$ satisfying inequality (1.57) can be found and classical shakedown theory does not deliver comprehensive results, even for loads for which limit states physically exist. We bypass this problem by assimilating the crack tip to a notch, following the concept of material block introduced by Neuber [129] and used in the same spirit as in the present work by Huang and Stein [79].
So, following Creager [32], the stress distribution in the neighborhood of the root of the notch is given by

$$r_f = r + n\ \varepsilon \tag{1.60}$$

with, according to Figure 1.11, r_f as effective notch root radius, ε as length of the Neuber material block (assumed to be a material constant), and n as factor depending of the loading type. The factor n is equal to 2 in mode I. Following this concept, the effective notch radius is equal to the original notch radius augmented of n time the dimension of the Neuber material block.

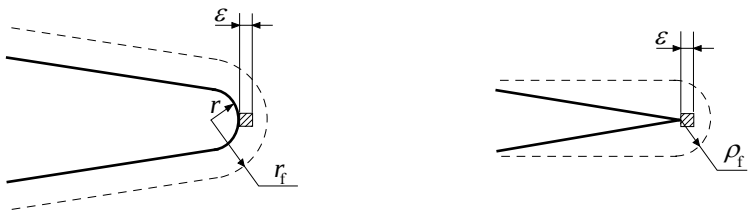

Figure 1.11. Modified notch and crack.

In the case of a sharp crack, the effective crack tip radius, denoted ρ_f, can be obtained just by putting $r = 0$ in eqn. (1.60)

$$\rho_f = n\ \varepsilon. \tag{1.61}$$

Eqn. (1.61) indicates implicitly that the crack can be treated as a notch with tip radius ρ_f. Physically, Neubers material block may be interpreted as being the sum of the minimum number of individual microscopic material particles (such as grains in polycrystalline

metals). The properties of which may differ from each other, but in average they should have the property of the macroscopic material. In [79], ρ_f is put to be about ten time the size of a grain, for mode I loading. Following this suggestion we write

$$\varepsilon \approx 5\ \xi. \tag{1.62}$$

8.2. Shakedown stress intensity factor

We consider an elastic-plastic plate, subjected to uniaxial loads $P(t)$. The values of $P(t)$ vary arbitrarily with time t, but remain between prescribed loads $P_{\min}$ and $P_{\max}$. One then looks for the maximum value of the load factor α, such that the plate will shake down under the loads $\alpha P(t)$. This load factor can be determined as solution of the following optimisation problem

$$\alpha_{SD} = \max_{\mathring{\boldsymbol{\sigma}}^{(r)},\, a_{Lim}} \alpha \tag{1.63}$$

with the subsidiary conditions

$$a_{Lim}(\alpha, \mathring{\boldsymbol{\sigma}}^{(r)}) - a_c < 0 \qquad \text{in } V \tag{1.64}$$

$$\text{Div}\, \mathring{\boldsymbol{\sigma}}^{(r)} = 0 \qquad \text{in } V \tag{1.65}$$

$$\mathbf{n} \cdot \mathring{\boldsymbol{\sigma}}^{(r)} = 0 \qquad \text{on } \partial V_p \tag{1.66}$$

$$\mathscr{F}(\alpha\, \boldsymbol{\sigma}^{(c)}(P) + \mathring{\boldsymbol{\sigma}}^{(r)}(\mathbf{x}),\, \sigma_Y) \le 0 \qquad \text{in } V \tag{1.67}$$

With the shakedown load factor α_{SD} computed for a cracked plate loaded in mode I, we will compute the stress intensity factor (eqn. (1.52)) corresponding to the shakedown state by

$$K_{SD} = \alpha_{SD}\, P \sqrt{\pi\, a_{Lim}}. \tag{1.68}$$

8.2.1. Comparison of the values of K_{SD} to the fatigue threshold

To validate the proposed approach, a comparison is made between the values of K_{SD} computed in the case of a rectangular plate solicited in mode I, the fatigue threshold K_S given by Wasen et al. [177] and the shakedown stress intensity factor K_{sh} given by Huang and Stein [79] for some materials. The characteristics of these materials are given in the Table 1:

Material	*Designation*	ξ (μm)	σ_Y (MPa)
Docol 350	A	8	260
SS 141147	B	15	185
HP steel	C	29	210
HP steel	D	45	160
HP steel	E	82	120

Table 1.1. Diameter of the grain and mechanical material data.

According to the results given in the Table 2, we remark that the values of K_{SD} agree with the values of K_{sh} given by Huang and Stein [79]. On the other hand, we notice a disparity with the fatigue threshold K_S given by Wasen et al. [177] for materials A and E. However, the results indicate that indeed K_{SD} can be considered as fatigue threshold.

Material	K_S	K_{sh}	K_{SD}
A	5.4	8.9	8.43
B	6.0	7.6	6.49
C	6.2	9.5	8.22
D	6.7	8.1	6.8
E	8.2	7.8	5.73

Table 1.2. Fatigue threshold and shakedown stress intensity factor.

8.2.2. Influence of the microstructure on the values of K_{SD}

For the materials given in Table 1.1, we show in Figure 1.12 the influence of the grain size on the obtained shakedown stress intensity factor K_{SD} (Table 2) normalized by the corresponding yield stress σ_Y. As expected, the results show that the ratio K_{SD}/σ_Y is an almost linear function of $\xi^{1/2}$ as it has been expressed in eqn. (1.54) by [153, 169, 177]

$$\frac{K_{SD}}{\sigma_Y} = a_2 + b_2\, \xi^{1/2} \tag{1.69}$$

By comparing the equation (1.68) to (1.69) relative to the fatigue threshold, one notes that the yield stress σ_Y influences the shakedown stress intensity factor K_{SD}. This can be explained by the fact that the shakedown stress intensity factor is computed in supporter counts the yield stress and the largest admissible crack length.

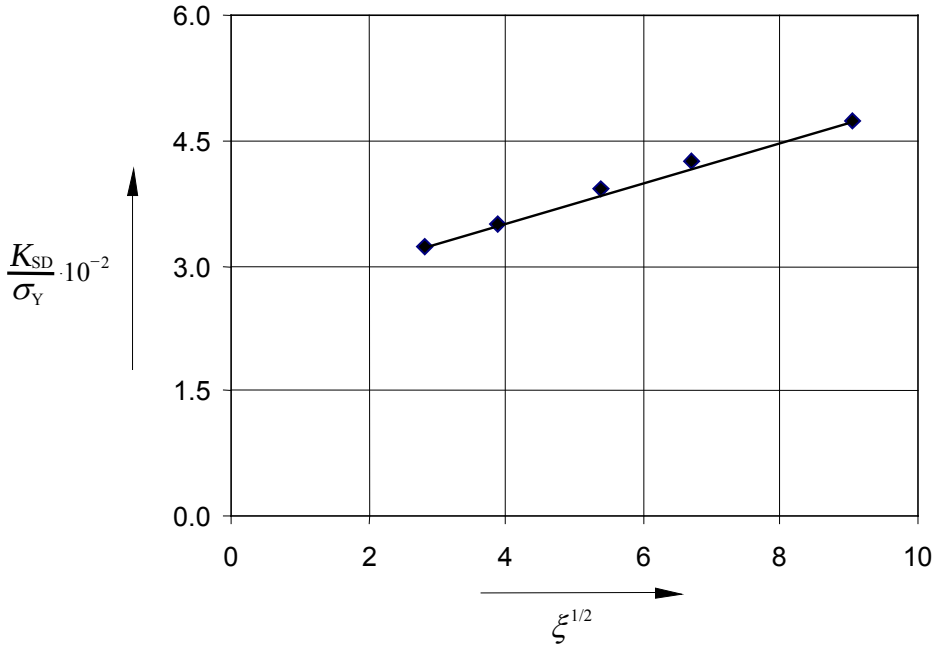

Figure 1.12. Variation of K_{SD}/σ_Y with $\xi^{1/2}$.

9. Conclusions

In this chapter, possibilities how to extend the validity of Direct Methods to other than linear elastic-ideal plastic or linear elastic- unlimited linear hardening material behaviour have been presented. More precisely, the following items have been discussed: application of the General Standard Material Model, introduction of material damage and stress intensity factor and the notion of the Sanctuary of Elasticity.

The phenomenon of damage is taken into account by an internal scalar variable in the senses of thermodynamics of irreversible processes, which give corresponding constitutive laws coupled with kinetical equations. Ductile plastic damage is taken into account by using the models of Lemaitre and Shichun-Hua, these are a function of the effective stress and the accumulated plastic strains. It should be mentioned, that the consideration of a scalar-valued damage variable is in practice rather restrictive. However, the presented approach could be extended to the case of more sophisticated models of damage.

The stress intensity factors have been computed for some chosen materials. Comparison with results from literature showed rather good, respectively fair agreement with the values obtained by using the developed lower-bound direct method. A linear functional relationship was observed between the shakedown stress intensity factor and the diameter of the grain of the material for the examples treated herein as it has been suggested in Taylor [169], Radhakrishna [153] and Wasen et al. [177]. We conclude that at least in the investigated cases, the computed shakedown stress intensity factors can be considered as fatigue threshold.

Chapitre 2

Adaptation des structures minces avec effets géométriques

Shakedown of thin-walled structures with geometrical effects

Collaborations liées à ce chapitre :

- Dr. J. Gross-Weege, I.F.M., Duisburg-Huckingen
- Dr. I. Kreja, Université Technologique de Gdansk
- Dr. J.B. Tritsch, USTL

Table of contents

1. Introduction

The primary purpose of this chapter is to extend the lower bound direct method to damaged structures accounting for geometrical effects. This extension is a combination of the formulations proposed by Hachemi and Weichert [64] and Tritsch and Weichert [173].
To model effects of geometrical changes due to deformation, the multiplicative decomposition of the total deformation gradient into an elastic and plastic parts as proposed by Lee [102] is used for the development of the theoretical framework. For that, a global intermediate configuration is introduced in the deformation process corresponding to a state of deformation satisfying the compatibility conditions. This configuration contains elastic and plastic residual deformations. This general formulation however, delivers constructive methods for shakedown analysis, if additional assumptions on the deformation pattern are introduced [178]. Here, the most simple case is studied, where the considered body or structure is subjected to initial loads, inducing large displacements and initial damage such that it is in the reference configuration in equilibrium. The body is then subjected to additional variable in time or cyclic loading, causing small additional displacement, in comparison with the previous ones, and additional damage. In this case, the response of the reference configuration is calculated incrementally. The lower bound of the load factor against failure due to non-shakedown or inadmissible damage is calculated by optimisation program.
For the numerical applications, we concentrate on thin-walled shells and plates under mechanical and thermal variable loads, taking certain geometrical effects into account that may occur during the loading history.

2. Formulation of the problem

We consider the behaviour of a three-dimensional elastic-perfectly plastic body $\mathcal{B}$ under the action of quasistatically varying external agencies $\mathbf{a}^*$. In the initial configuration C_i at the time $t = 0$, $\mathcal{B}$ occupies the volume V_0. The motion of $\mathcal{B}$ is described by the use of Cartesian coordinates, where the positions of the particles of $\mathcal{B}$ in the undeformed and deformed state are given by the coordinates $\mathbf{X} = [X_1, X_2, X_3]$ and $\mathbf{x} = [x_1, x_2, x_3]$, respectively. The actual configuration C_t of $\mathcal{B}$ is then defined by the displacement function $\mathbf{u}$:

$$\mathbf{u}(\mathbf{X}, t) = \mathbf{x}(\mathbf{X}, t) - \mathbf{X} \tag{2.1}$$

Under this assumptions the boundary value problem referred to the initial undeformed configuration is defined by:

(i) *Statical equations*

$$\text{Div}\,(\mathbf{T}) = -\,\mathbf{f}^{*} \qquad \text{in } V_0 \tag{2.2}$$

$$\mathbf{n}.\mathbf{T} = \mathbf{p}^{*} \qquad \text{on } \partial V_{0p} \tag{2.3}$$

with

$$\mathbf{T} = \mathbf{F}\,\mathbf{S} \tag{2.4}$$

(ii) *Kinematical equations*

$$\mathbf{u} = \mathbf{u}^{*} \qquad \text{on } \partial V_{0u} \tag{2.5}$$

$$\mathbf{F} = \mathbf{I} + \text{grad}(\mathbf{u}) \qquad \text{in } V_0 \tag{2.6}$$

$$\mathbf{E} = \frac{1}{2}(\mathbf{C} - \mathbf{I}) \qquad \text{in } V_0 \tag{2.7}$$

with

$$\mathbf{C} = \mathbf{F}^{T}\mathbf{F} \tag{2.8}$$

Here, **T** and **S** are the unsymmetric first Piola-Kirchhoff stress tensor and the symmetric second Piola-Kirchhoff stress tensor whereas **F** and **E** are the deformation gradient and the Green-Lagrange strain tensor, respectively. **I** denotes the metric tensor of second rank and **n** is the outer normal vector to ∂V_0 in C_i.

Elastic-plastic deformations are usually described by means of a fictitious intermediate configuration C_κ, derived from the multiplicative decomposition of the deformation gradient **F** into an elastic part $\mathbf{F}^{e}$ and a plastic part $\mathbf{F}^{p}$ [102]:

$$\mathbf{F} = \mathbf{F}^{e}\,\mathbf{F}^{p} \tag{2.9}$$

where $\mathbf{F}^{e}$ is obtained by unloading all infinitesimal neighbourhoods of the body $\mathcal{B}$. This decomposition provides the relation between elastic, plastic and total deformation valid for finites strains and leads to an additive decomposition of the Green-Lagrange strain tensor **E** into a purely plastic part $\mathbf{E}^{p}$ and an elastic part $\mathbf{E}^{e}$ depending on the plastic deformation [55]:

$$\mathbf{E} = \mathbf{E}^{e} + \mathbf{E}^{p} \tag{2.10}$$

with

$$\mathbf{E}^{e} = \frac{1}{2}(\mathbf{F}^{p})^{T}\left[(\mathbf{F}^{e})^{T}(\mathbf{F}^{e}) - \mathbf{I}\right](\mathbf{F}^{p}) \quad \text{and} \quad \mathbf{E}^{p} = \frac{1}{2}\left[(\mathbf{F}^{p})^{T}(\mathbf{F}^{p}) - \mathbf{I}\right] \tag{2.11}$$

3. Lower bound theorem

3.1. General assumptions

Here the combination of extensions of Melan's shakedown theorem as to be found in Hachemi and Weichert [64] and Tritsch and Weichert [173] is given. For that, an intermediate configuration C_x is introduced in the deformation process corresponding to a state of deformation satisfying the compatibility conditions. This in general time-dependent and unknown configuration is obtained by removing external loads from the considered body and we get a multiplicative decomposition of the deformation gradient tensor (Figure 2.1)

$$\begin{aligned} \mathbf{F} &= \mathbf{F}^{(e)}\,\mathbf{F}^{(x)} \\ &= (\mathbf{F}^{(e)}\,\mathbf{F}^{(re)})\,\mathbf{F}^{p} \end{aligned} \tag{2.12}$$

where $\mathbf{F}^{(e)}$ denotes the free elastic deformation gradient, $\mathbf{F}^{(x)}$ the deformation gradient in the intermediate configuration C_x containing plastic and elastic residual deformations and $\mathbf{F}^{(re)}$ the elastic residual deformation gradient (see [172, 173]). In this case, the Green-Lagrange strain tensor $\mathbf{E}$ is expressed by

$$\begin{aligned} \mathbf{E} &= \mathbf{E}^{(e)} + \mathbf{E}^{(x)} \\ &= \mathbf{E}^{(e)} + \mathbf{E}^{(re)} + \mathbf{E}^{p} \end{aligned} \tag{2.13}$$

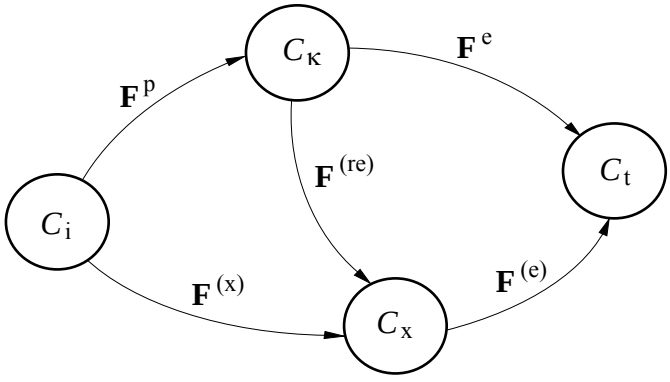

Figure 2.1. Kinematics of elastic-plastic deformation.

3.2. Statement of the theorem

If there exists a safety factor $\alpha > 1$ and a time-independent state of effective residual stresses $\overset{\circ}{\widetilde{\mathbf{S}}}^{(r)}$, satisfying the following relations:

$$\text{Div}\,(\mathbf{F}^{(x)}\,\overset{\circ}{\mathbf{S}}^{(r)}) = 0 \qquad \text{in } V_0 \tag{2.14}$$

$$\mathbf{n}.(\mathbf{F}^{(x)}\,\overset{\circ}{\mathbf{S}}^{(r)}) = 0 \qquad \text{on } \partial V_{0p} \tag{2.15}$$

$$\mathscr{F}\,(\alpha\,\widetilde{\mathbf{S}}^{(e)} + \overset{\circ}{\widetilde{\mathbf{S}}}^{(r)},\, \sigma_Y) \le 0 \qquad \text{in } V_0 \tag{2.16}$$

then the body $\mathcal{B}$ will shake down with respect to the given loading $\mathbf{a}^*$.

3.3. Proof of the theorem

The proof of this theorem is analogous to that of the linear theory (cf. Chapter 1). For this, the bounded quadratic form is introduced defined by [182]:

$$W = \frac{1}{2}\int_{(V_0)} (\mathbf{S}^{(r)} - \overset{\circ}{\mathbf{S}}^{(r)}) \mathbf{:} \widetilde{\mathbf{L}}^{-1} \mathbf{:} (\mathbf{S}^{(r)} - \overset{\circ}{\mathbf{S}}^{(r)})\, dV_0 \tag{2.17}$$

where $\mathbf{S}^{(r)}$ and $\overset{\circ}{\mathbf{S}}^{(r)}$ are the actual time-dependent second Piola-Kirchhoff residual stresses tensor and the time-independent second Piola-Kirchhoff residual stresses tensor, respectively.

Using the following definitions

$$\mathbf{S}^{(r)} = \mathbf{S} - \mathbf{S}^{(e)} \tag{2.18}$$

$$\overset{\circ}{\mathbf{S}}^{(r)} = \mathbf{S}^{(s)} - \mathbf{S}^{(e)} \tag{2.19}$$

$$\Delta Y = \frac{1}{2}(\widetilde{\mathbf{S}} - \widetilde{\mathbf{S}}^{(s)}) \mathbf{:} \mathbf{L}^{-1} \mathbf{:} (\widetilde{\mathbf{S}} - \widetilde{\mathbf{S}}^{(s)}) \tag{2.20}$$

$$\dot{\mathbf{E}}^{(re)} = \dot{\mathbf{E}} - \dot{\mathbf{E}}^{(e)} - \dot{\mathbf{E}}^{p} \tag{2.21}$$

we get the time-derivative of eqn. (2.17)

$$\dot{W} = -\int_{(V_0)} (\mathbf{S} - \mathbf{S}^{(s)}) : \dot{\mathbf{E}}^{p}\, dV_0 \; - \int_{(V_0)} \Delta Y\, \dot{D}\, dV_0 \tag{2.22}$$

In view of inequality (1.19) and (1.24) it follows that $\dot{W} \geq 0$ and furthermore, $\dot{W}$ is equal to zero only if $\dot{\mathbf{E}}^{p} = 0$ and $\dot{D} = 0$. So Melan's argument holds: As W is non-negative by definition, plastic flow $\dot{\mathbf{E}}^{p}$ and damage evolution $\dot{D}$ cease beyond a certain time instant if a state of effective stresses $\tilde{\tilde{\mathbf{S}}}^{(r)}$ exists, fulfilling the relations (2.14-15). We say that $\mathcal{B}$ shakes down in this case (for details we refer to [182]).

3.4. Particular case allowing for practicable methods

This general formulation does not deliver a constructive method in the context of shakedown theory due to the fact that we need to know all quantities describing the state of deformations in the global intermediate configuration. Additional assumptions have to be introduced. In the simplest case we assume that the loads $\mathbf{a}^{*}$ are of a special type: Up to an instant t^{R} the body $\mathcal{B}$ undergoes finite and given displacement $\mathbf{u}^{R}$ with respect to the initial configuration C_i at time $t = 0$ in such a way that $\mathcal{B}$ is in the known configuration C_R in equilibrium under time-independent loads $\mathbf{a}^{R*}$. For times $t > t^{R}$ the body $\mathcal{B}$ is submitted to additional variable loads $\mathbf{a}^{r*}$ such that :

$$\mathbf{a}^{*}(\mathbf{X}, t) = \mathbf{a}^{R*}(\mathbf{X}) + \mathbf{a}^{r*}(\mathbf{X}, t) \tag{2.23}$$

and occupies the actual configuration C_t (see e.g. [57, 149, 154, 178]). Since the actual configuration should also be an equilibrium configuration and the following equations hold:

(i) *Statical equations*

$$\mathrm{Div}\,(\mathbf{T}^{R} + \mathbf{T}^{r}) = -\mathbf{f}^{R*} - \mathbf{f}^{r*} \qquad \text{in } V_0 \tag{2.24}$$

$$\mathbf{n}.(\mathbf{T}^{R} + \mathbf{T}^{r}) = \mathbf{p}^{R*} + \mathbf{p}^{r*} \qquad \text{on } \partial V_{0p} \tag{2.25}$$

with

$$\mathbf{T}^{R} + \mathbf{T}^{r} = (\mathbf{F}^{r}\,\mathbf{F}^{R})(\mathbf{S}^{R} + \mathbf{S}^{r}) \tag{2.26}$$

(ii) *Kinematical equations*

$$\mathbf{u} = \mathbf{u}^{R} + \mathbf{u}^{r} \qquad \text{in } V_0 \qquad (2.27)$$

$$\mathbf{F} = \mathbf{F}^{r}\,\mathbf{F}^{R} = \mathbf{I} + \text{grad}(\mathbf{u}^{R}) + \text{grad}(\mathbf{u}^{r}) \quad \text{in } V_0 \qquad (2.28)$$

$$\mathbf{E} = \mathbf{E}^{R} + \mathbf{E}^{r} = \frac{1}{2}(\mathbf{C} - \mathbf{I}) \qquad \text{in } V_0 \qquad (2.29)$$

$$\mathbf{u} = \mathbf{u}^{R*} + \mathbf{u}^{r*} \qquad \text{on } \partial V_{0u} \qquad (2.30)$$

with

$$\mathbf{C} = (\mathbf{F}^{r}\,\mathbf{F}^{R})^{T}(\mathbf{F}^{r}\,\mathbf{F}^{R}) \qquad (2.31)$$

where all quantities caused by the time-independent loads $\mathbf{a}^{R*}$ are marked by a superscript (^{R}), whereas the additional field quantities caused by the time-dependent loads $\mathbf{a}^{r*}$ are marked by superscript (^{r}). The additional field quantities caused by $\mathbf{a}^{r*}$ have to satisfy the following equations:

(i) *Statical equations*

$$\text{Div}\,(\mathbf{T}^{r}) = -\,\mathbf{f}^{r*} \qquad \text{in } V_0 \qquad (2.32)$$

$$\mathbf{n}.\mathbf{T}^{r} = \mathbf{p}^{r*} \qquad \text{on } \partial V_{0p} \qquad (2.33)$$

with

$$\mathbf{T}^{r} = \mathbf{H}^{r}\,\mathbf{F}^{R}\,\mathbf{S}^{R} + \mathbf{F}^{R}\,\mathbf{S}^{r} + \mathbf{H}^{r}\,\mathbf{F}^{R}\,\mathbf{S}^{r} \qquad (2.34)$$

(ii) *Kinematical equations*

$$\mathbf{F}^{r} = \mathbf{I} + \mathbf{H}^{r} \qquad \text{in } V_0 \qquad (2.35)$$

$$\mathbf{E}^{r} = \frac{1}{2}(\mathbf{F}^{R})^{T}[(\mathbf{H}^{r})^{T} + \mathbf{H}^{r} + (\mathbf{H}^{r})^{T}\,\mathbf{H}^{r}](\mathbf{F}^{R}) \qquad \text{in } V_0 \qquad (2.36)$$

$$\mathbf{u}^{r} = \mathbf{u}^{r*} \qquad \text{on } \partial V_{0u} \qquad (2.37)$$

with

$$\mathbf{H}^{r} = \text{grad}_{R}(\mathbf{u}^{r}) \qquad (2.38)$$

In the sequel, we restrict our considerations to loading histories characterized by the motion of a fictitious comparison body $\mathcal{B}^{(c)}$, having at time t^{R} the same field quantities as $\mathcal{B}$ but reacting, in contrast to $\mathcal{B}$, purely elastically to the additional time-dependent loads $\mathbf{a}^{r*}$, superimposed on $\mathbf{a}^{R*}$ for $t > t^{R}$ (Figure 2.2) (cf. [57, 154, 178]). Henceforth, all quantities related to this comparison problem are indicated by superscript (^{c}). Obviously, eqn. (2.32-38) also hold for the comparison problem with the only exception, that in the

comparison body $\mathcal{B}^{(c)}$ no additional plastic strains and no damage can occur. The differences between the states in $\mathcal{B}$ and $\mathcal{B}^{(c)}$ are then described by the difference fields:

$$\Delta\mathbf{u} = \mathbf{u}^{r} - \mathbf{u}^{r(c)}\,; \quad \Delta\mathbf{F} = \mathbf{F}^{r} - \mathbf{F}^{r(c)}\,; \quad \Delta\mathbf{E} = \mathbf{E}^{r} - \mathbf{E}^{r(c)} \tag{2.39}$$

$$\Delta\mathbf{T} = \mathbf{T}^{r} - \mathbf{T}^{r(c)}\,; \quad \Delta\mathbf{S} = \mathbf{S}^{r} - \mathbf{S}^{r(c)} \tag{2.40}$$

and have to fulfil the following equations:

$$\mathrm{Div}\,(\Delta\mathbf{T}) = 0 \qquad \text{in } V_0 \tag{2.41}$$

$$\mathbf{n}.(\Delta\mathbf{T}) = 0 \qquad \text{on } \partial V_{0p} \tag{2.42}$$

and

$$\Delta\mathbf{F} = \mathbf{H}^{r} - \mathbf{H}^{r(c)} \qquad \text{in } V_0 \tag{2.43}$$

$$\Delta\mathbf{E} = \frac{1}{2}(\mathbf{F}^{R})^{T}[(\Delta\mathbf{F})^{T} + (\Delta\mathbf{F})](\mathbf{F}^{R}) + \frac{1}{2}(\mathbf{F}^{R})^{T}[(\mathbf{H}^{r})^{T}(\mathbf{H}^{r}) - (\mathbf{H}^{r(c)})^{T}(\mathbf{H}^{r(c)})](\mathbf{F}^{R}) \qquad \text{in } V_0 \tag{2.44}$$

$$\Delta\mathbf{u} = 0 \qquad \text{on } \partial V_{0u} \tag{2.45}$$

with

$$\Delta\mathbf{T} = (\Delta\mathbf{F})\,\mathbf{F}^{R}\,\mathbf{S}^{R} + \mathbf{F}^{R}\,(\Delta\mathbf{S}) + \mathbf{H}^{r}\,\mathbf{F}^{R}\,\mathbf{S}^{r} - \mathbf{H}^{r(c)}\,\mathbf{F}^{R}\,\mathbf{S}^{r(c)} \tag{2.46}$$

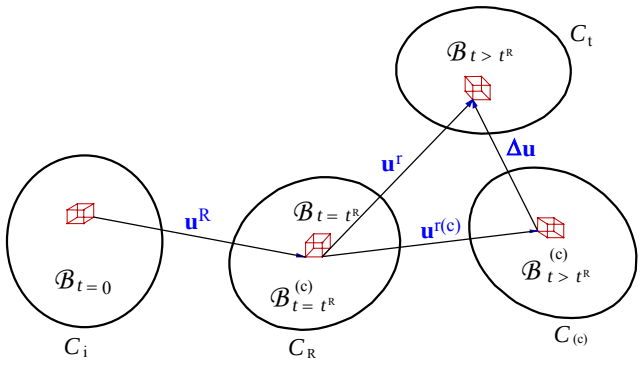

Figure 2.2. Evolution of real body $\mathcal{B}$ and comparison body $\mathcal{B}^{(c)}$.

In the following, we restrict our considerations to situations where the state of deformation and the state of stress in $\mathcal{B}$ are subjected to small variations in time [57, 178]. Consequently, we neglect in the governing eqn. (2.39-46) all terms, which are non-linear in the time-dependent additional field quantities marked by a superscript (^{r}). This excludes to study buckling effects induced by the additional time-dependent loads. Then the following extension of Melan's theorem holds:

If there exists a time-independent field of effective residual stresses $\Delta\overset{\sim}{\overset{\circ}{\mathbf{S}}}$ such that the following relations holds:

$$(i)\quad \mathrm{Div}\,(\mathbf{F}^{\mathrm{R}}\mathbf{S}^{\mathrm{R}}) = -\,\mathbf{f}^{\mathrm{R}*} \qquad \text{in } V_0 \qquad (2.47)$$

$$\mathbf{n}.(\mathbf{F}^{\mathrm{R}}\mathbf{S}^{\mathrm{R}}) = \mathbf{p}^{\mathrm{R}*} \qquad \text{on } \partial V_{0\mathrm{p}} \qquad (2.48)$$

$$\mathbf{u} = \mathbf{u}^{\mathrm{R}*} \qquad \text{on } \partial V_{0\mathrm{u}} \qquad (2.49)$$

$$(ii)\quad \mathrm{Div}\,(\Delta\overset{\circ}{\mathbf{T}}) = 0 \qquad \text{in } V_0 \qquad (2.50)$$

$$\mathbf{n}.(\Delta\overset{\circ}{\mathbf{T}}) = 0 \qquad \text{on } \partial V_{0\mathrm{p}} \qquad (2.51)$$

$$\Delta\overset{\circ}{\mathbf{u}} = 0 \qquad \text{on } \partial V_{0\mathrm{u}} \qquad (2.52)$$

with $\Delta\overset{\circ}{\mathbf{T}} = (\Delta\overset{\circ}{\mathbf{F}})\,\mathbf{F}^{\mathrm{R}}\mathbf{S}^{\mathrm{R}} + \mathbf{F}^{\mathrm{R}}(\Delta\overset{\circ}{\mathbf{S}})$

$$(iii)\quad \mathscr{F}\,(\alpha\,\tilde{\mathbf{S}}^{\mathrm{r(c)}} + \tilde{\mathbf{S}}^{\mathrm{R}} + \Delta\overset{\sim}{\overset{\circ}{\mathbf{S}}}),\ \sigma_{\mathrm{Y}}) \le 0 \qquad \text{in } V_0 \qquad (2.53)$$

for all time $t > t^{\mathrm{R}}$, then the original body $\mathcal{B}$ will shakedown under given program of loading $\mathbf{a}^*$. The damage parameter D^{r} induced by additional variable loads $\mathbf{a}^{\mathrm{r}*}$ is given by eqn. (1.43).

Then the safety factor against failure due to non-shakedown or inadmissible damage is defined by the following optimisation problem [182]:

$$\alpha_{SD} = \max_{\Delta\overset{\circ}{\mathbf{T}},\,D}\ \alpha \qquad (2.54)$$

with the subsidiary conditions

$$D - D_c < 0 \qquad \text{in } V_0 \qquad (2.55)$$

$$\mathrm{Div}\,(\Delta\overset{\circ}{\mathbf{T}}) = 0 \qquad \text{in } V_0 \qquad (2.56)$$

$$\mathbf{n}.(\Delta\overset{\circ}{\mathbf{T}}) = 0 \qquad \text{on } \partial V_{0\mathrm{p}} \qquad (2.57)$$

$$\mathscr{F}\,(\alpha\,\tilde{\mathbf{S}}^{\mathrm{r(c)}} + \tilde{\mathbf{S}}^{\mathrm{R}} + \Delta\overset{\sim}{\overset{\circ}{\mathbf{S}}}),\ \sigma_{\mathrm{Y}}) \le 0 \qquad \text{in } V_0 \qquad (2.58)$$

where

$$\Delta\overset{\circ}{\mathbf{T}} = (\Delta\overset{\circ}{\mathbf{F}})\,\mathbf{F}^{\mathrm{R}}\mathbf{S}^{\mathrm{R}} + \mathbf{F}^{\mathrm{R}}(\Delta\overset{\circ}{\mathbf{S}}) \ \text{ and } \ D = D^{\mathrm{R}} + D^{\mathrm{r}}.$$

4. Application to shell-like structures

The practical approach presented above in the case of geometrical non-linearity is applied to shell-like structures. For this, we use generalised material laws expressed in terms of stress and strain resultants. This enables us to derive a strictly two-dimensional formulation, which is advantageous from a computational point of view. The classical non-linear shell theory of Donnell-Mushtari-Vlasov will be used, which gives sufficiently accurate results within imposed range of applicability (see, e.g. [59, 156, 180]).

4.1. Basic shell relations

In the following, we restrict our consideration to shallow-shells undergoing moderate rotations about tangents and small rotations about normals to the mid-surface $\mathcal{M}$ of the shell. Let P the region of the three-dimensional Euclidean space E occupied by the shell in its undeformed configuration C_i, parameterised by the curvilinear coordinates $(\theta^1, \theta^2, \theta^3)$ such that $-h/2 \le \theta^3 \le h/2$; h is the thickness of the undeformed shell, assumed to be small compared with the smallest radius of curvature R of the mid-surface $\mathcal{M}$; i.e. $h/R << 1$ (Figure 2.3) (see, e.g. [7]). $\mathcal{M}$ is described by the position vector in the undeformed configuration by

$$\mathbf{r} = \mathbf{X}^k (\theta^\alpha)\, \mathbf{i}_k \; ; \; k = 1, 2, 3; \; \alpha = 1, 2 \tag{2.59}$$

where $\mathbf{i}_k$ is the orthonormal basis of a Cartesian system of coordinates with origin $O \in E$. Then, by usual definitions, we have

– base vectors: $\mathbf{a}_\alpha = \mathbf{r}_{,\alpha}$; $\mathbf{a}^\alpha = a^{\alpha\beta}\, \mathbf{a}_\beta$ (2.60)

– unit normal vector: $\mathbf{a}_3 = 1/2\; \varepsilon^{\alpha\beta}\, \mathbf{a}_\alpha \times \mathbf{a}_\beta$; $\mathbf{a}^3 = \mathbf{a}_3$ (2.61)

– metric tensor: $a_{\alpha\beta} = \mathbf{a}_\alpha \cdot \mathbf{a}_\beta$; $a^{\alpha\beta} = \mathbf{a}^\alpha \cdot \mathbf{a}^\beta$ (2.62)

– curvature tensors: $b_{\alpha\beta} = -\, \mathbf{a}_\alpha \cdot \mathbf{a}_{3,\beta}$; $b_\alpha^\beta = a_{\alpha\gamma}\, a^{\gamma\beta}$ (2.63)

– determinant: $a = |a_{\alpha\beta}| = a_{11}\, a_{22} - (a_{12})^2$ (2.64)

Here, $(\cdot)_{,\alpha}$ denotes partial derivatives with respect to θ^α. Greek and Latin indices take the values 1, 2 and 1, 2, 3, respectively. $\varepsilon^{\alpha\beta}$ denotes the contravariant components of the permutation tensor with $\varepsilon^{12} = -\varepsilon^{21} = a^{-1/2}$ and $\varepsilon^{11} = \varepsilon^{22} = 0$. The symbol $(\cdot)$ and $(\times)$ between two vectors represent scalar product and cross product, respectively. At line C, bounding the middle surface $\mathcal{M}$, we introduce an orthonormal vector system $\boldsymbol{\nu}$, $\mathbf{t}$, $\mathbf{a}_3$, where $\mathbf{t} = \partial\mathbf{r}/\partial s$ is the unit tangent vector, s being the arc length along C, and $\boldsymbol{\nu} = \mathbf{t} \times \mathbf{a}_3$ denotes the outward unit normal vector.

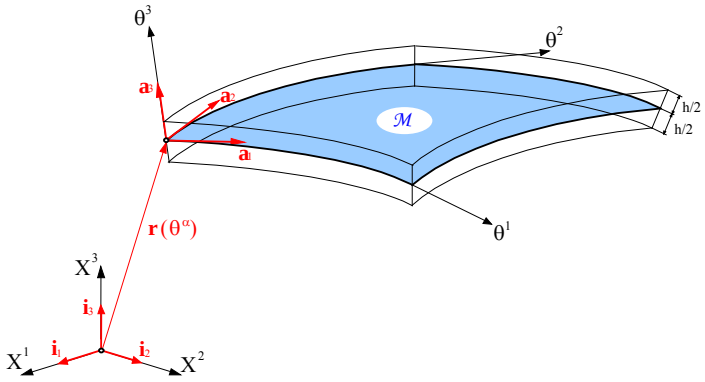

Figure 2.3. Shell geometry.

The deformation of the shell middle surface from the undeformed configuration $\mathcal{M}$ into the deformed configuration $\overline{\mathcal{M}}$ can be described by the displacement field

$$\mathbf{u} = \overline{\mathbf{r}} - \mathbf{r} = u^\alpha\, \mathbf{a}_\alpha + u^3\, \mathbf{a}_3 \tag{2.65}$$

The deformation of the shell can be defined by the middle surface strain tensor $\boldsymbol{\gamma}$ and the change of curvature $\boldsymbol{\chi}$

$$\gamma_{\alpha\beta} = \frac{1}{2}\,(u_\alpha|_\beta + u_\beta|_\alpha - 2\, b_{\alpha\beta}\, u_3 + u_{3,\alpha}\, u_{3,\beta}) \qquad \text{in } \mathcal{M} \tag{2.66}$$

$$\chi_{\alpha\beta} = -\, u_3|_{\alpha\beta} \qquad \text{in } \mathcal{M} \tag{2.67}$$

where a vertical stroke preceding a subscript indicates covariant differentiation with respect to the corresponding direction.

To complete the set of kinematical equations, the geometrical boundary conditions on the part C_u of C are given by

$$u_\nu = u^\alpha \ \nu_\alpha = u^*_\nu \qquad \text{on } C_u \qquad (2.68)$$
$$u_t = u^\alpha \ t_\alpha = u^*_t \qquad \text{on } C_u \qquad (2.69)$$
$$u_3 = u^*_3 \qquad \text{on } C_u \qquad (2.70)$$
$$\beta_\nu = -\, u_{3,\alpha} \ \nu^\alpha = \beta^*_\nu \qquad \text{on } C_u \qquad (2.71)$$

where prescribed quantities are indicated by an asterisk and β_ν denotes the rotation about tangent to the boundary line. However, the statical equations are given in the following form

$$N^{\alpha\beta}|_\beta + p^{\alpha *} = 0 \qquad \text{in } \mathcal{M} \qquad (2.72)$$
$$(M^{\alpha\beta}|_\alpha + u_{3,\alpha} \ N^{\alpha\beta})|_\beta + b_{\alpha\beta} \, N^{\alpha\beta} + p^{3*} = 0 \qquad \text{in } \mathcal{M} \qquad (2.73)$$
$$\nu_\alpha \ \nu_\beta \, N^{\alpha\beta} = N^*_{\nu\nu} \qquad \text{on } C_p \qquad (2.74)$$
$$t_\alpha \ \nu_\beta \, N^{\alpha\beta} = N^*_{t\nu} \qquad \text{on } C_p \qquad (2.75)$$
$$\nu_\beta \, (M^{\alpha\beta}|_\alpha + u_{3,\alpha} \ N^{\alpha\beta}) - M_{t\nu,\alpha} \, t^\alpha = N^*_{n\nu} - M^*_{t\nu,t} \qquad \text{on } C_p \qquad (2.76)$$
$$\nu_\alpha \ \nu_\beta \, M^{\alpha\beta} = M^*_{\nu\nu} \qquad \text{on } C_p \qquad (2.77)$$

Here, C_p denotes the part of C, where static boundary conditions are prescribed and $p^{\alpha *}$ and p^{3*} are the components of the distributed surface loads per unit area of the undeformed middle surface $\mathcal{M}$. **N** and **M** denote the symmetric stress resultant tensor and the symmetric stress couple tensor, respectively.

4.2. Stress-resultant constitutive relations

The strain measures $\boldsymbol{\gamma}$, $\boldsymbol{\chi}$ can be additively decomposed into elastic parts $\boldsymbol{\gamma}^e$, $\boldsymbol{\chi}^e$ and plastic parts $\boldsymbol{\gamma}^p$, $\boldsymbol{\chi}^p$, such that

$$\gamma_{\alpha\beta} = \gamma^e_{\alpha\beta} + \gamma^p_{\alpha\beta} \qquad (2.78)$$
$$\chi_{\alpha\beta} = \chi^e_{\alpha\beta} + \chi^p_{\alpha\beta} \qquad (2.79)$$

For isotropic linear elastic material behaviour, the strain measures $\boldsymbol{\gamma}^{e}$, $\boldsymbol{\chi}^{e}$ are given by the relations

$$\gamma_{e,\alpha\beta} = \frac{1}{A} G_{\alpha\beta\gamma\lambda}\, \tilde{N}^{\gamma\lambda} \tag{2.80}$$

$$\chi_{e,\alpha\beta} = \frac{1}{B} G_{\alpha\beta\gamma\lambda}\, \tilde{M}^{\gamma\lambda} \tag{2.81}$$

where $\mathbf{G}$ is the positive definite elasticity tensor and A and B are the extensional and bending stiffness, respectively, defined by

$$G_{\alpha\beta\gamma\lambda} = \frac{1}{2(1-\nu)} \left[a_{\alpha\gamma}\, a_{\beta\lambda} + a_{\alpha\lambda}\, a_{\beta\gamma} - \frac{2\nu}{1+\nu} a_{\alpha\beta}\, a_{\gamma\lambda} \right] \tag{2.82}$$

and

$$A = \frac{E\,h}{1-\nu^2}, \quad B = \frac{E\,h^3}{12(1-\nu^2)} \tag{2.83}$$

The plastic measures $\boldsymbol{\gamma}^{p}$, $\boldsymbol{\chi}^{p}$ are given by the normality rule

$$\dot{\gamma}^{p}_{\alpha\beta} = \dot{\lambda}_N \frac{\partial \mathscr{F}}{\partial N^{\alpha\beta}} \tag{2.84}$$

$$\dot{\chi}^{p}_{\alpha\beta} = \dot{\lambda}_M \frac{\partial \mathscr{F}}{\partial M^{\alpha\beta}} \tag{2.85}$$

where $\dot{\lambda}_N$ and $\dot{\lambda}_M$ are non-negative proportionality factors. In the following we use a so-called subsequent yield condition derived by Bieniek and Funaro [13] and modified by several authors to take into account hardening parameter. As it has been suggested by Gross-Weege and Weichert [58], we use a simplified two-surface yield condition, expressed exclusively in terms of the effective stress resultants

$$\mathscr{F}_I(\tilde{\mathbf{N}}, \tilde{\mathbf{M}}^{*}) = I_{NN} + \frac{9}{4} I^{*}_{MM} \pm 3\, I^{*}_{NM} - 1 = 0 \tag{2.86}$$

$$\mathscr{F}_L(\tilde{\mathbf{N}}, \tilde{\mathbf{M}}) = I_{NN} + I_{MM} \pm \frac{1}{\sqrt{3}} I_{NM} - 1 = 0 \tag{2.87}$$

with

$$I_{\mathrm{NN}} = I_{\alpha\beta\gamma\lambda}\frac{\widetilde{N}^{\alpha\beta}\widetilde{N}^{\gamma\lambda}}{N_{\mathrm{p}}^{2}};\ I_{\mathrm{MM}} = I_{\alpha\beta\gamma\lambda}\frac{\widetilde{M}^{\alpha\beta}\widetilde{M}^{\gamma\lambda}}{M_{\mathrm{p}}^{2}};\ I_{\mathrm{NM}} = I_{\alpha\beta\gamma\lambda}\frac{\widetilde{N}^{\alpha\beta}\widetilde{M}^{\gamma\lambda}}{N_{\mathrm{p}}\,M_{\mathrm{p}}} \tag{2.88}$$

and

$$I_{\alpha\beta\gamma\lambda} = \frac{3}{2}a_{\alpha\gamma}\,a_{\beta\lambda} - \frac{1}{2}a_{\alpha\beta}\,a_{\gamma\lambda} \tag{2.89}$$

$$N_{\mathrm{p}} = \sigma_{\mathrm{Y}}\,h,\ M_{\mathrm{p}} = \sigma_{\mathrm{Y}}\,h^{2}/4. \tag{2.90}$$

Here $\mathscr{F}_{\mathrm{I}}$ and $\mathscr{F}_{\mathrm{L}}$ denote the initial yield surface [13] and the limit yield surface [80], respectively. N_{p} and M_{p} denote the uniaxial yield force and the uniaxial yield moment, respectively, and σ_{Y} is the uniaxial yield stress. I^{*}_{MM} and I^{*}_{NM} are also given by eqn. (2.88) if we replace $\mathbf{M}$ by the differences $\mathbf{M} - \mathbf{M}^{*}$, where $\mathbf{M}^{*}$ plays the role of a "*hardening*" parameter whose evolution is defined by

$$\dot{M}^{*\alpha\beta} = \begin{cases} C^{\alpha\beta\gamma\lambda}\,\dot{\chi}^{\mathrm{p}}_{\gamma\lambda} & \text{for } \mathscr{F}_{\mathrm{I}} = 0 \text{ and } \dot{\mathscr{F}}_{\mathrm{I}} > 0 \\ 0 & \text{for } \mathscr{F}_{\mathrm{I}} < 0 \text{ or } \mathscr{F}_{\mathrm{I}} = 0 \text{ and } \dot{\mathscr{F}}_{\mathrm{I}} < 0 \end{cases} \tag{2.91}$$

where

$$C^{\alpha\beta\gamma\lambda} = a^{\alpha\gamma}\,a^{\beta\lambda}\frac{E\,h^{3}}{12}$$

4.3. A stress-resultant formulation of shakedown theorem

The problem: An elastic-plastic shell P is at time $t = t^{\mathrm{R}}$ in equilibrium in the configuration C_{R} under the time-independent external loading $\mathbf{a}^{\mathrm{R}}$. Will the shell shakedown under the action of additional variable loads $\mathbf{a}^{\mathrm{r}}$?

Proposition: The shell P shakes down if there exist time-independent fields of effective bending moments and effective membrane forces $\widetilde{\mathbf{M}}^{*}$, $\Delta\widetilde{\mathbf{N}}$ and $\Delta\widetilde{\mathbf{M}}$, such that for $t > t^{\mathrm{R}}$ the following conditions are valid

$$\Delta \overset{\circ}{N}{}^{\alpha\beta}|_{\beta} = 0 \qquad \text{in } \mathcal{M} \qquad (2.92)$$

$$(\Delta \overset{\circ}{M}{}^{\alpha\beta}|_{\alpha} + u^{\mathrm{R}}_{3,\alpha} \Delta \overset{\circ}{N}{}^{\alpha\beta} + \Delta \mathring{u}_{3,\alpha} N^{\mathrm{R}\alpha\beta})|_{\beta} + b_{\alpha\beta} \Delta \overset{\circ}{N}{}^{\alpha\beta} = 0 \qquad \text{in } \mathcal{M} \qquad (2.93)$$

$$\nu_{\alpha}\ \nu_{\beta}\ \Delta \overset{\circ}{N}{}^{\alpha\beta} = 0 \qquad \text{on } \mathcal{C}_{\mathrm{p}} \qquad (2.94)$$

$$t_{\alpha}\ \nu_{\beta}\ \Delta \overset{\circ}{N}{}^{\alpha\beta} = 0 \qquad \text{on } \mathcal{C}_{\mathrm{p}} \qquad (2.95)$$

$$\nu_{\beta}\ (\Delta \overset{\circ}{M}{}^{\alpha\beta}|_{\alpha} + u^{\mathrm{R}}_{3,\alpha} \Delta \overset{\circ}{N}{}^{\alpha\beta} + \Delta \mathring{u}_{3,\alpha} N^{\mathrm{R}\alpha\beta}) - \Delta \overset{\circ}{M}_{\mathrm{tv},\alpha}\ t^{\alpha} = 0 \qquad \text{on } \mathcal{C}_{\mathrm{p}} \qquad (2.96)$$

$$\nu_{\alpha}\ \nu_{\beta}\ \Delta \overset{\circ}{M}{}^{\alpha\beta} = 0 \qquad \text{on } \mathcal{C}_{\mathrm{p}} \qquad (2.97)$$

$$\Delta \mathring{u}_{3} = 0 \qquad \text{on } \mathcal{C}_{\mathrm{u}} \qquad (2.98)$$

$$\beta_{\nu} = -\ \Delta \mathring{u}_{3,\alpha}\ \nu^{\alpha} = 0 \qquad \text{on } \mathcal{C}_{\mathrm{u}} \qquad (2.99)$$

$$\mathscr{F}_{\mathrm{I}} \left(\frac{\mathbf{N}^{\mathrm{r(c)}}}{1-D} + \frac{\mathbf{N}^{\mathrm{R}}}{1-D} + \frac{\Delta \overset{\circ}{\mathbf{N}}}{1-D} ; \frac{\mathbf{M}^{\mathrm{r(c)}}}{1-D} + \frac{\mathbf{M}^{\mathrm{R}} - \mathbf{M}^{*\mathrm{R}}}{1-D} + \frac{\Delta \overset{\circ}{\mathbf{M}} - \overset{\circ}{\mathbf{M}}{}^{*}}{1-D}, \sigma_{\mathrm{Y}} \right) < 0 \text{ in } \mathcal{M} \qquad (2.100)$$

$$\mathscr{F}_{\mathrm{L}} \left(\frac{\mathbf{N}^{\mathrm{r(c)}}}{1-D} + \frac{\mathbf{N}^{\mathrm{R}}}{1-D} + \frac{\Delta \overset{\circ}{\mathbf{N}}}{1-D} ; \frac{\mathbf{M}^{\mathrm{r(c)}}}{1-D} + \frac{\mathbf{M}^{\mathrm{R}}}{1-D} + \frac{\Delta \overset{\circ}{\mathbf{M}}}{1-D}, \sigma_{\mathrm{U}} \right) < 0 \qquad \text{in } \mathcal{M} \qquad (2.101)$$

with

$$D = D^{\mathrm{R}} + D^{\mathrm{r}} \qquad (2.102)$$

In eqn. (2.92-102), the quantities fields induced by the time-independent loads $\mathbf{a}^{\mathrm{R}*}$ are indicated by superscript $(^{\mathrm{R}})$, however the quantities resulting from time-dependent additional loads $\mathbf{a}^{\mathrm{r}*}$ are indicated by $(^{\mathrm{r}})$ (see, e.g. [95, 174]).

5. Numerical applications

On the basis of the concepts developed in the chapter 1 and the preceding sections, the specialised **S**hakedown **A**nd **Li**mit-**A**nalysis software "SALIA" has been used [10, 16, 53, 56, 65, 157, 175]. For illustration, some numerical examples of axisymmetric shells will be considered. Lower bounds of the safety factor are derived taking into account, in the case of geometrical changes, the influence of the reference state by determining the state of stresses $\mathbf{S}^{\mathrm{R}}$, displacement $\mathbf{u}^{\mathrm{R}}$ and damage parameter D^{R} in the reference configuration C_{R} under the time-independent load $\mathbf{a}^{\mathrm{R}*}$. The symmetry of shell and loads is assumed which allows to limit calculations to half of the shell.

5.1. Clamped conical shell

In the first example, we consider a clamped conical shell subjected to external uniform pressure (Figure 2.4). The von Mises-sandwich yield criteria is used. We compare, in the case of limit analysis ($p = \mu\, p_0$, $\mu = \mu^- = \mu^+$), results obtained by SALIA with the lower and upper bounds of the limit load, given by Chwala and Biron [25], the quasi-lower and upper bounds given by Nguyen Dang Hung et al. [130] who also use von Mises-sandwich yield criteria and with results given by Morelle [124] who uses the Tresca-sandwich yield condition (Table 2.1). In the case of shakedown analysis ($p = \mu\, p^0$, $0 \le \mu \le \mu^+$), we compare our results with those obtained by Morelle [124] using Tresca-sandwich yield condition (Table 2.2).

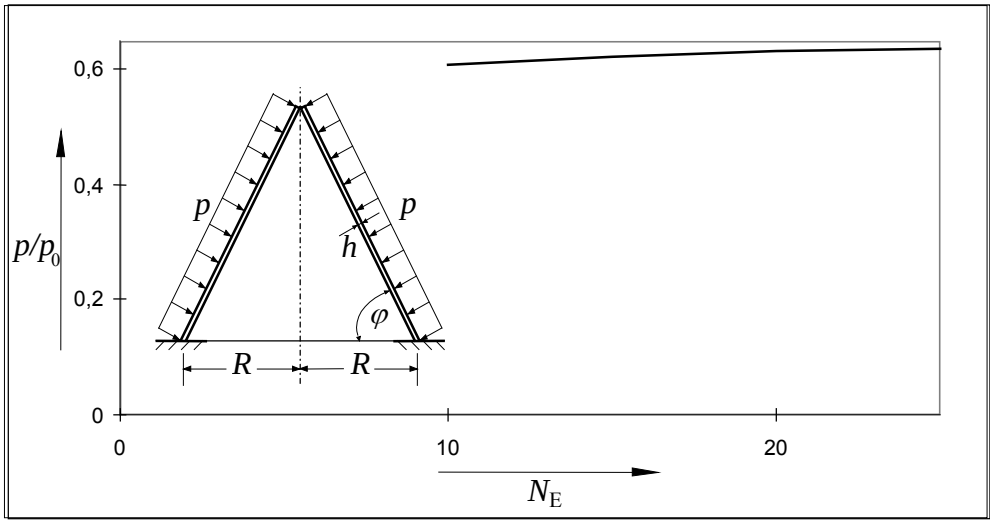

Figure 2.4. Conical shell under external pressure.
Convergence of the shakedown load in terms of the number of elements.

Figure 2.4 also shows the convergence of the results for this example as function of the number (N_E) of equal size finite elements. One observes that few elements are sufficient to get reasonable results if one assumes an asymptotic behaviour of the solution as Figure 2.4 suggests. These results are obtained by taking the following values for geometry, material properties and loads:

$$h/R = 1/25;\ \varphi = 63°27;\ E = 1.6\times10^5 \text{ MPa};\ \nu = 0.3;\ \sigma_Y = 360 \text{ MPa};\ p_0 = 2\ \sigma_Y\, h/R.$$

Author	*Criterion*	*Approach*	N_E	p/p_0
Chwala and Biron [25]	von Mises	upper bound	2	0.6859
Chwala and Biron [25]	von Mises	upper bound	3	0.6655
Chwala and Biron [25]	von Mises	lower bound	4	0.6303
Nguyen Dang Hung et al. [130]	von Mises	quasi-lower bound	8	0.6270
Nguyen Dang Hung et al. [130]	von Mises	quasi-lower bound	10	0.6203
Nguyen Dang Hung et al. [130]	von Mises	upper bound	6	0.6787
Nguyen Dang Hung et al. [130]	von Mises	upper bound	8	0.6758
Morelle [124]	Tresca	lower bound	41	0.5920
Morelle [124]	Tresca	upper bound	41	0.6021
Present solution	von Mises	lower bound	10	0.6088
Present solution	von Mises	lower bound	20	0.6333

Table 2.1. Limit analysis of a conical shell.

Author	*Criterion*	*Approach*	N_E	p/p_0
Morelle [124]	Tresca	lower bound	11	0.578
Morelle [124]	Tresca	lower bound	41	0.591
Morelle [124]	Tresca	upper bound	11	0.645
Morelle [124]	Tresca	upper bound	41	0.602
Present solution	von Mises	lower bound	10	0.608
Present solution	von Mises	lower bound	20	0.631

Table 2.2. Shakedown analysis of a conical shell.

5.2. Circular plate

The conical shell described above is reduced to an annular plate by setting $\varphi = 0°$. Here, three cases are investigated:

(i) limit analysis of a circular plate with a central hole loaded by uniformly distributed pressure;

(ii) shakedown analysis of a circular plate under the action of uniform pressure and a bending moment;

(iii) shakedown analysis of a circular plate under the action of uniform pressure and variable temperature.

5.2.1. Circular plate with a central circular hole

A circular plate with a central circular hole is considered, Figure 2.5. This problem has been treated analytically by Hodge [77] and numerically by Morelle and Nguyen Dang Hung [123], who derived lower bounds for the limit loads, using the Tresca-sandwich yield criterion. In our case, we adopt the von Mises-sandwich yield criterion. Fig. 4 shows the variation of limit loads with the ratio between the radius r of the hole and outer radius R of the plate ($b = r/R$). The difference of the results between the two yield criteria is of the order of 10 per cent. The analytical lower bound given by Hodge [77] is $p/p_0 = 1/(1 + b - 2b^2)$. The following quantities have been adopted in the numerical analysis: $h/R = 1/100$; $E = 1.6\times10^5$ MPa; $\nu = 0.3$; $\sigma_Y = 360$ MPa; $p_0 = 1.5\ \sigma_Y\ (h/R)^2$.

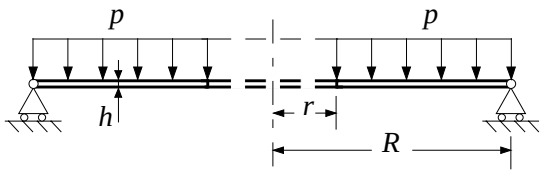

Figure 2.5. Circular plate with central hole.

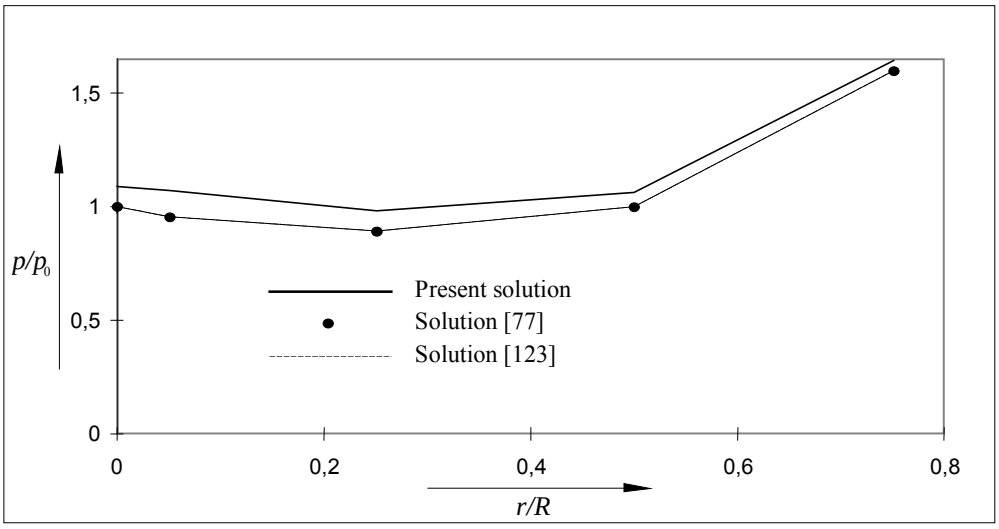

Figure 2.5. Variation of limit load with the ratio r/R.

5.2.2. Circular plate under uniform pressure and a bending moment

The shakedown analysis was carried out for a simply supported circular plate loaded as shown in Figure 2.6 by two independent variable loads, the uniform pressure p ($p = \mu_1 p_0$, $0 \le \mu_1 \le \mu_1^+$) and a bending moment ($M = \mu_2 M_0$, $\mu_2^- \le \mu_2 \le \mu_2^+$). This example has also been treated by König [88] and Morelle [125] using the Tresca yield condition for uniform and sandwich cross-section, respectively. The first author gives the lower bound via an analytical method and the second via a numerical method. The following values of geometrical dimensions and material properties have been adopted in the numerical analysis : $h/R = 1/100$; $E = 1.6\times10^5$ MPa; $\nu = 1/3$ and $\sigma_Y = 360$ MPa. For the graphical representation of the results the following quantities of loads are used: $p_0 = 1.5\ \sigma_Y\ (h/R)^2$ and $M_0 = \sigma_Y\ h^2/4$.

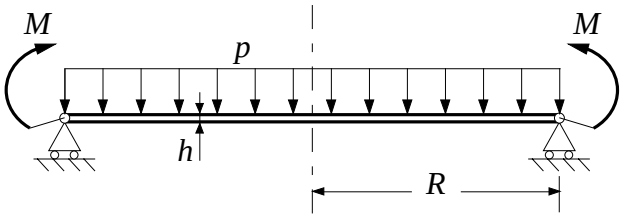

Figure 2.6. Circular plate under uniform pressure and a bending moment.

Two different classes of material behaviour are considered :

- elastic perfectly plastic material behaviour without damage, Figure 2.7. Both failure mechanisms are studied, namely failure due to alternating plasticity and failure due to accumulated plasticity. Curves (a) correspond to the failure due to alternating plasticity by considering uniform cross-section and curves (b) correspond to the failure due to accumulated plasticity by considering sandwich cross-section;
- elastic perfectly plastic material behaviour with ductile damage (Figure 2.8) using the models of Lemaitre [104] and Shichun and Hua [158] presented in chapter 1. Only the failure mechanism due to accumulated plasticity is investigated because of the choice of the adopted damage models. We observe a stronger sensitivity of the shakedown load on the uniform pressure then on the moment variation. The range of the allowable safe moment variation is characterised by the failure mechanism of alternating plasticity.

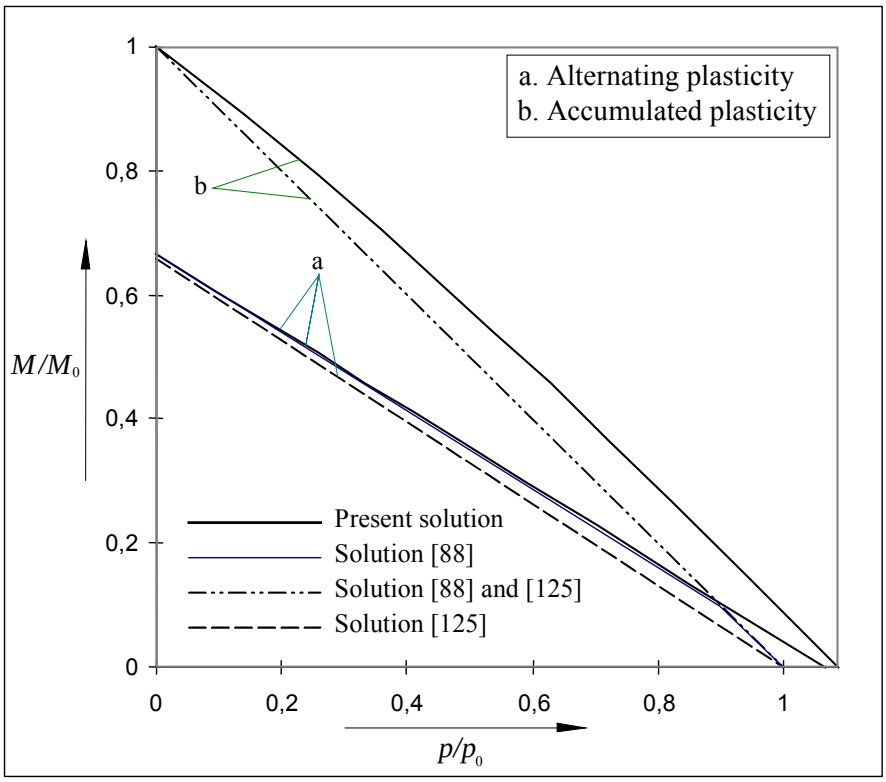

Figure 2.7. Loading domains of circular plate without damage.

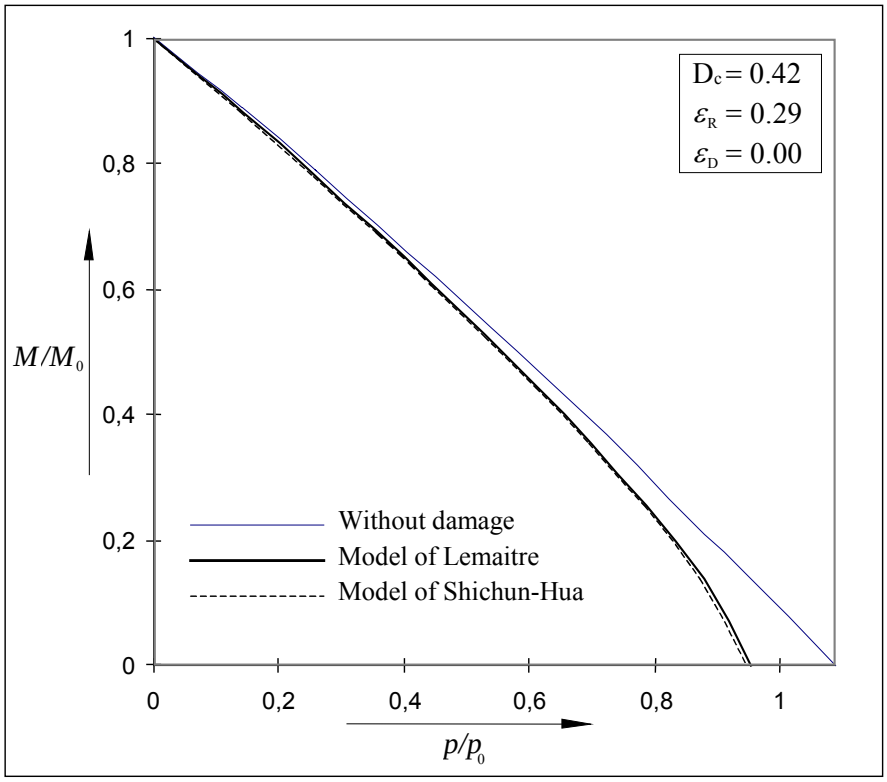

Figure 2.8. Influence of ductile damage.

5.2.3. Circular plate under uniform pressure and variable temperature

A clamped circular plate under uniform pressure p and variable temperature ϑ is considered (Figure 2.9). The distribution of ϑ across the thickness is assumed linear. Two different cases of material behaviour are studied :

- perfectly plastic material behaviour without damage (Figure 2.10);
- elastic perfectly plastic material behaviour with ductile damage (Figure 2.11), by using the model of Lemaitre [104] and Shichun and Hua [158].

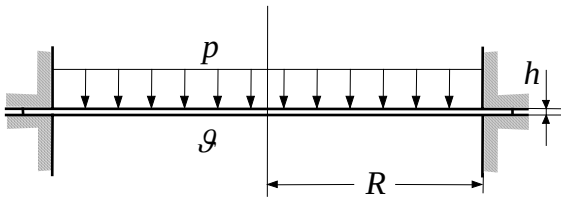

Figure 2.9. Clamped circular plate under uniform pressure and variable temperature.

The following values for geometry, material properties and loads have been adopted in the numerical analysis:

$$h/R = 1/25;\ E = 1.6\times10^{5}\ \text{MPa};\ \nu = 0.3;\ \sigma_Y = 360\ \text{MPa};\ \alpha_\vartheta = 0.2\times10^{-4}\ \text{K}^{-1};$$
$$p_0 = 4\sigma_Y h^2/((1+\nu)R^2);\ \vartheta_0 = 6(1-\nu)\sigma_Y/(E\alpha_\vartheta).$$

For the undamaged behaviour, we compare our results with those obtained numerically by Gokhfeld and Cherniavsky [54]. They used the statical method in the rigorous formulation, use being made of a special simplex method applying Tresca yield condition. For this case, the following loading conditions are investigated:

- the uniform pressure p is constant whereas the temperature $\vartheta = \mu\ \vartheta_0$ is variable $(0 \le \mu \le \mu^+)$;
- both the uniform pressure $p = \mu_1\ p_0$ and temperature $\vartheta = \mu_2\ \vartheta_0$ vary independently $(0 \le \mu_1 \le \mu_1^+;\ 0 \le \mu_2 \le \mu_2^+)$.

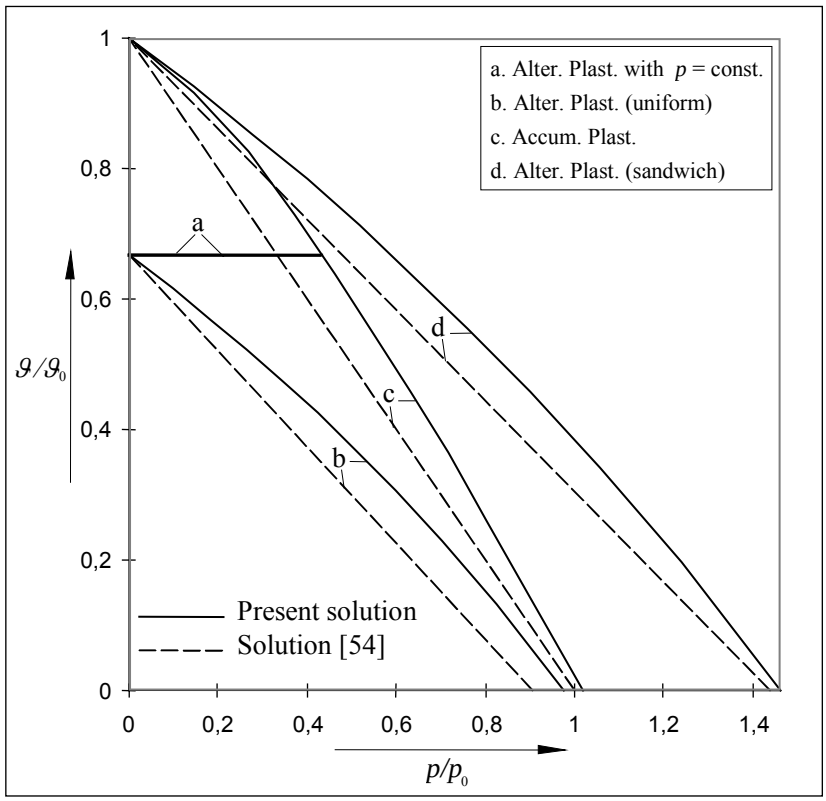

Figure 2.10. Loading domains of circular plate without damage.

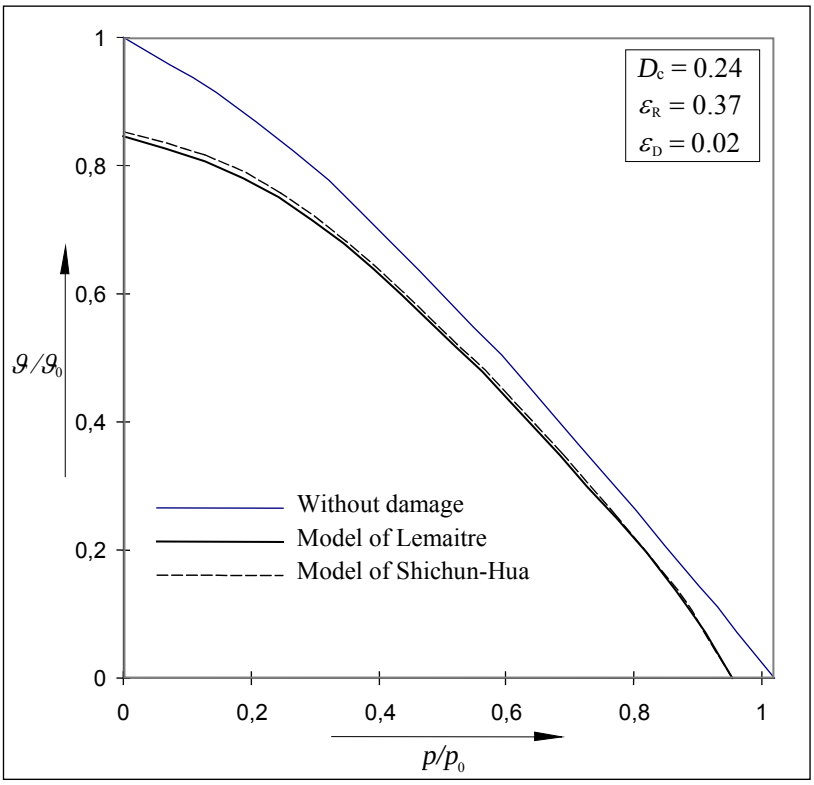

Figure 2.11. Influence of ductile damage.

The obtained shakedown domain is shown in Figure 2.10, where the results given by Gokhfeld and Cherniavsky [54] are represented. Curves (b) and (d) correspond to the failure due to alternating plasticity for uniform and sandwich plate, respectively, and curves (c) correspond to failure due to accumulated plastic deformation for uniform cross-section. When the loading program is defined by a variable thermal load at constant pressure, alternating plasticity (curves a) is relevant. In this case the drop in load-carrying capacity resulting from thermal loads is of the order of 33 per cent.
The shakedown domain in the case of combined plasticity and damage is shown in Figure 2.11 for uniform cross-section. The results show a considerable reduction of shakedown loads due to ductile damage compared to the undamaged behaviour, particularly when the thermal variable load is dominant.

5.3. Cylindrical shell under internal pressure and variable temperature

A cylindrical shell is subjected to internal pressure and a linear temperature distribution across the thickness (Figure 2.12). Temperature ϑ varies between ϑ_i and ϑ_a, where ϑ_a is the temperature on the outer wall of the shell and is assumed to be 0°C. For this case, the following loading conditions are investigated:

- the internal pressure p is constant whereas the temperature $\vartheta_i = \mu\ \vartheta_0$ is variable ($0 \le \mu \le \mu^+$);
- both internal pressure $p = \mu_1\ p_0$ and temperature $\vartheta_i = \mu_2\ \vartheta_0$ vary independently within the bounds $0 \le \mu_1 \le \mu_1^+$ and $0 \le \mu_2 \le \mu_2^+$.

The following types of material behaviour are considered:

- elastic perfectly-plastic material behaviour (Figure 2.13). The yield stress σ_Y is a function of the actual temperature with $\sigma_Y = \sigma_{Y_0}(1 + A\vartheta + B\vartheta^2)$, where σ_{Y_0}, A and B are given material parameters;
- linear kinematical hardening material behaviour, the ratio of the tensile strength σ_U to the yield stress σ_Y is equal to 1.2 (Figure 2.14). The tensile strength σ_U and the yield stress σ_Y are temperature-dependent.

The following values for geometry, material properties and loads have been adopted in the numerical analysis:

$$h/R = 1/10;\ L/R = 1/2;\ E = 1.6\times10^{5}\ \text{MPa};\ \nu = 0.3;\ \sigma_{Y_0} = 205\ \text{MPa};$$
$$\alpha_\vartheta = 0.2\times10^{-4}\ \text{K}^{-1};\ A = -1.83\times10^{-3}\ \text{K}^{-1};\ B = 1.83\times10^{-6}\ \text{K}^{-2};$$
$$p_0 = \sigma_{Y_0} h/R;\ \vartheta_0 = 2(1-\nu)\sigma_{Y_0}/(E\alpha_\vartheta).$$

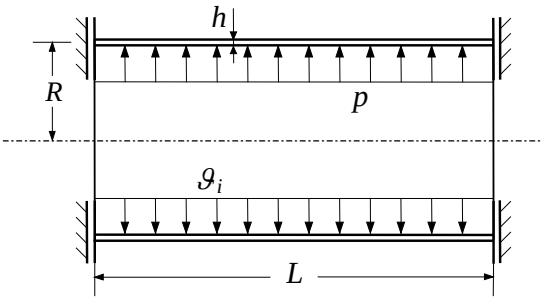

Figure 2.12. Cylindrical shell under internal pressure and variable temperature.

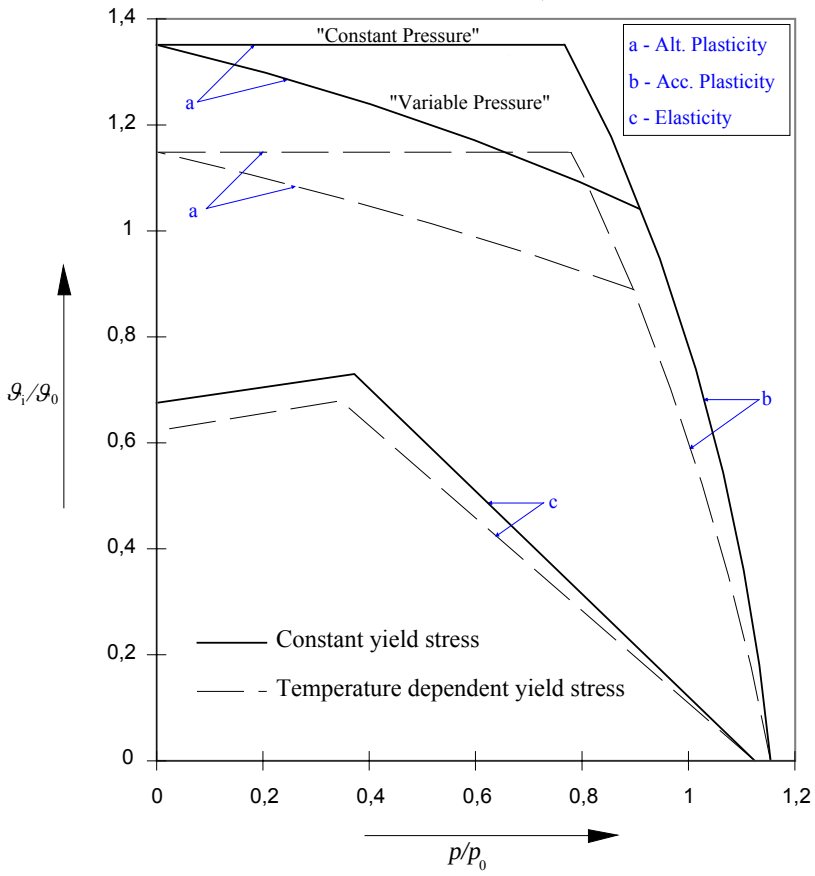

Figure 2.13. Loading domains.

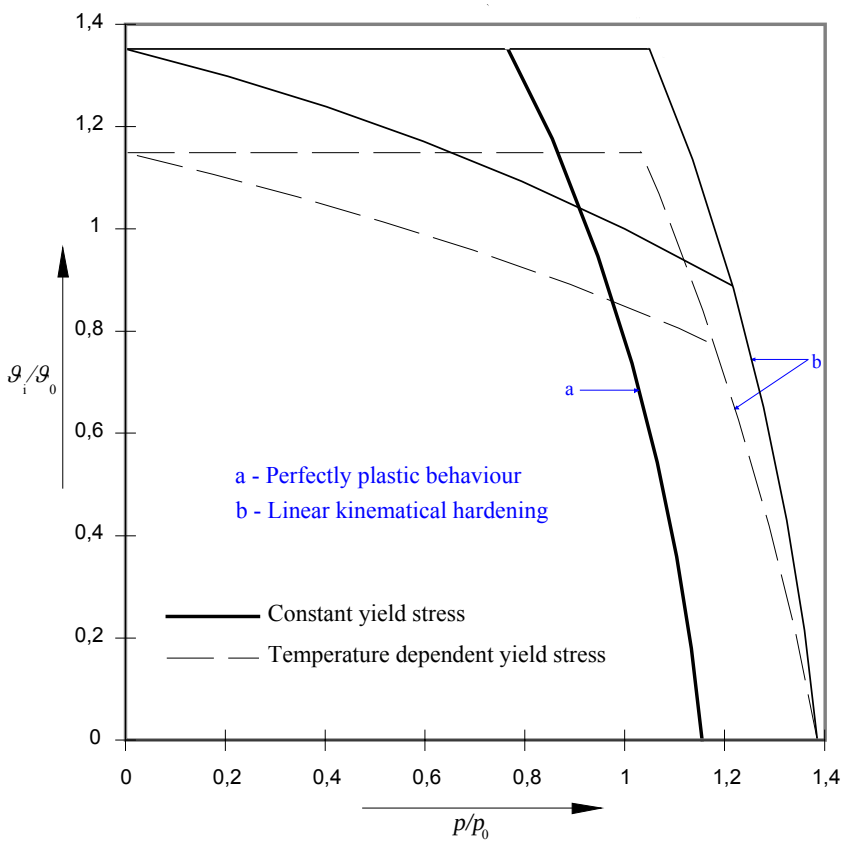

Figure 2.14. Influence of kinematical hardening.

5.4. Geometrical effect

5.4.1. Cylindrical shell under internal pressure

To take into account the influence of large displacements, we consider a short clamped cylindrical shell studied by Gross-Weege [56, 57] with sandwich cross-section, length L, radius R and wall-thickness h (Figure 2.15), where $L/R = 1/10$ and $h/R = 1/200$. The shell is subjected to internal pressure p,

$$p = p^{R} + p^{r}$$

where p^{R} is a time-independent reference pressure and $p^{R} = \mu(t)\, p^{R}$ is a time-dependent additional pressure, where μ(t) varies between fixed bounds μ^{-} and μ^{+}, so that $\mu^{-} \le \mu \le \mu^{+}$. This is a typical problem in process engineering, when fluctuations of pressure in the neighborhood of the nominal pressure in pipelines and other pressure vessels may occur. To determine the state of stresses $\mathbf{S}^{R}$, displacement $\mathbf{u}^{R}$ and damage parameter D^{R} in the reference configuration C_R under the time-independent reference pressure p^{R}, a modified

version of the NONSAP step-by-step finite element program [8] of Kreja et al. [99] to take into account ductile damage model of Lemaitre [104] has been used.

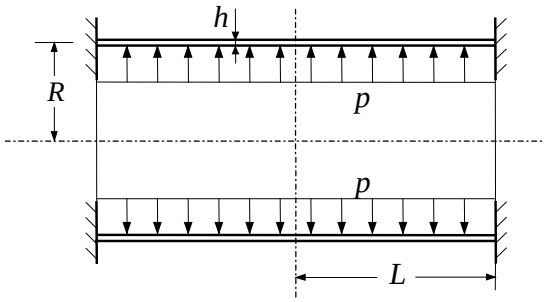

Figure 2.15. Cylindrical shell under internal pressure.

For this example, the following values for material and damage properties are adopted:

$$E = 2.1\times10^5 \text{ MPa};\ \nu = 0.3;\ D_c = 0.42,\ \varepsilon_R = 0.25 \text{ and } \varepsilon_D = 0.0.$$

The shakedown load domains for different values of the uniaxial yield stress are shown in Figure 2.16. For the sake of comparison, the results of undamaged shell are represented as well as geometrical linear solution using the von Mises sandwich yield condition.

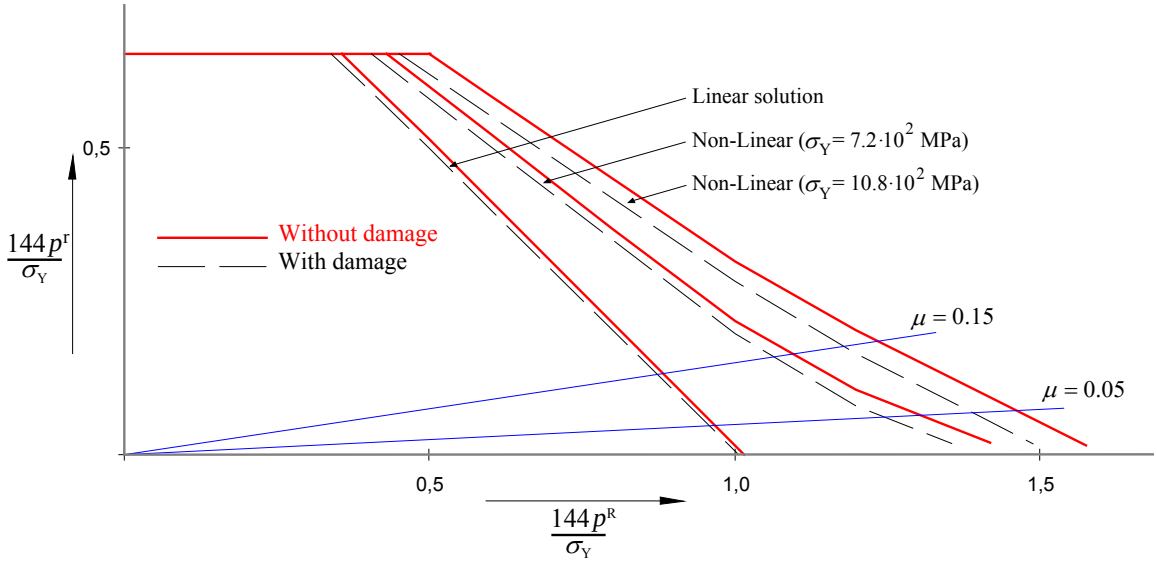

Figure 2.16. Shakedown load domain for cylindrical shell under internal pressure.

5.4.2. Cylindrical shell under internal pressure and a bending moment

The cylindrical shell described above with the following dimensions L/R = 1/10 and h/R = 1/100 is loaded as shown in Figure 2.17 by two independent loads, the internal pressure $p = \mu_1 p_0$ and a bending moment $M = \mu_2 M_0$ ($0 \le \mu_1 \le \mu_1^+$; $0 \le \mu_2 \le \mu_2^+$). The following values of material properties $E = 1.6\times10^5$ MPa, $\nu = 0.3$, $\sigma_Y = 360$ MPa, $D_c = 0.42$, $\varepsilon_R = 0.29$, $\varepsilon_D = 0.0$.

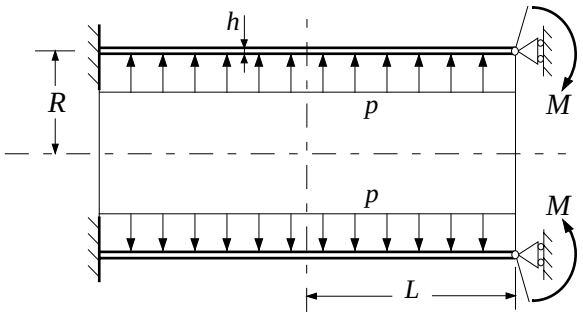

Figure 2.17. Cylindrical shell under internal pressure and bending moment.

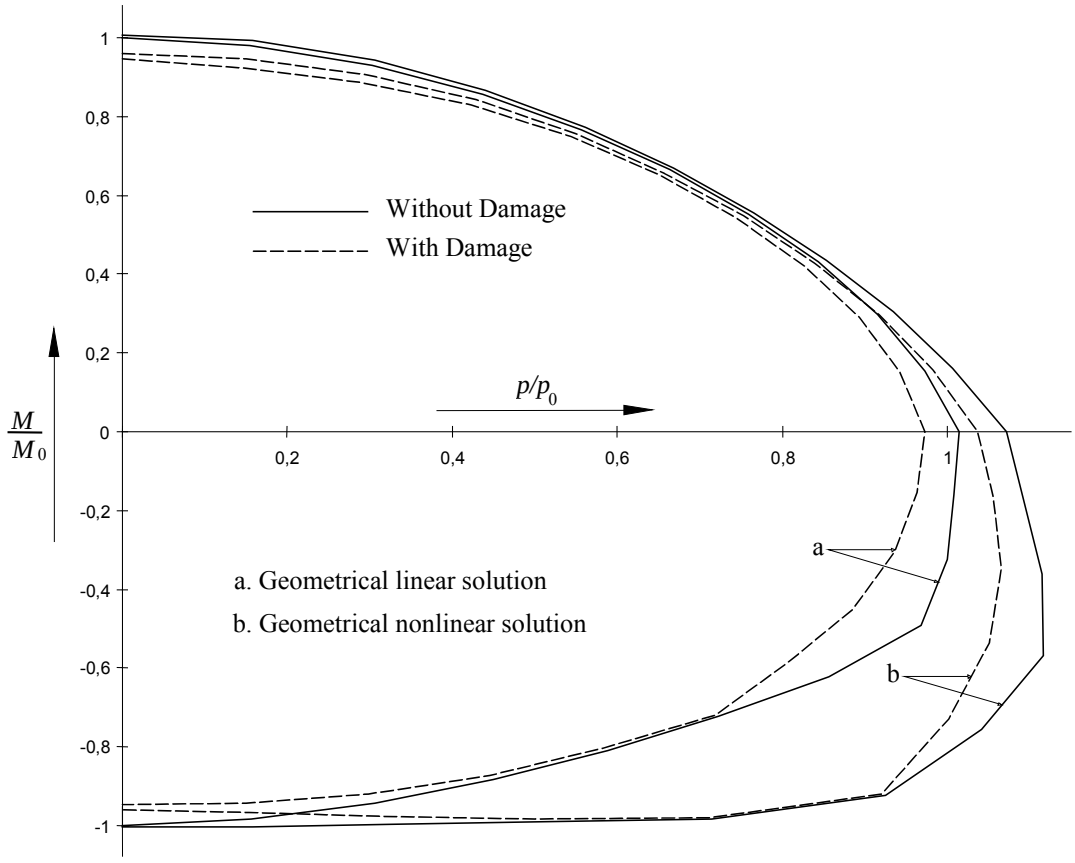

Figure 2.18. Shakedown load domain for cylindrical shell under internal pressure and bending moment.

For this example, the Ilyuschin yield condition [80] is used. The obtained shakedown domain is shown in Figure 2.18, where also the results of undamaged behaviour are presented. Curves (a) and (b) correspond to the shakedown limit load due to incremental collapse for uniform cross-sections. We observe in the major part of the loading space a significant difference between geometrical linear, curves (a), and geometrical nonlinear, curves (b), analysis and between damaged and undamaged behaviour.

5.4.3. Conical shell under internal pressure and an axial ring load

A simply supported conical shell with smaller radius R_i, external radius R_e, wall-thickness h and angle φ is considered (Figure 2.19). This kind of mechanical structures is found in valve systems. The shell is submitted to an axial ring load at the large radius edge and internal pressure. Both internal pressure and axial ring load can vary independently within the bounds $Q = \mu_1 Q_0$ and $p = \mu_2 p_0$ ($0 \le \mu_1 \le \mu_1^+$; $0 \le \mu_2 \le \mu_2^+$). The following magnitudes of geometric dimensions were adopted in the numerical analysis: $R_i/R_e = 3/4$, $h/R = 1/200$ and $\varphi = 60°$ with the same mechanical properties then the example 5.4.2. The following initial values of loads are considered: $Q_0 = 1.2\times10^3$ N/mm and $p_0 = 1.6$ MPa.

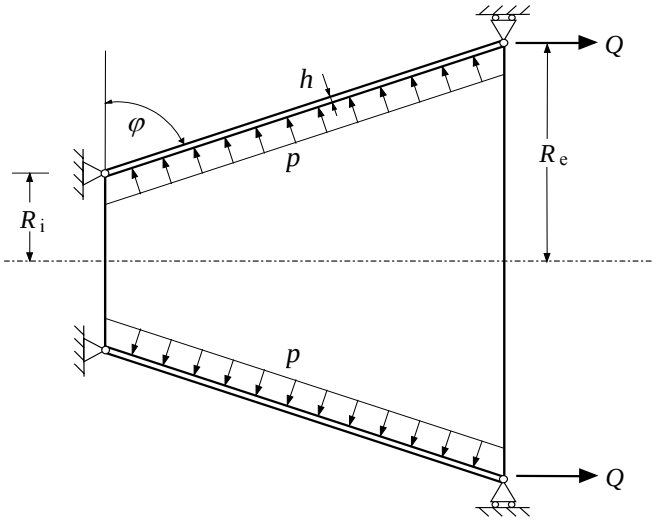

Figure 2.19. Conical shell under internal pressure and axial ring load.

It can be seen in Figure 2.20, that the shakedown domain does not increase significantly due to the consideration of geometric effects and damage has not great influence when the axial force Q acts in the same axial direction as pressure p. However, the effects are more important when these loads acts in the opposite direction.

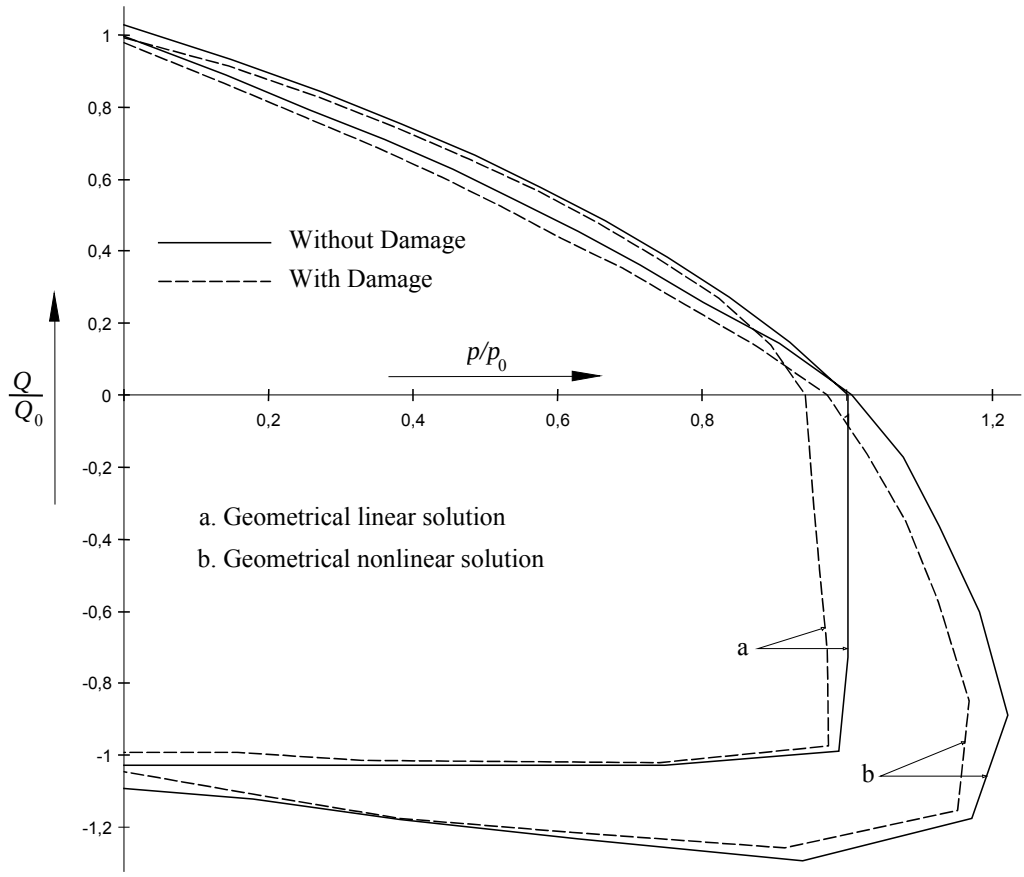

Figure 2.18. Shakedown load domain for conical shell under internal pressure and axial ring load.

6. Conclusions

The presented extension of lower bound direct method accounting for geometrical non-linearities and plastic ductile damage and its numerical applications is meant to contribute to the improvement of direct methods for the assessment of structures under variable loads beyond the elastic limit. Although the methodology of the extension of the theorem is quite general, the class of materials considered in this chapter as in the chapter 1 is rather restricted: in particular, anisotropic damage evolution and more general models of interaction between plasticity and damage seem to be important issues for further research. The methodology developed in the first chapter for geometrical linear theory has been validated and applied to plates and thin-walled shells under mechanical and thermal variable loads. The obtained results show in general a reduction of shakedown loads due to

ductile damage compared to the undamaged behaviour. In the applications to thin-walled shells subjected to finite displacements and moderate rotations only special loading cases were considered, where external loads may vary randomly within a given range in the neighbourhood of a prescribed service-load. More general loading should be considered in the future. It appears that the consideration of geometrical non-linearities can have a stabilizing or destabilizing effect. The combination of an incremental analysis with the shakedown analysis seems to be promising; so one observes in the first of the presented examples that for certain loading cases, the deformations exceed the limit of moderate rotations so that the validity of the Donnel-Mushtari-Vlasov theory becomes questionable.

Altogether, the presented results indicate that this method is well adopted for the numerical determination of the safety factor with respect to non-shakedown and inadmissible damage. Nevertheless, quite a number of open questions remains to be answered. Among them, a sound experimental validation of the proposed method is of major importance. Unfortunately, we observed a considerable lack of adapted and reliable experimental data in literature. Therefore, in the next future, special research effort should be put on experimental shakedown analysis in conjunction with theoretical and numerical modelling.

Chapitre 3

Adaptation des composites avec des microstructures périodiques

Shakedown of composites with periodic microstructures

Collaborations liées à ce chapitre:

- Prof. O. Débordes ; Dr. S. Bourgeois ; Dr. H. Magoariec, EGIM & LMA
- Dr. F. Schwabe ; M. N. Pellegrini, RWTH Aachen

Table of contents

1. Introduction

Local failure under variable loading can be considered as being caused by repeated, dissipative events occurring on the micro-structural level of materials. In this chapter, the scale chosen for observation of these effects will be called “micro-scale”, small compared to the scale for measuring the macroscopic dimensions of a mechanical structural element and large compared to the atomistic scale. We suppose that on this microscopic level the laws and methods of classical continuum-mechanics are applicable, but that the different components of the material can be recognised, forming a mechanical structure by itself on this level of observation. The interaction between these components determines the local response of the material, in particular the mechanisms leading to local damage and overall failure. Therefore, the study of these mechanisms on the micro-level of specific materials under complex loads can be helpful to better understand the causes of failure and methods developed for this purpose can be used in a constructive manner for the design of materials.

A particularly interesting class of materials for this kind of studies are composite materials. Their heterogeneity causes in general large gradients of the mechanical field quantities, initiating local damage and overall failure by the interaction of different local effects, which depend upon the mechanical and geometrical properties of the individual components of the composite. For certain types of composites realistic modelling should take into account not only inelastic behaviour of the matrix material but also debonding of the interfaces between matrix and reinforcements. Special attention has to be paid to the realistic reproduction of the mechanical behaviour of interfaces between matrix and reinforcements, observed in experiments [19]. It is important not only to understand and to model the mechanical effects for this type of materials on the micro-structural level but to link them to the characteristic macroscopic material properties. Here, averaging techniques such as the homogenisation technique [164] are proposed to bridge the gap between local (microscopic) and global (macroscopic) properties.

It is shown in this chapter, how direct methods, namely limit and shakedown analysis, can help to assess composites which exhibit plastic deformations on the micro-scale and how this theory can be used in a constructive manner for the design of materials. In this contribution, the debonding process is modelled within the framework of interface damage mechanics, where the displacement discontinuities created by the progressive decohesion are related to constitutive equations extended by an anisotropic damage model [37].

2. Composites with periodic microstructures

The theoretical discussion of the effective properties of composites with periodic microstructures is similar to the more general discussion of the effective properties of random media, except that the information on the microstructure is complete in the periodic case, whereas it is only partial in the random case.

The question of the effective properties of a composite implicitely assumes that the problem contains two scales which can be separated. The microscopic scale (local scale) is small enough for the heterogeneities to be separately identified. The macroscopic scale (overall scale) is large enough, compared to the microscopic scale, for the heterogeneities to be smeared-out. The effective properties at the microscopic scale of the composite are determined from geometrical and material data available from the study of a representative volume element. For periodic composites, these data are completely specified from geometrical and material properties of a unit cell which generates by periodic repetition the whole microstructure of the composite. The macroscopic behaviour of this heterogeneous material is observed on the scale **x** and the microscopic behaviour on the scale **y** (see e.g. Figure 3.1).

A periodic medium is defined by a unit cell and 3 vectors (in dimension 3) of translation invariance. The unit cell is not uniquely defined. However, the effective behaviour of the composite computed from different unit cells generating the same microstructure should coincide (since the physical effective properties of the composite are well defined independently of the choice of the unit cell). The choice of the unit cell is often motivated by the differences in geometrical symmetries which can be used to simplify the numerical solution of the local problem.

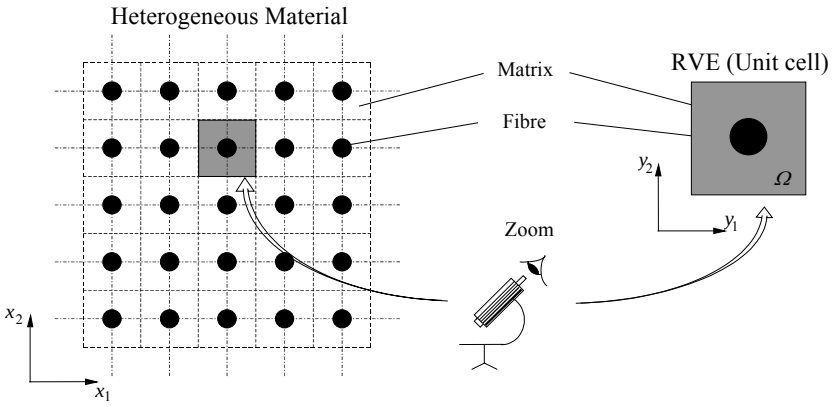

Figure 3.1. Heterogeneous media with unit cell.

2.1. Periodic fields

Consider a large sample of a periodic composite containing a large number of cells. Assume first this sample has been homogeneised and behaves as a homogeneised body. Then, imposing an affine displacement on the boundary of the sample will result in a homogeneous strain **E** through the body. This homogeneous strain generates a homogeneous stress **Σ** and the homogenised constitutive relations express the relation between **σ** and **ε**. Then, sufficiently far away from the boundary of the sample, the local stress and strain fields **σ** and **ε** conform themselves to the periodic arrangement of the cells. These fields are periodic at the microscopic scale and can be determined on a single unit cell Ω.

2.1.1. Periodic stress fields

The local stress field **σ**, in addition to being periodic, is in equilibrium throughout the entire periodic medium. Therefore, **σ** satisfies the equilibrium conditions inside Ω and on the boundary of Ω, expressing that the boundaries between neighbouring unit cells are equilibrated. It follows that **σ** is a divergence-free field in Ω and that the tractions on opposite sides of $\partial\Omega$ are opposite. The equilibrium conditions for the local stress read as

$$\text{Div}\,\boldsymbol{\sigma} = 0 \quad \text{in } \Omega, \quad \boldsymbol{\sigma}.\mathbf{n} \quad \text{anti-periodic on } \partial\Omega. \tag{3.1}$$

The overall stress tensor is defined as the average of the microscopic stress tensor

$$\langle \boldsymbol{\sigma} \rangle = \frac{1}{|\Omega|} \int_{\Omega} \boldsymbol{\sigma}(\mathbf{u}) \, \mathrm{d}\Omega = \boldsymbol{\Sigma}. \tag{3.2}$$

2.1.2. Periodic strain fields

Let $\mathbf{y}$ denote the position of a point in the unit cell. The local strain field $\boldsymbol{\varepsilon}(\mathbf{u}(\mathbf{y}))$ can be split into the overall strain $\mathbf{E}(\mathbf{x})$ which would be the actual strain field in the unit cell if it were homogeneous, and a correction $\boldsymbol{\varepsilon}(\mathbf{u}^{\mathrm{per}})$ which accounts for the presence of heterogeneities. This correction derives from a displacement field $\mathbf{u}^{\mathrm{per}}$. $\mathbf{E}$ gives the deformation of the lattice and $\boldsymbol{\varepsilon}(\mathbf{u}^{\mathrm{per}})$ is therefore a fluctuation about this mean deformation. Its average consequently vanishes. It can then be proved that $\mathbf{u}^{\mathrm{per}}$ is a periodic field, up to a rigid body motion which can be disregarded, since the only quantity of interest here is strain. The displacement and strain fields in the unit cell Ω, therefore admit the following decomposition

$$\mathbf{u}(\mathbf{y}) = \mathbf{E}.\mathbf{y} + \mathbf{u}^{\mathrm{per}}(\mathbf{y}) \tag{3.3}$$

and

$$\boldsymbol{\varepsilon}(\mathbf{u}(\mathbf{y})) = \mathbf{E}(\mathbf{x}) + \boldsymbol{\varepsilon}(\mathbf{u}^{\mathrm{per}}(\mathbf{y})). \tag{3.4}$$

By periodicity of $\mathbf{u}^{\mathrm{per}}$ it is understood that all components of $\mathbf{u}^{\mathrm{per}}$ take identical values on points of the boundary $\partial\Omega$ of the unit cell which are deduced by translation parallel to the directions of invariance of the lattice. Note that the periodicity of $\mathbf{u}^{\mathrm{per}}$ implies that the average of $\boldsymbol{\varepsilon}(\mathbf{u}^{\mathrm{per}})$ on the unit cell vanishes and therefore that the average of $\boldsymbol{\varepsilon}$ is $\mathbf{E}$

$$\langle \boldsymbol{\varepsilon}(\mathbf{u}^{\mathrm{per}}) \rangle = \frac{1}{|\Omega|} \int_{\Omega} \boldsymbol{\varepsilon}(\mathbf{u}^{\mathrm{per}}) \, \mathrm{d}\Omega = 0 \tag{3.5}$$

and

$$\langle \boldsymbol{\varepsilon}(\mathbf{u}) \rangle = \frac{1}{|\Omega|} \int_{\Omega} \boldsymbol{\varepsilon}(\mathbf{u}) \, \mathrm{d}\Omega = \mathbf{E}. \tag{3.6}$$

By assuming that $\boldsymbol{\sigma}$ and $\mathbf{u}$ are in the form of (3.1) and (3.3), respectively, then, Hill's relationship holds [74]

$$\boldsymbol{\Sigma}:\mathbf{E} = \langle \boldsymbol{\sigma}:\boldsymbol{\varepsilon} \rangle = \frac{1}{|\Omega|} \int_{\Omega} \boldsymbol{\sigma}:\boldsymbol{\varepsilon} \, \mathrm{d}\Omega \tag{3.7}$$

where

$$\mathbf{\Sigma}(\mathbf{x}) = <\boldsymbol{\sigma}(\mathbf{y})> = \frac{1}{|\Omega|}\int_{\Omega} \boldsymbol{\sigma}(\mathbf{y})\, d\Omega \tag{3.8}$$

and

$$\mathbf{E}(\mathbf{x}) = <\boldsymbol{\varepsilon}(\mathbf{y})> = \frac{1}{|\Omega|}\int_{\Omega} (\mathbf{u} \otimes_s \mathbf{n})\, dS \tag{3.9}$$

which means that the average of the microscopic (virtual) internal work is equals the macroscopic (virtual) work of internal forces.

2.2. Decohesive effect

We consider in particular the problem of materials reinforced by straight fibres. In the case of transverse loading, this justifies the hypothesis of plane state of strains. Thus, the problem is reduced to a two-dimensional case with periodicity in the fibre section plane. A significant characteristic of fibre-reinforced composites is the limited strength of the interface between fibres and matrix. The micromechanical representative element of total surface Ω presented herein includes the fibre phase, the matrix phase occupying the domains Ω_+ and Ω_-, respectively and the cohesive zone represented by the band-shaped domain Ω_δ of width $\delta << 1$ ($\Omega = \Omega_- \cup \Omega_+ \cup \Omega_\delta$) as illustrated in Figure 3.2, defined by

$$\Omega_\delta = \left\{ \mathbf{y} = \mathbf{y}_0 + \epsilon \mathbf{n} \;\middle|\; \forall \mathbf{y}_0 \in \Gamma, -\frac{\delta}{2} \le \epsilon \le \frac{\delta}{2} \right\}. \tag{3.10}$$

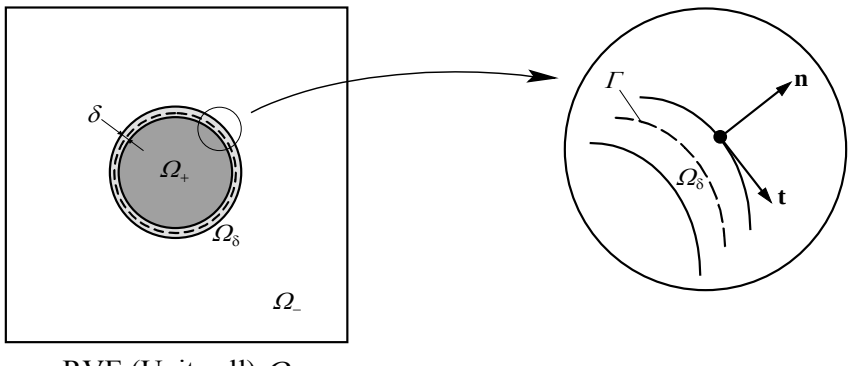

RVE (Unit cell) Ω

Figure 3.2. Discontinuity interface Γ.

The strain field corresponding to the displacement field is derived as

$$\boldsymbol{\varepsilon} = \nabla_s \underline{\mathbf{u}} + (\llbracket \mathbf{u} \rrbracket \otimes_s \mathbf{n}\delta_R), \quad \forall \mathbf{y} \in \Omega, \tag{3.11}$$

where $\underline{\mathbf{u}}$ is the continuous displacement field and $\llbracket \mathbf{u} \rrbracket$ is the displacement jump vector, i.e. $\llbracket \mathbf{u} \rrbracket = \mathbf{u}^+ - \mathbf{u}^-$. Here, $\mathbf{u}^+$ and $\mathbf{u}^-$ are the displacement vectors at the interior and the exterior borders of the interface zone. $\mathbf{n}$ is the unit vector and δ_R is the Dirac-delta function defined by

$$\delta_R = \begin{cases} 0 & \text{if } \mathbf{y} \in \Omega_- \\ \dfrac{1}{\delta} & \text{if } \mathbf{y} \in \Omega_\delta \\ 0 & \text{if } \mathbf{y} \in \Omega_+. \end{cases} \tag{3.12}$$

According to the restriction to geometrically linear theory, total strains $\boldsymbol{\varepsilon}(\mathbf{y})$ can be split into purely elastic $\boldsymbol{\varepsilon}^e$ and purely inelastic $\boldsymbol{\varepsilon}^{in}$ parts, respectively

$$\boldsymbol{\varepsilon}(\mathbf{y}) = \boldsymbol{\varepsilon}^e(\mathbf{y}) + \boldsymbol{\varepsilon}^{in}(\mathbf{y}), \quad \forall \mathbf{y} \in \Omega. \tag{3.13}$$

Consequently, the total strain field $\boldsymbol{\varepsilon}$ can be decomposed independently into a continuous strain field $\underline{\boldsymbol{\varepsilon}}$ and a regularised strain field $\boldsymbol{\varepsilon}_\delta$ within the interface in the following way

$$\boldsymbol{\varepsilon}(\mathbf{y}) = \underline{\boldsymbol{\varepsilon}}(\mathbf{y}) + \boldsymbol{\varepsilon}_\delta(\mathbf{y}), \quad \forall \mathbf{y} \in \Omega \tag{3.14}$$

with

$$\underline{\boldsymbol{\varepsilon}}(\mathbf{y}) = \underline{\boldsymbol{\varepsilon}}^e(\mathbf{y}) + \underline{\boldsymbol{\varepsilon}}^{in}(\mathbf{y}), \quad \forall \mathbf{y} \in \Omega_- \cup \Omega_+ \tag{3.15}$$

$$\boldsymbol{\varepsilon}_\delta(\mathbf{y}) = \boldsymbol{\varepsilon}_\delta^e(\mathbf{y}) + \boldsymbol{\varepsilon}_\delta^{in}(\mathbf{y}), \quad \forall \mathbf{y} \in \Omega_\delta. \tag{3.16}$$

For the plastic part of the matrix and/or fibre behaviour, we assume the validity of the normality rule for plastic flow in sub-differential form, such that

$$\dot{\underline{\boldsymbol{\varepsilon}}}^{in} \in \delta\varphi(\boldsymbol{\sigma}) \tag{3.17}$$

where $\delta\varphi(\boldsymbol{\sigma})$ denotes the sub-gradient of the plastic potential $\varphi(\boldsymbol{\sigma})$ which is the indicator

function of a convex domain F(**y**) of all plastically admissible stress states. Here and in the sequel, superposed dots denote the rate of the considered quantity. Then we have

$$\boldsymbol{\sigma}(\mathbf{y}) \in \mathrm{F}(\mathbf{y}), \quad \forall \mathbf{y} \in \Omega_- \cup \Omega_+ \tag{3.18}$$

where F(**y**) is defined by means of a yield function $f(\boldsymbol{\sigma}, \mathbf{y})$

$$\mathrm{F}(\mathbf{y}) = \{\boldsymbol{\sigma} \mid f(\boldsymbol{\sigma}, \mathbf{y}) \le 0, \ \forall \mathbf{y} \in \Omega_- \cup \Omega_+\}. \tag{3.19}$$

The convexity of $f(\boldsymbol{\sigma}, \mathbf{y})$ and the validity of the normality rule can be expressed by the maximum plastic work inequality

$$(\boldsymbol{\sigma} - \boldsymbol{\sigma}^{(s)}) : \underline{\dot{\boldsymbol{\varepsilon}}}^{in} > 0, \quad \forall \ \boldsymbol{\sigma}^{(s)}(\mathbf{y}) \in \overline{\mathrm{F}}(\mathbf{y}) \tag{3.20}$$

where $\boldsymbol{\sigma}^{(s)}$ is any safe state of stresses defined by

$$\overline{\mathrm{F}}(\mathbf{y}) = \{\boldsymbol{\sigma}^{(s)} \mid f(\boldsymbol{\sigma}^{(s)}, \mathbf{y}) < 0, \ \forall \mathbf{y} \in \Omega_- \cup \Omega_+\}. \tag{3.21}$$

2.3. Interfacial constitutive equations

The mechanical response of the interface is described by the relation between the normal and tangential relative displacements $[\![u_n]\!]$ and $[\![u_t]\!]$ and their respective normal and tangential tractions τ_n and τ_t. The relative displacement across the interface $[\![\mathbf{u}]\!]$ is decomposed into an elastic part $[\![\mathbf{u}^e]\!]$ and an inelastic part $[\![\mathbf{u}^{in}]\!]$

$$[\![\mathbf{u}]\!] = [\![\mathbf{u}^e]\!] + [\![\mathbf{u}^{in}]\!]. \tag{3.22}$$

At each point of the interface, we define [81, 106]

$$u_n = \mathbf{n}.[\![\mathbf{u}]\!], \ u_t = \mathbf{t}.[\![\mathbf{u}]\!] \tag{3.23}$$

and

$$\tau_n = \mathbf{n}.\boldsymbol{\tau}, \ \tau_t = \mathbf{t}.\boldsymbol{\tau} \tag{3.24}$$

where **n** and **t** form a right-hand coordinate system. The initiation and propagation of debonding between fibre and matrix is simulated by using a strain-based anisotropic damage model in the sense of Ju [82]. To this end, we separately introduce a normal damage variable d_n and a tangential damage variable d_t.

To describe the interface constitutive equations, we introduce a thermodynamical potential

$$\Psi = \frac{1}{2} [\![\mathbf{u}^e]\!]^T \cdot \tilde{\mathbf{Q}}_\delta \cdot [\![\mathbf{u}^e]\!] \tag{3.25}$$

with

$$[\![\mathbf{u}^e]\!] = [\![u_n^e]\!]\, \mathbf{n} + [\![u_t^e]\!]\, \mathbf{t} \tag{3.26}$$

and

$$\tilde{\mathbf{Q}}_\delta = (\mathbf{I} - \mathbf{d})\mathbf{Q}_\delta = (1 - d_n) Q_{\delta_n}\, \mathbf{n} \otimes_s \mathbf{n} + (1 - d_t) Q_{\delta_t}\, \mathbf{t} \otimes_s \mathbf{t} \tag{3.27}$$

where $\mathbf{Q}_\delta$ represents the interface stiffness, i.e. $\mathbf{Q}_\delta = \mathbf{n}\cdot\mathbf{L}\cdot\mathbf{n}/\delta$. Here, **L** denotes the fourth order elasticity tensor. This leads to define respectively, the traction forces as functions of elastic displacement discontinuities and damage variables, and the thermodynamic forces associated with damage variables (see. eg. [37])

$$\boldsymbol{\tau} = \frac{\partial \Psi}{\partial [\![\mathbf{u}^e]\!]} = \tilde{\mathbf{Q}}_\delta \cdot [\![\mathbf{u}^e]\!] \quad \text{and} \quad \mathbf{Y} = -\frac{\partial \Psi}{\partial \mathbf{d}} = \frac{1}{2} [\![\mathbf{u}^e]\!]^T \cdot \mathbf{Q}_\delta \cdot [\![\mathbf{u}^e]\!]. \tag{3.28}$$

In the sequel superposed tilda indicates quantities related to the damaged state of the cohesive zone. It is assumed that both debonding and damage process are irreversible with no cross-healing effect. Then, in the form of the Clausius-Duhem inequality, we assume the 2nd principle of thermodynamics to be satisfied by the two independent inequalities

$$\boldsymbol{\tau} . [\![\dot{\mathbf{u}}^{in}]\!] \geq 0 \tag{3.29}$$

and

$$\mathbf{Y} . \dot{\mathbf{d}} \geq 0 \tag{3.30}$$

or, in index notation

$$\tau_n [\![\dot{u}_n^{in}]\!] + \tau_t [\![\dot{u}_t^{in}]\!] \geq 0 \tag{3.31}$$

and

$$\frac{1}{2} Q_{\delta_n} [\![u_n^e]\!]^2 \dot{d}_n + \frac{1}{2} Q_{\delta_t} [\![u_t^e]\!]^2 \dot{d}_t \geq 0. \tag{3.32}$$

The inelastic parts of the relative displacements are expressed by the normality rule

$$[\![\dot{u}_n^{in}]\!] = \dot{\lambda} \frac{\partial g}{\partial \tau_n}, \quad [\![\dot{u}_t^{in}]\!] = \dot{\lambda} \frac{\partial g}{\partial \tau_t} \tag{3.33}$$

where $\dot{\lambda}$ is the plastic multiplier and g the inelastic gap potential defined by

$$g(\boldsymbol{\tau}, \mathbf{d}, \mathbf{y}) = \left[\left(\frac{\tau_n}{1-d_n} \right)^2 + \frac{1}{\beta^2} \left(\frac{\tau_t}{1-d_t} \right)^2 \right]^{1/2} - \sigma_{max} \leq 0, \quad \forall \mathbf{y} \in \Omega_\delta \tag{3.34}$$

which is a positive convex and differentiable function. This implies that the maximum plastic work inequality is valid, i.e.

$$(\boldsymbol{\tau} - \boldsymbol{\tau}^{(s)}) . [\![\dot{\mathbf{u}}^{in}]\!] > 0, \quad \forall \boldsymbol{\tau}^{(s)}(\mathbf{y}) \in \bar{G}(\mathbf{y}) \tag{3.35}$$

where

$$\bar{G}(\mathbf{y}) = \left\{ \boldsymbol{\tau}^{(s)} \,|\, g(\boldsymbol{\tau}^{(s)}, \mathbf{d}, \mathbf{y}) < 0, \quad \forall \mathbf{y} \in \Omega_\delta \right\}. \tag{3.36}$$

Here, σ_{max} is a measure of bond strength of the cohesive zone and β is the interface shear-to-normal strength ratio. As example for a simple explicite form of eqn. (3.34), we mention the equations for the damage variables proposed by Bazant and Prat [9]

$$d_n = 1 - \exp\left[- \left(\frac{\kappa_n}{a_n} \right)^n \right], \quad d_t = 1 - \exp\left[- \left(\frac{\kappa_t}{a_t} \right)^t \right] \tag{3.37}$$

where the constants (n, a_n) and (t, a_t) are material parameters to be determined from experiment. The history parameters κ_n and κ_t are the damage thresholds at the current time t, they memorise the maximum values attained by $[\![u_n]\!]$ and $[\![u_t]\!]$ in the following way

$$\kappa_n = \max \left[\kappa_{n_0}, \max_{t \in [0, T]} [\![u_n]\!] \right], \quad \kappa_t = \max \left[\kappa_{t_0}, \max_{t \in [0, T]} [\![u_t]\!] \right] \tag{3.38}$$

where κ_{n_0} and κ_{t_0} are the initial damage thresholds before any loading is applied.

3. Formulation of shakedown problem

3.1. Statement

Adopting these definitions and hypotheses, the statical shakedown theorem can be stated as follows:

If there exist a real number $\alpha > 1$, a time-independent field of periodic residual stresses $\mathring{\boldsymbol{\sigma}}^{(r)}$, a time-independent vector of traction forces $\mathring{\boldsymbol{\tau}}^{(r)}$ at the interface and an admissible domain P of macroscopic states of stress $\boldsymbol{\Sigma}$:

$$P = \left\{ \boldsymbol{\Sigma} \,\middle|\, \exists \boldsymbol{\sigma}^{(s)}, \exists \boldsymbol{\tau}^{(s)} \,;\; \boldsymbol{\sigma}^{(s)}(\mathbf{y}) \in \overline{F}(\mathbf{y}),\; \boldsymbol{\tau}^{(s)}(\mathbf{y}) \in \overline{G}(\mathbf{y}) \right\} \tag{3.39}$$

then the composite material shakes down to the given domain of loading. Safe states of stresses $\boldsymbol{\sigma}^{(s)}$ and traction forces $\boldsymbol{\tau}^{(s)}$ are defined, resp., by

$$\boldsymbol{\sigma}^{(s)} = \alpha\, \boldsymbol{\sigma}^{(c)} + \mathring{\boldsymbol{\sigma}}^{(r))} \tag{3.40}$$

and

$$\boldsymbol{\tau}^{(s)} = \alpha\, \boldsymbol{\tau}^{(c)} + \mathring{\boldsymbol{\tau}}^{(r)} \tag{3.41}$$

such that

$$\overline{F}(\mathbf{y}) = \left\{ \boldsymbol{\sigma}^{(s)} \;\middle|\; f(\boldsymbol{\sigma}^{(s)}, \mathbf{y}) \le 0,\; \forall \mathbf{y} \in \Omega_- \cup \Omega_+ \right\} \tag{3.42}$$

and

$$\overline{G}(\mathbf{y}) = \left\{ \boldsymbol{\tau}^{(s)} \,\middle|\, g(\boldsymbol{\tau}^{(s)}, \mathbf{d}, \mathbf{y}) \le 0,\; \forall \mathbf{y} \in \Omega_\delta \right\}. \tag{3.43}$$

Here, $\boldsymbol{\sigma}^{(c)}$ and $\boldsymbol{\tau}^{(c)}$ are respectively, the stress field and the traction forces vector in a purely elastic representative volume element under the same boundary conditions as for the RVE of the original problem such that the following relations hold

$$\operatorname{Div} \boldsymbol{\sigma}^{(c)} = 0 \qquad \text{in } \Omega \tag{3.44}$$

$$[\![\boldsymbol{\sigma}^{(c)}]\!].\mathbf{n}_\Gamma = 0 \qquad \text{on } \Gamma \tag{3.45}$$

$$\mathbf{u}^{(c)} - \mathbf{E}.\mathbf{y} \quad \text{periodic} \qquad \text{on } \partial\Omega \tag{3.46}$$

$$\boldsymbol{\sigma}^{(c)}.\mathbf{n} \quad \text{anti-periodic} \qquad \text{on } \partial\Omega \tag{3.47}$$

$$\boldsymbol{\sigma}^{(c)} = \mathbf{L}:(\boldsymbol{\varepsilon}(\mathbf{u}^{per}) + \mathbf{E}) \qquad \text{in } \Omega. \tag{3.48}$$

However, the field of the residual stresses $\mathring{\boldsymbol{\sigma}}^{(r)}$ satisfies

$$\text{Div}\,\mathring{\boldsymbol{\sigma}}^{(r)} = \mathbf{0} \quad \text{in } \Omega \tag{3.49}$$

$$[\![\mathring{\boldsymbol{\sigma}}^{(r)}]\!].\mathbf{n}_{\Gamma} = 0 \quad \text{on } \Gamma \tag{3.50}$$

$$\mathring{\boldsymbol{\sigma}}^{(r)}.\mathbf{n} \quad \text{anti-periodic} \quad \text{on } \partial\Omega \tag{3.51}$$

$$<\mathring{\boldsymbol{\sigma}}^{(r)}> = 0 \quad \text{in } \Omega \tag{3.52}$$

and, additionally

$$<\boldsymbol{\sigma}^{(s)}(\mathbf{y})> = \boldsymbol{\Sigma}(\mathbf{x}), \tag{3.53}$$

where $\mathbf{n}_{\Gamma}$ is the normal unit vector at any point of Γ.

Particular case

If one considers that the boundary conditions on the edges of the representative volume element are uniform constraints $\boldsymbol{\Sigma}$ as suggested by Suquet [164] (see also [120]), then we have to consider the following conditions

$$\text{Div}\,\boldsymbol{\sigma}^{(c)} = 0 \quad \text{in } \Omega \tag{3.54}$$

$$[\![\boldsymbol{\sigma}^{(c)}]\!].\mathbf{n}_{\Gamma} = 0 \quad \text{on } \Gamma \tag{3.55}$$

$$\boldsymbol{\sigma}^{(c)}.\mathbf{n} = \boldsymbol{\Sigma}.\mathbf{n} \quad \text{on } \partial\Omega \tag{3.56}$$

and

$$\text{Div}\,\mathring{\boldsymbol{\sigma}}^{(r)} = \mathbf{0} \quad \text{in } \Omega \tag{3.57}$$

$$[\![\mathring{\boldsymbol{\sigma}}^{(r)}]\!].\mathbf{n}_{\Gamma} = 0 \quad \text{on } \Gamma \tag{3.58}$$

$$\mathring{\boldsymbol{\sigma}}^{(r)}.\mathbf{n} = 0 \quad \text{on } \partial\Omega \tag{3.59}$$

If on the contrary one assumes that the boundary conditions on the edges of the representative volume element are uniform strains $\mathbf{E}$, then the following conditions have to be considered

$$\text{Div}\,\boldsymbol{\sigma}^{(c)} = 0 \quad \text{in } \Omega \tag{3.60}$$

$$[\![\boldsymbol{\sigma}^{(c)}]\!].\mathbf{n}_{\Gamma} = 0 \quad \text{on } \Gamma \tag{3.61}$$

$$\mathbf{u}^{(c)} = \mathbf{E}.\mathbf{y} \quad \text{on } \partial\Omega \tag{3.62}$$

$$\boldsymbol{\sigma}^{(c)} = \mathbf{L}:\boldsymbol{\varepsilon}^{(c)} \quad \text{in } \Omega. \tag{3.63}$$

and

$$\text{Div}\,\mathring{\boldsymbol{\sigma}}^{(r)} = \mathbf{0} \qquad \text{in } \Omega \tag{3.64}$$

$$[\![\mathring{\boldsymbol{\sigma}}^{(r)}]\!].\mathbf{n}_{\Gamma} = 0 \qquad \text{on } \Gamma \tag{3.65}$$

$$<\mathring{\boldsymbol{\sigma}}^{(r)}> = 0 \qquad \text{in } \Omega \tag{3.66}$$

$$<\boldsymbol{\sigma}^{(s)}(\mathbf{y})> = \boldsymbol{\Sigma}(\mathbf{x}). \tag{3.67}$$

3.2. Proof

The proof of this statement is analogous to that of the classical static shakedown theorems [121]. For this, a bounded quadratic form is introduced defined by [70]

$$W = \frac{1}{2}\int_{\Omega_+\cup\Omega_-} (\boldsymbol{\sigma}^{(r)} - \mathring{\boldsymbol{\sigma}}^{(r)}):\mathbf{L}^{-1}:(\boldsymbol{\sigma}^{(r)} - \mathring{\boldsymbol{\sigma}}^{(r)})\,d\Omega + \frac{1}{2}\int_{\Omega_\delta} (\boldsymbol{\sigma}_\delta^{(r)} - \mathring{\boldsymbol{\sigma}}_\delta^{(r)}):\tilde{\mathbf{L}}^{-1}:(\boldsymbol{\sigma}_\delta^{(r)} - \mathring{\boldsymbol{\sigma}}_\delta^{(r)})\,d\Omega \tag{3.68}$$

where the time-dependent and time-independent residual stresses and traction forces are defined as follows

$$\boldsymbol{\sigma}^{(r)}(\mathbf{y}, t) = \boldsymbol{\sigma}(\mathbf{y}, t) - \boldsymbol{\sigma}^{(c)}(\mathbf{y}, t), \quad \mathring{\boldsymbol{\sigma}}^{(r)}(\mathbf{y}) = \boldsymbol{\sigma}^{(s)}(\mathbf{y}, t) - \boldsymbol{\sigma}^{(c)}(\mathbf{y}, t) \tag{3.69}$$

$$\boldsymbol{\tau}^{(r)}(\mathbf{y}, t) = \boldsymbol{\tau}(\mathbf{y}, t) - \boldsymbol{\tau}^{(c)}(\mathbf{y}, t), \quad \mathring{\boldsymbol{\tau}}^{(r)}(\mathbf{y}) = \boldsymbol{\tau}^{(s)}(\mathbf{y}, t) - \boldsymbol{\tau}^{(c)}(\mathbf{y}, t). \tag{3.70}$$

With the following definitions

$$\boldsymbol{\sigma}^{(r)} = \mathbf{L}:\underline{\boldsymbol{\varepsilon}}^{(r)}; \quad \mathring{\boldsymbol{\sigma}}^{(r)} = \mathbf{L}:\underline{\mathring{\boldsymbol{\varepsilon}}}^{(r)}, \quad \forall \mathbf{y} \in \Omega_+\cup\Omega_- \tag{3.71}$$

$$\boldsymbol{\sigma}_\delta^{(r)} = \tilde{\mathbf{L}}:\boldsymbol{\varepsilon}_\delta^{(r)}; \quad \mathring{\boldsymbol{\sigma}}_\delta^{(r)} = \tilde{\mathbf{L}}:\mathring{\boldsymbol{\varepsilon}}_\delta^{(r)}, \quad \forall \mathbf{y} \in \Omega_\delta \tag{3.72}$$

and

$$\dot{\boldsymbol{\sigma}}^{(r)} = \mathbf{L}:\underline{\dot{\boldsymbol{\varepsilon}}}^{(r)}; \quad \dot{\mathring{\boldsymbol{\sigma}}}^{(r)} = \mathbf{0}, \quad \forall \mathbf{y} \in \Omega_+\cup\Omega_- \tag{3.73}$$

$$\dot{\boldsymbol{\sigma}}_\delta^{(r)} = \tilde{\mathbf{L}}:\dot{\boldsymbol{\varepsilon}}_\delta^{(r)} + \dot{\tilde{\mathbf{L}}}:\boldsymbol{\varepsilon}_\delta^{(r)}; \quad \dot{\mathring{\boldsymbol{\sigma}}}_\delta^{(r)} = \dot{\tilde{\mathbf{L}}}:\mathring{\boldsymbol{\varepsilon}}_\delta^{(r)}, \quad \forall \mathbf{y} \in \Omega_\delta \tag{3.74}$$

we get the time-derivative of equation (3.68)

$$\dot{W} = \int_{\Omega_+\cup\Omega_-} (\boldsymbol{\sigma}^{(r)} - \mathring{\boldsymbol{\sigma}}^{(r)}) : \underline{\dot{\boldsymbol{\varepsilon}}}^{(r)} \, d\Omega + \int_{\Omega_\delta} (\boldsymbol{\sigma}_\delta^{(r)} - \mathring{\boldsymbol{\sigma}}_\delta^{(r)}) : \dot{\boldsymbol{\varepsilon}}_\delta^{(r)} \, d\Omega$$
$$- \frac{1}{2} \int_{\Omega_\delta} (\tilde{\boldsymbol{\sigma}}_\delta^{(r)} - \tilde{\mathring{\boldsymbol{\sigma}}}_\delta^{(r)}) : \mathbf{L}^{-1} : (\tilde{\boldsymbol{\sigma}}_\delta^{(r)} - \tilde{\mathring{\boldsymbol{\sigma}}}_\delta^{(r)}) \, \dot{\mathbf{d}} \, d\Omega. \tag{3.75}$$

The strain rates $\underline{\dot{\boldsymbol{\varepsilon}}}^{(r)}$ and $\dot{\boldsymbol{\varepsilon}}_\delta^{(r)}$ can be cast as

$$\underline{\dot{\boldsymbol{\varepsilon}}}^{(r)} = \underline{\dot{\boldsymbol{\varepsilon}}} - \underline{\dot{\boldsymbol{\varepsilon}}}^{(c)} - \underline{\dot{\boldsymbol{\varepsilon}}}^{in}, \quad \forall \mathbf{y} \in \Omega_+\cup\Omega_- \tag{3.76}$$
$$\dot{\boldsymbol{\varepsilon}}_\delta^{(r)} = \dot{\boldsymbol{\varepsilon}}_\delta - \dot{\boldsymbol{\varepsilon}}_\delta^{(c)} - \dot{\boldsymbol{\varepsilon}}_\delta^{in}, \quad \forall \mathbf{y} \in \Omega_\delta \tag{3.77}$$

such that

$$\underline{\dot{\boldsymbol{\varepsilon}}}^{(c)} = \nabla_s \underline{\dot{\mathbf{u}}}^{(c)} \; ; \quad \underline{\dot{\boldsymbol{\varepsilon}}}^{(r)} + \underline{\dot{\boldsymbol{\varepsilon}}}^{in} = \nabla_s \underline{\dot{\mathbf{u}}}^{R}, \quad \forall \mathbf{y} \in \Omega_+\cup\Omega_- \tag{3.78}$$
$$\dot{\boldsymbol{\varepsilon}}_\delta^{(c)} = \frac{1}{\delta}([\![\dot{\mathbf{u}}^{(c)}]\!] \otimes_s \mathbf{n}); \quad \dot{\boldsymbol{\varepsilon}}_\delta^{(r)} + \dot{\boldsymbol{\varepsilon}}_\delta^{in} = \frac{1}{\delta}([\![\dot{\mathbf{u}}^{R}]\!] \otimes_s \mathbf{n}), \quad \forall \mathbf{y} \in \Omega_\delta \tag{3.79}$$

and by using the virtual work principle, we get

$$\int_{\Omega_+\cup\Omega_-} (\boldsymbol{\sigma}^{(r)} - \mathring{\boldsymbol{\sigma}}^{(r)}) : (\underline{\dot{\boldsymbol{\varepsilon}}} - \underline{\dot{\boldsymbol{\varepsilon}}}^{(c)}) \, d\Omega = 0 \;\text{ and }\; \int_{\Omega_\delta} (\boldsymbol{\sigma}_\delta^{(r)} - \mathring{\boldsymbol{\sigma}}_\delta^{(r)}) : (\dot{\boldsymbol{\varepsilon}}_\delta - \dot{\boldsymbol{\varepsilon}}_\delta^{(c)}) \, d\Omega = 0 \tag{3.80}$$

Therefore, we get finally the following expression for $\dot{W}$

$$\dot{W} = \int_{\Omega_+\cup\Omega_-} (\boldsymbol{\sigma}^{(r)} - \mathring{\boldsymbol{\sigma}}^{(r)}) : \underline{\dot{\boldsymbol{\varepsilon}}}^{in} \, d\Omega - \int_{\Gamma} (\boldsymbol{\tau} - \boldsymbol{\tau}^{(s)}) . [\![\dot{\mathbf{u}}^{in}]\!] \, dS$$
$$- \frac{1}{2} \int_{\Gamma} (\tilde{\boldsymbol{\tau}} - \tilde{\boldsymbol{\tau}}^{(s)}) . \mathbf{Q}^{-1} . (\tilde{\boldsymbol{\tau}} - \tilde{\boldsymbol{\tau}}^{(s)}) \, \dot{\mathbf{d}} \, dS. \tag{3.81}$$

In view of inequalities (3.20), (3.30) and (3.35) it follows that $\dot{W} \le 0$ and furthermore, $\dot{W}$ is equal to zero only if $\underline{\dot{\boldsymbol{\varepsilon}}}^{in} = 0$, $[\![\dot{\mathbf{u}}^{in}]\!] = 0$ and $\dot{\mathbf{d}} = 0$. So Melan's argument holds: As W is non-negative by definition, plastic flow and damage evolution within the interface cease beyond a certain time instant if the fields $\mathring{\boldsymbol{\sigma}}^{(r)}$ and $\mathring{\boldsymbol{\tau}}^{(r)}$ exist, fulfilling the relations (3.44-52). We say that the RVE shakes down in this case.

3.3. Relative displacement bounding

As in the presented approach damage **d** is functions of the damage threshold **κ** (eqn. (3.37)), bounds for damage can be given in this special case by bounding the relative displacement $[\![\mathbf{u}]\!]$ which can be estimated from the extremal values of $[\![\mathbf{u}^{(c)}]\!]$ and $[\![\mathbf{u}^{R}]\!]$

$$\text{Max } [\![\mathbf{u}]\!] \leq \text{Max } [\![\mathbf{u}^{(c)}]\!] + \text{Max } [\![\mathbf{u}^{R}]\!]. \tag{3.82}$$

A bound for $[\![\mathbf{u}^{(c)}]\!]$ is straightforward to obtain since is linear in terms of the load multipliers. To evaluate the bound to $[\![\mathbf{u}^{R}]\!]$, we use the reciprocal relation of elasticity extended to the case of non-compatible strains which are identified here with the plastic strains

$$\int_{\partial\Omega} \hat{\mathbf{P}}.\mathbf{u}\, dS = \int_{\Omega} \hat{\boldsymbol{\sigma}}:\boldsymbol{\varepsilon}\, d\Omega \tag{3.83}$$

where $\hat{\boldsymbol{\sigma}}(\mathbf{y}, \mathbf{y}_0)$ stands for the purely elastic stress field in the RVE$^{(c)}$ loaded by concentrated force $\hat{\mathbf{P}}$ at point $\mathbf{y}_0$. Using the relation (3.83), we deduce then

$$\int_{\Gamma} \hat{\mathbf{P}}.[\![\mathbf{u}]\!]\, dS = \int_{\Omega_\delta} \hat{\boldsymbol{\sigma}}:\boldsymbol{\varepsilon}_\delta\, d\Omega \tag{3.84}$$

or in detail

$$\int_{\Gamma} \hat{\mathbf{P}}.[\![\mathbf{u}^{(c)}]\!]\, dS + \int_{\Gamma} \hat{\mathbf{P}}.[\![\mathbf{u}^{R}]\!]\, dS = \int_{\Omega_\delta} \hat{\boldsymbol{\sigma}}:\boldsymbol{\varepsilon}_\delta^{(c)}\, d\Omega + \int_{\Omega_\delta} \hat{\boldsymbol{\sigma}}:\boldsymbol{\varepsilon}_\delta^{(r)}\, d\Omega + \int_{\Omega_\delta} \hat{\boldsymbol{\sigma}}:\boldsymbol{\varepsilon}_\delta^{in}\, d\Omega \tag{3.85}$$

Using the Betti-Maxwell relation,

$$\int_{\Omega_\delta} \hat{\boldsymbol{\sigma}}:\boldsymbol{\varepsilon}_\delta^{(r)}\, d\Omega = \int_{\Omega_\delta} \boldsymbol{\sigma}_\delta^{(r)}:\hat{\boldsymbol{\varepsilon}}\, d\Omega = 0 \tag{3.86}$$

we obtain

$$\int_{\Gamma} \hat{\mathbf{P}}.[\![\mathbf{u}^{(c)}]\!]\, dS = \int_{\Omega_\delta} \hat{\boldsymbol{\sigma}}:\boldsymbol{\varepsilon}_\delta^{(c)}\, d\Omega \tag{3.87}$$

and

$$\int_{\Gamma} \hat{\mathbf{P}}.[\![\mathbf{u}^{\mathrm{R}}]\!]\, \mathrm{d}S = \int_{\Omega_\delta} \hat{\boldsymbol{\sigma}}:\boldsymbol{\varepsilon}_\delta^{\mathrm{in}}\, \mathrm{d}\Omega. \tag{3.88}$$

If the yield surface contains the origin of the coordinate system and the material is initially virgin then there exist two constants ζ and ξ such that

$$\zeta \|\dot{\boldsymbol{\varepsilon}}_\delta^{\mathrm{in}}\| \le \boldsymbol{\sigma}_\delta:\dot{\boldsymbol{\varepsilon}}_\delta^{\mathrm{in}} \le \xi \|\dot{\boldsymbol{\varepsilon}}_\delta^{\mathrm{in}}\| \tag{3.89}$$

where

$$\zeta = \inf \frac{\boldsymbol{\sigma}_\delta:\dot{\boldsymbol{\varepsilon}}_\delta^{\mathrm{in}}}{(\dot{\boldsymbol{\varepsilon}}_\delta^{\mathrm{in}}:\dot{\boldsymbol{\varepsilon}}_\delta^{\mathrm{in}})^{1/2}}, \quad \xi = \sup \frac{\boldsymbol{\sigma}_\delta:\dot{\boldsymbol{\varepsilon}}_\delta^{\mathrm{in}}}{(\dot{\boldsymbol{\varepsilon}}_\delta^{\mathrm{in}}:\dot{\boldsymbol{\varepsilon}}_\delta^{\mathrm{in}})^{1/2}} \tag{3.90}$$

and

$$\|\dot{\boldsymbol{\varepsilon}}_\delta^{\mathrm{in}}\| = (\dot{\boldsymbol{\varepsilon}}_\delta^{\mathrm{in}}:\dot{\boldsymbol{\varepsilon}}_\delta^{\mathrm{in}})^{1/2} = \left([\![\dot{u}_{\mathrm{n}}^{\mathrm{in}}]\!]^2 + [\![\dot{u}_{\mathrm{t}}^{\mathrm{in}}]\!]^2\right)^{1/2}. \tag{3.91}$$

For initially virgin material, according to Dorosz [38], we have

$$\|\boldsymbol{\varepsilon}_\delta^{\mathrm{in}}\| \le \int_0^t \|\dot{\boldsymbol{\varepsilon}}_\delta^{\mathrm{in}}\|\, \mathrm{d}t, \tag{3.92}$$

This allows to bound the relative residual displacement by

$$\begin{aligned} \left| \int_{\Gamma} \hat{\mathbf{P}}.[\![\mathbf{u}^{\mathrm{R}}]\!]\, \mathrm{d}S \right| &= \left| \int_{\Omega_\delta} \hat{\boldsymbol{\sigma}}:\boldsymbol{\varepsilon}_\delta^{\mathrm{in}}\, \mathrm{d}\Omega \right| \\ &\le \int_{\Omega_\delta} \|\hat{\boldsymbol{\sigma}}\|\, \|\boldsymbol{\varepsilon}_\delta^{\mathrm{in}}\|\, \mathrm{d}\Omega \\ &\le \int_{\Omega_\delta} \|\hat{\boldsymbol{\sigma}}\| \frac{1}{\zeta} \left(\int_0^t \boldsymbol{\sigma}:\dot{\boldsymbol{\varepsilon}}_\delta^{\mathrm{in}}\, \mathrm{d}t \right) \mathrm{d}\Omega \end{aligned} \tag{3.93}$$

Thus the inequality (3.93) leads to estimate the maximum relative residual displacement as

$$\left| [\![\mathbf{u}^{R}]\!] \right| \leq \max_{\Omega} \left(\frac{\|\hat{\boldsymbol{\sigma}}(\mathbf{y}, y_0)\|}{\zeta} \right) \frac{\alpha}{\alpha - 1} \int_{\Omega_\delta} \overset{\circ}{\boldsymbol{\sigma}}{}_{\delta}^{(r)} : \mathbf{C}^{-1} : \overset{\circ}{\boldsymbol{\sigma}}{}_{\delta}^{(r)} \, d\Omega \tag{3.94}$$

Therefore, the proposed shakedown condition for the determination of the macroscopic admissible domain against failure due to an unlimited accumulation of plastic deformations or local debonding can then be expressed by the following optimisation problem:

$$(\mathcal{P}) \begin{cases} \alpha_{SD} = \max\limits_{\overset{\circ}{\boldsymbol{\tau}}{}^{(r)}, \overset{\circ}{\boldsymbol{\sigma}}{}^{(r)}, \mathbf{d}} \alpha \\ \text{s.t.} \\ \overset{\circ}{\boldsymbol{\tau}}(\mathbf{y}) \in G(\mathbf{y}), \quad \forall \mathbf{y} \in \Omega_\delta \\ \overset{\circ}{\boldsymbol{\sigma}}(\mathbf{y}) \in F(\mathbf{y}), \quad \forall \mathbf{y} \in \Omega_+ \cup \Omega_- \\ <\boldsymbol{\sigma}^{(s)}> = \boldsymbol{\Sigma}. \end{cases} \tag{3.95}$$

The condition (3.95b) is considered as a failure criterion of the interface and the condition (3.95c) assures that the safe state of stresses is statically and plastically admissible.

4. Discrete formulation

To evaluate the macroscopic admissible loading domain, this constrained optimisation problem ($\mathcal{P}$) (eqn. (3.95)) is implemented numerically in order to solve the shakedown analysis problem (the elastic and limit analysis are considered as particular cases) (see [109, 157]). The finite element method based on the discretisation of the displacements is used. After discretisation of the unit cell, there are three principal tasks to be performed:

- to choose an appropriate discretisation for the loading domain,
- to write the discrete form of $\mathcal{P}_{\text{strain/stress}}$ with respect the boundary conditions (eqn. (3.44-48)). This permits to calculate the purely elastic stresses at each integration point for each loading path and to express the corresponding yield function, which represents the inequality constraints,
- to write the discrete form of $\mathcal{P}_{\text{res}}$ with respect the boundary conditions (eqn. (3.49-52)), which represents the equality conditions which must be satisfied by $\overset{\circ}{\boldsymbol{\sigma}}{}^{(r)}$.

4.1. Discretisation of the time variable

Up to now, no restrictions have been made to the load domain $\mathcal{L}$. Thus $\mathcal{L}$ can be of arbitrary form. However in many practical cases the number of independent loads is restricted, each varying between some given bounds. If the number of such independent loads is n, then the load domain is defined by an n-dimensional polyhedron

$$\mathcal{L} = \left\{ \mathrm{P} / \ \mathrm{P}\,(\mathbf{y}, t) = \sum_{k=1}^{n} \mu_k(t)\ \mathrm{P}_0^k(\mathbf{y}), \quad \mu_k \in [\mu_k^-, \mu_k^+] \right\} \tag{3.96}$$

where P is the vector of generalised loads, μ_k are scalar multipliers with upper and lower bounds μ_k^+ and μ_k^-, respectively. P_0^k represents n fixed and independent generalised loads (e.g. macroscopic strains, macroscopic stresses, temperature changes or combinations of them). For subsequent considerations the corners of the polyhedron (load domain $\mathcal{L}$) are numbred by the index j, such that $j = 1, \ldots, NV$, where NV denotes the total number of corners. The loads, which correspond to each corner of $\mathcal{L}$ are characterised symbolically by P_j (see on Figure 3.3 the bi-dimensional case ($n = 2$), when two different loads are applied on the RVE). In view of the convexity of the yield function f (eqn. (3.19)) and due to the above assumption on the load domain $\mathcal{L}$ it has been shown [91] that

$$f\left(\alpha\, \boldsymbol{\sigma}^{(\mathrm{c})}(\mathbf{y}, t) + \mathring{\boldsymbol{\sigma}}^{(\mathrm{r})}(\mathbf{y})\right) \le 0 \tag{3.97}$$

is fulfilled at any time t, if

$$f\left(\alpha\, \boldsymbol{\sigma}^{(\mathrm{c})}(\mathrm{P}_j) + \mathring{\boldsymbol{\sigma}}^{(\mathrm{r})}\right) \le 0 \tag{3.98}$$

holds for all $j \in [1, NV]$ and for all $i \in [1, NG]$.

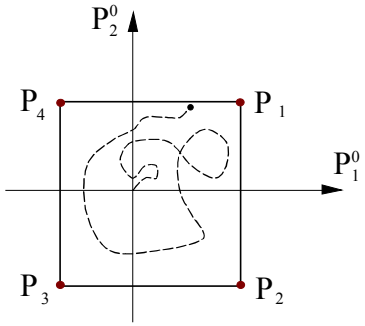

Figure 3.3. Two-dimensional representation of load domain.

4.2. Variational formulation on the unit cell

This analysis presents two local problems, $\mathcal{P}_{\text{strain/stress}}$ and $\mathcal{P}_{\text{res}}$, which have to be solved to obtain the data for the constrained optimisation problem ($\mathcal{P}$) and which can both be written under the same general form (see [71, 108, 109])

$$\mathcal{P}_{gen} \begin{cases} \text{div } \mathbf{s} = 0 \quad \text{in } \Omega \\ \mathbf{s.n} = 0 \text{ anti-periodic on } \partial\Omega \\ [\![\mathbf{s}]\!].\mathbf{n}_{\Gamma} = 0 \text{ on } \Gamma \\ <\mathbf{s}> = \mathbf{S} \end{cases} \tag{3.99}$$

where $\mathbf{s}$ designs either $\boldsymbol{\sigma}^{(c)}$ or $\mathring{\boldsymbol{\sigma}}^{(r)}$ and $\mathbf{S}$ either the macroscopic stress field $\boldsymbol{\Sigma}$ or the null tensor $\mathbf{0}$ (because $<\mathring{\boldsymbol{\sigma}}^{(r)}> = 0$). In variational form, these cellular problems are expressed by the use of the virtual work principle on the equilibrium equation (3.99a) with the kinematic relation defined by the decomposition (3.3). By integration by parts and taking into account the average conditions (3.2) and (3.6) and the periodicity relations (3.99b)-(3.99c), this system $\mathcal{P}_{gen}$ can be replaced by the unique following formulation

$$\forall \delta\mathbf{u}^{\text{per}}, \forall \mathbf{E}, \qquad \int_{\Omega} \mathbf{s}:(\boldsymbol{\varepsilon}(\delta\mathbf{u}^{\text{per}}) + \delta\mathbf{E})\, d\Omega = |\Omega|\, \mathbf{S}:\delta\mathbf{E}. \tag{3.100}$$

Taking into account that either $\mathbf{s} = \mathbf{L}:(\boldsymbol{\varepsilon}(\mathbf{u}^{\text{per}}) + \mathbf{E})$ for $\mathcal{P}_{\text{strain/stress}}$ or $\mathbf{s} = \mathring{\boldsymbol{\sigma}}^{(r)}$ for $\mathcal{P}_{\text{res}}$, this formulation emphasizes the degrees of freedom which have to be considered on the unit cell. On one hand the local degrees of freedom $\mathbf{u}^{\text{per}}$ which describe the fluctuations of the displacement field due to the heterogeneities, and on the other hand the global degrees of freedom $\mathbf{E}$ which represent the strains average of the cell which would occur in the homogeneous case. The nodal associated forces to $\mathbf{E}$ are the components of the macroscopic stress field $\boldsymbol{\Sigma}$ multiplied by the volume of the unit cell. Practically, after having meshed the unit cell, an additional node, the degrees of freedom related to the macroscopic strains, is added to all the elements of the mesh. This fictive node is called "macroscopic node" [35] and is added to the connectivity table of each element *e* such that the vector of elementary degrees of freedom is given by

$$\{\mathbf{u}^{e}\} = \begin{Bmatrix} \mathbf{u}^{\text{per}} \\ \mathbf{E} \end{Bmatrix} \tag{3.101}$$

and a new matrix $[\mathbf{B}^{\text{hom},e}]$ is substituted to the classical one $[\mathbf{B}^{e}]$ constituted by the derivatives of the shape functions and linking strains and displacements

$$[\mathbf{B}^{\text{hom},e}] = [\mathbf{B}^{e}, \mathbf{I}] \tag{3.102}$$

such that

$$\begin{aligned} \{\boldsymbol{\varepsilon}^{e}\} &= [\mathbf{B}^{\text{hom},e}]\ \{\mathbf{u}^{e}\} \\ &= [\mathbf{B}^{e}]\ \{\mathbf{u}^{\text{per},e}\} + \{\mathbf{E}\} \end{aligned} \tag{3.103}$$

Finally, we get the discrete form of $\mathcal{P}_{\text{gen}}$

$$\forall \delta\mathbf{u}^{\text{per}},\ \forall \mathbf{E},\qquad \sum_{e=1}^{NE} \langle \delta\mathbf{u}^{\text{per},e},\ \delta\mathbf{E}\rangle \sum_{i=1}^{NGE} \omega_{\text{i}}\ [B_{\text{i}}^{\text{hom},e}]^{\text{T}}\ \{s_{\text{i}}\}\ \det J = |\Omega|\ \langle \delta\mathbf{E}\rangle\{\mathbf{S}\} \tag{3.104}$$

where *NE* denotes the total number of elements, *e* the current element, $\delta\mathbf{u}^{\text{per},e}$ the vector of the virtual displacements of the nodes of the element and *NGE* its number of Gaussian points. The discrete formulation (eqn. (3.104)) leads to the above-mentioned discrete forms of the elastic problem $\mathcal{P}_{\text{strain/stress}}$ and of the specific formulation representing $\mathcal{P}_{\text{res}}$.

*(i) Elastic proble*m: in this case, $\mathbf{s} = \boldsymbol{\sigma}^{(\text{c})}$ and $\mathbf{S} = \boldsymbol{\Sigma}$

Using the kinematic relation (3.3), the discrete form (eqn. (3.104)) leads to a classical linear system

$$[\mathbf{K}]\ \{\mathbf{u}^{\text{per}}, \mathbf{E}\}^{\text{T}} = \{\mathbf{0}, |\Omega|\boldsymbol{\Sigma}\}^{\text{T}} \tag{3.105}$$

where $[\mathbf{K}]$ results from the assembly of the elementary stiffness matrix

$$[\mathbf{K}^{\text{hom},e}] = \sum_{i=1}^{NGE} \omega_{\text{i}}\ [B_{\text{i}}^{\text{hom},e}]^{\text{T}}\ [\mathbf{L}^{e}]\ [B_{\text{i}}^{\text{hom},e}]\ \det J. \tag{3.106}$$

Applying a macroscopic strain or stress, becomes then the same as applying a displacement or a force.

(*ii*) *Residual stresses proble*m: in this case, $\mathbf{s} = \mathring{\boldsymbol{\sigma}}^{(r)}$ and $\mathbf{S} = \mathbf{0}$

The discrete form (eqn. (3.104)) becomes a linear system of equations, which constitutes the equality constraints of the optimisation problem and is the discrete form of $\mathcal{P}_{res}$,

$$[\mathbf{C}]\ \{\mathring{\boldsymbol{\sigma}}^{(r)}\} = \{\mathbf{0}\} \tag{3.107}$$

where [**C**] is here called *equilibrium matri*x. This matrix results also from the assembly of the elementary equilibrium matrix

$$[\mathbf{C}^e] = \sum_{i=1}^{NGE} \omega_i\, [B_i^{\text{hom},e}]^T \det J \tag{3.108}$$

where $\mathring{\boldsymbol{\sigma}}^{(r)}$ is constituted by the residual stresses at the Gauss points. For the elastic problem as for the residual stresses, the periodicity relations are represented by linear constraints between the degrees of freedom of the nodes. In the two cases, they are taken into account before the assembly of the elementary matrix [$\mathbf{K}^{\text{hom},e}$] or [$\mathbf{C}^e$] by an elimination method.

5. Validations and applications

5.1. Flat aluminium alloy sheets

To validate the presented method, flat aluminium alloy sheets with periodically arranged slits of varying length and pattern of periodicity are investigated [187]. The calculations have been made on representative unit cells by using the lower-bound direct method and homogenisation technique of periodic media with the assumption of plane stress (eqn. (3.60-67)). The mechanical characteristics of the homogeneous and isotropic aluminium utilised are as follows: Young's modulus $E = 67200$ MPa; Poisson's ratio $\nu = 0.318$ and the conventional yield stress at 0.1% of axial elongation $\sigma_Y = 137$ MPa. The following dimensionless lengths of the openings were considered: $r = l/L = 0.5$ and 0.7 with $t = 1$ mm.

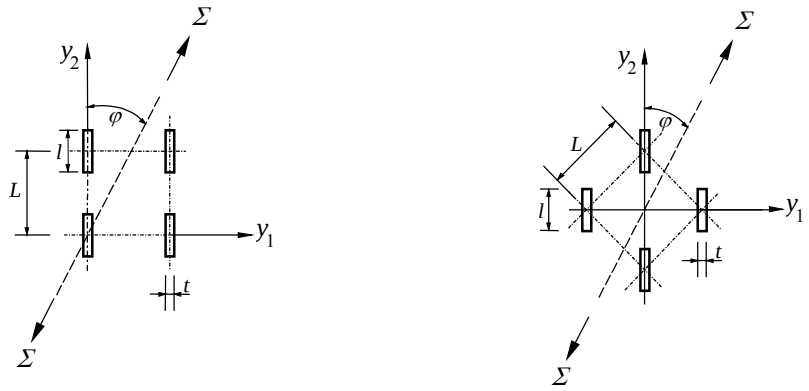

(a) rectangular pattern (b) rotated pattern

Figure 3.4. Arrangement of rectangular opening

In Figure 3.4, two considered patterns of openings with the pitch L = 10 mm are specified. It follows, therefore, that two different types of symmetries regarding the rectangular openings were considered. In the first case the rectangular openings orientation follows the pitch, whereas in the second this orientation makes an angle φ = 45° with the square grid specifying the pitch. In Figure 3.5, a comparison of the obtained results, using the software SALIA, with experimental values [107] of uniaxial macroscopic tensile strength as function of the load orientation are shown for the two considered patterns. It should be noted that the solution of the elastic reference problem for the shakedown analysis corresponds to a slit, where the sharp corners have been replaced by rounded corners with radius t/10. The fact that the calculated solution (Figure 3.5b) is non-conservative compared to the experimental results may be related to this approximation.

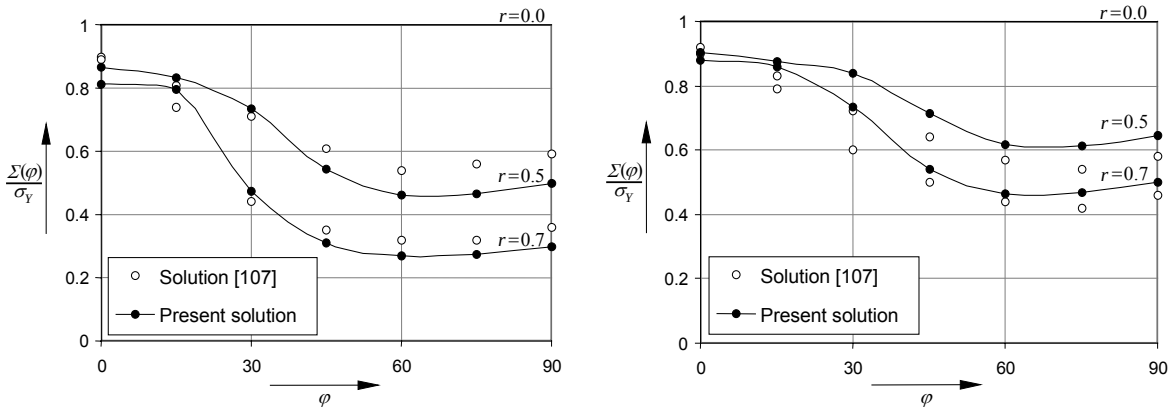

(a) rectangular pattern (b) rotated pattern

Figure 3.5. Uniaxial macroscopic tensile strength versus inclinations φ.

5.2. Fibre-reinforced composites

For the limit and shakedown analysis of fibre-reinforced composite materials, we consider a typical problem for an aluminium/alumina composite assuming perfect bonding between fibres and matrix [187]. For given regular quadratic, rotated and hexagonal patterns of periodicity of reinforced elastic fibres in ductile matrix as illustrated in Figure 3.6, given material properties of the fibres and matrix (Table 3.1), one has to determine the admissible macroscopic stresses. The adopted mechanical characteristics for the matrix and the fibres are:

Material	Matrix(Al)	Fibre (Al_2O_3)
Young's Modulus E (GPa)	70	370
Poisson's ratio ν	0.3	0.3
Yield stress σ_Y (MPa)	80	—

Table 3.1. Mechanical characteristics of fibre-reinforced composite.

The Figure 3.7 presents the variation of the admissible value of macroscopic stress ($\Sigma_1 = \Sigma_2 = \Sigma$), normalised by the yield stress of the matrix σ_Y, with fibre volume fraction where the results obtained by Zahl and Schmauder [188] for respectively, rectangular, rotated and hexagonal patterns are represented. The admissible rectangular macroscopic domains for quadratic arrangement are shown in Figure 3.8, where the bounds of elastic, limit and shakedown domains are represented. These bounds are obtained for different values of fibre volume fraction ($V_f / V = \pi D^2 / 4L^2 = 0\%–50\%$) using SALIA.

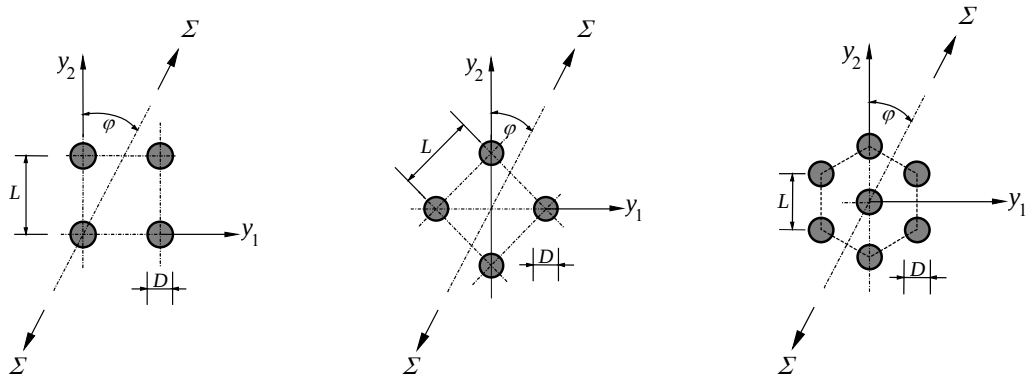

(a) rectangular pattern (b) rotated pattern (c) hexagonal pattern

Figure 3.6. Arrangement of fibre-reinforced composite.

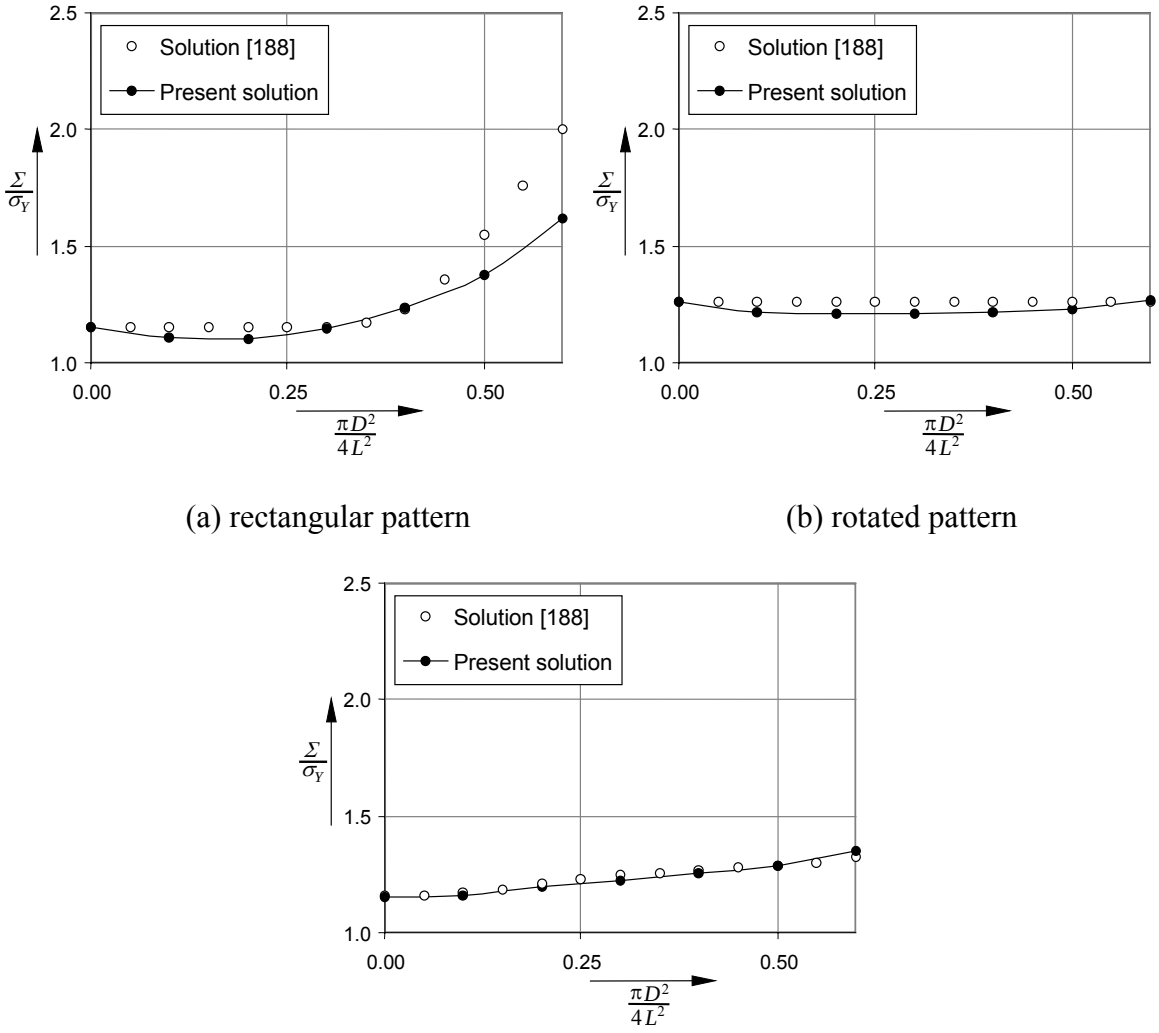

(a) rectangular pattern (b) rotated pattern

(c) hexagonal pattern

Figure 3.7. Variation of macroscopic stress with fibre volume fraction

The given regular and rotated quadratic patterns of periodicity of the fibre-reinforced composite described above, have been investigated under constant distribution of temperature $\Delta\vartheta$ with the following coefficients of isotropic thermal expansion $\alpha_\vartheta = 22\times10^{-6}\ \mathrm{K}^{-1}$ and $\alpha_\vartheta = 8\times10^{-6}\ \mathrm{K}^{-1}$ for the matrix and fibre, respectively. The results show the sensitivity of the composite to prescribed thermal loads by considering the volume fraction of fibres $V_\mathrm{f}/V = 60\%$. In Figure 3.9, the results show the variation of shakedown domains in the space of macroscopic strains for the composite under compression with the temperature amplitude normalized by $\Delta\vartheta_0 = 100$ K. The results show that the thermal residual stresses induced by the thermal loads strongly affect the size and the shape of the shakedown domains. The influence of the thermal loads is much stronger for the regular patterns than for the rotated patterns.

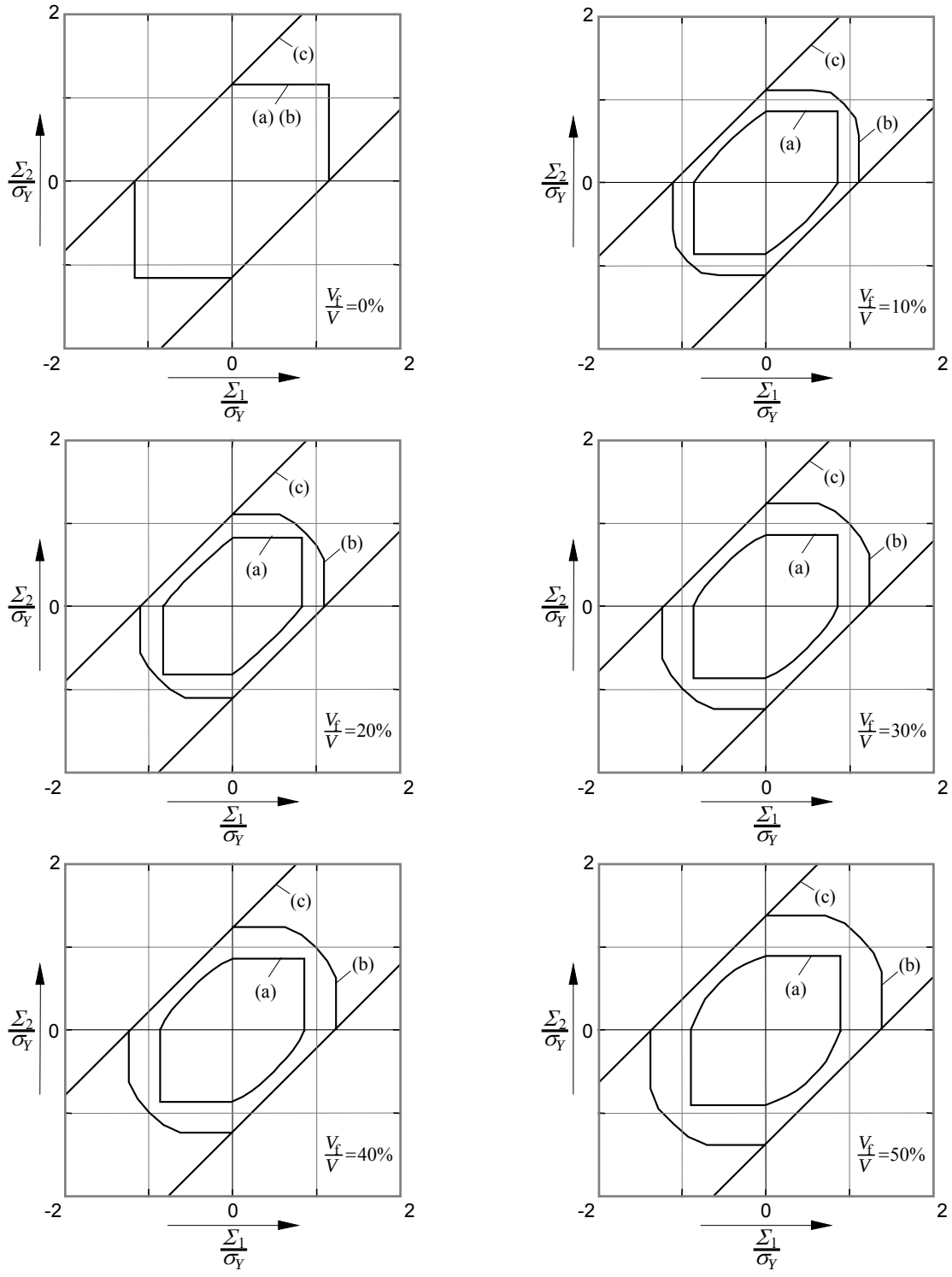

(a) elastic domains, (b) shakedown domains, (c) limit domains

Figure 3.8. Admissible domains of macroscopic stresses.

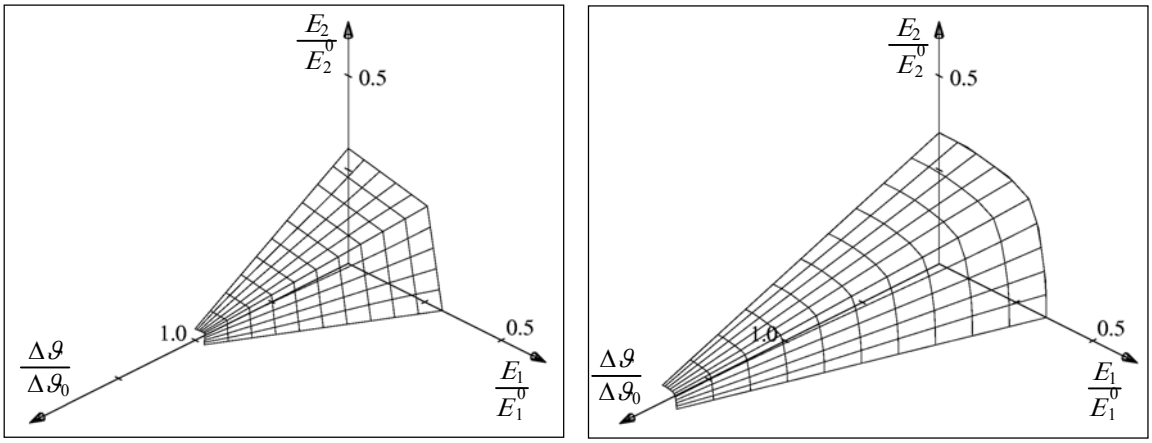

(a) rectangular pattern (b) rotated pattern

Figure 3.9. Variation of shakedown domains with amplitude of temperature.

5.3. Layered composites

The heterogeneous medium investigated herein, consists of a three-dimensional periodic material with two layers perpendicular to the direction x_3 [108]. The periodicity properties of the material leads to consider a parallelepiped unit cell constituted by one of each layer as shown in the Figure 3.10. The calculations are performed with the software SIC [6] (see |109]). The chosen mechanical properties are shown in the Table 3.2, where the thickness ratio is $h_1/h_2 = 1/2$.

Material	Layer 1	Layer 2
Young's Modulus E (Gpa)	210	160
Poisson's ratio ν	0.3	0.27
Yield stress σ_Y (MPa)	180	270

Table 3.2. Mechanical characteristics of layers.

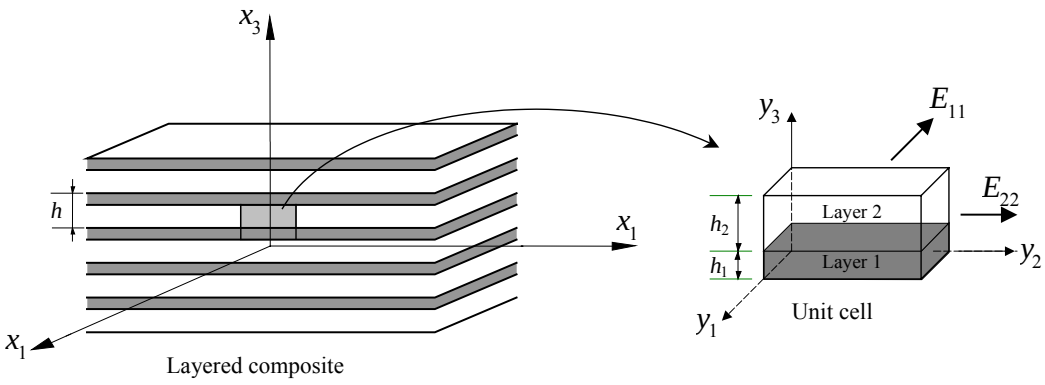

Figure 3.10. Layered composite.

The objective is to determine the elastic, limit and shakedown domains under bi-axial tension in the space of macroscopic strains in order to compare the present results with those obtained analytically [68]. Here, the half-plane is considered due to the symmetry of the macroscopic admissible domain with respect to the origin of the yield criterion (Figure 3.11).

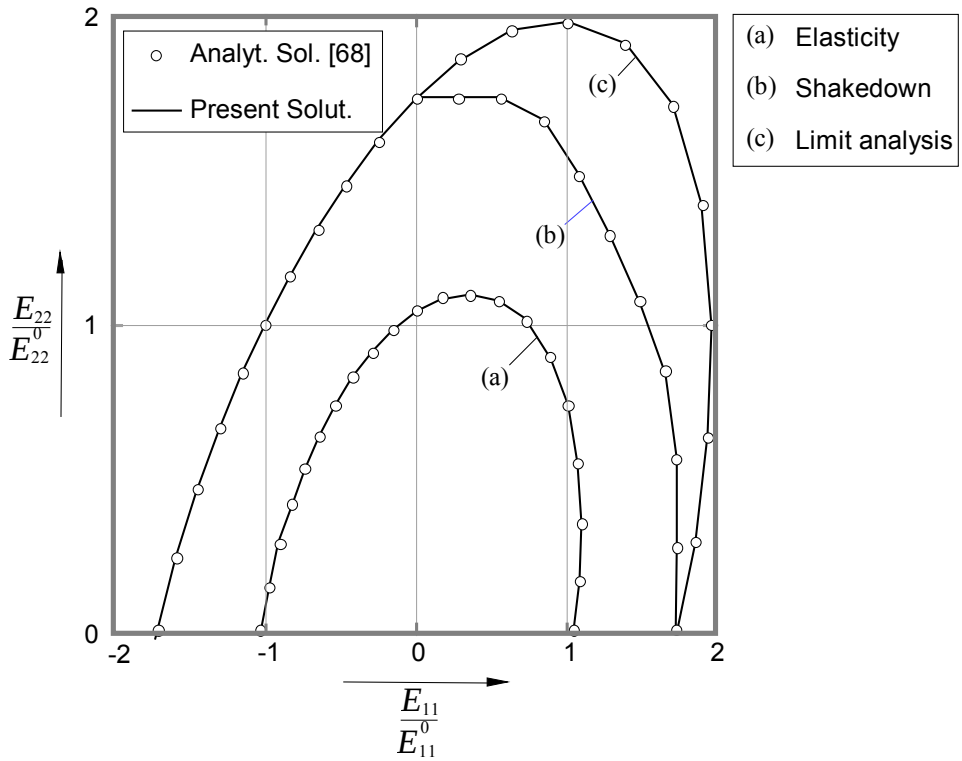

Figure 3.11. Loading domains in the space of macroscopic strains.

5.4. Perforated sheet

We consider a three-dimensional periodically perforated aluminium sheet loaded in its plane by macroscopic stresses |108]. The chosen unit cell is represented in Figure 3.12. For symmetric reasons only an eighth of the unit cell is considered. The unit cell is meshed with the same type of elements as for the layered composite using the software SIC. The mechanical characteristics of the homogeneous and isotropic matrix are as follows: Young's modulus $E = 69550$ MPa; Poisson's ratio $\nu = 0.337$ and yield stress $\sigma_Y = 159$ MPa, where the porosity is defined by the relation $2r/d = 0.3$.

The admissible loading domains in the space of macroscopic stresses are shown in Figure 3.13, where the results are compared with those obtained by an incremental computation under the assumption of plane stress [34]. The gap between the computations under plane stress and presents results can be explained by the fact that in [34] the restrictive assumption of plane stress is used whereas we impose only the real conditions, which are on the upper and lower surfaces of the sheet. For this reason it is plausible that the safe domain calculated in [34] is smaller than the domain calculated by the here presented method.

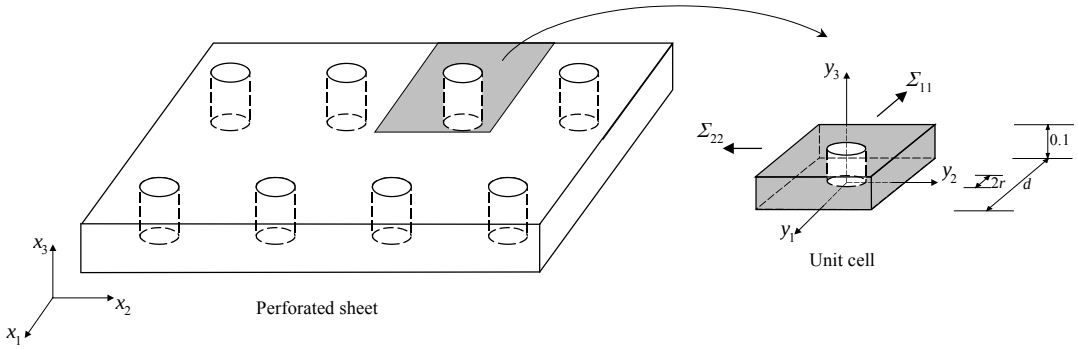

Figure 3.12. Perforated sheet.

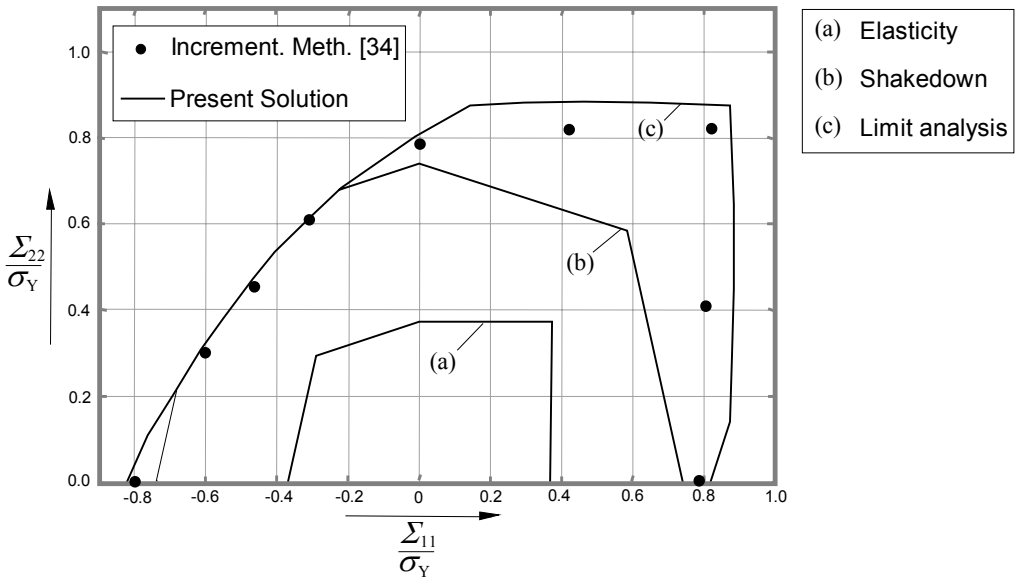

Figure 3.13. Loading domains in the space of macroscopic stresses.

5.5. Debonding effect

In the presented numerical example, debonding between fibres and matrix material is taken into account, as it has been developed above, by introducing a cohesive zone [70]. For given regular quadratic patterns of periodicity of reinforced elastic fibres in ductile matrix as illustrated in Figure 3.14, given material properties of the fibres, matrix and interface (Table 3.3), the admissible macroscopic stress Σ is determined as function of the load orientation φ for different values of $\sigma_{\max}$ where the perfect bonding case is represented. The following dimensions were considered for the analysis: $l/L = 0.5$, $t = 1$ mm, $\delta = 5$ μm and $\beta = 1$.

Material	Matrix	Fibre	Interface
Young's Modulus E (GPa)	67.2	370	0.67
Poisson's ratio ν	0.318	0.318	0.0
Yield stress σ_Y (MPa)	137	—	68.5

Table 3.3. Mechanical characteristics of fibre-reinforced composite.

The results in Figure 3.14 have been obtained under the assumption of plane stress. The results show that the influence of debonding on the response of the considered composite, in comparison with perfect bonding case, is more important when the load is applied in the direction y_1.

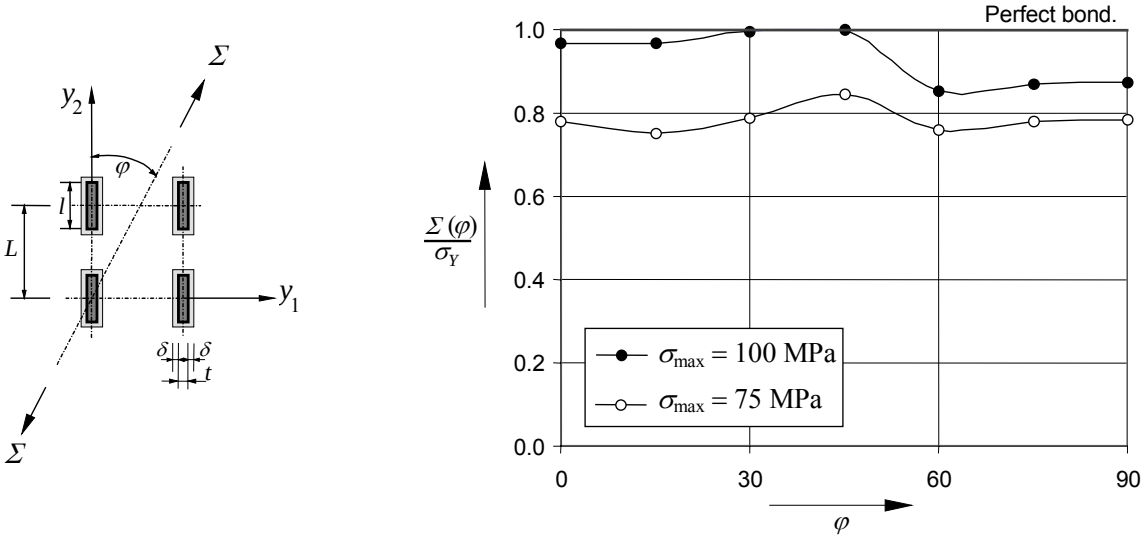

Figure 3.14. Admissible macroscopic stress versus load orientation φ.

6. Conclusions

Motivated by the use of composite materials in a number of fields, such as aerospace, biomechanic and civil engineering, especially in applications where high stiffness-to-weight and strength-to-weight ratios are required, Direct Methods have been developed in this chapter to predict long-term behaviour of such materials. The development of such materials demands an optimal design of the microstructure and a fundamental understanding of the role of the microstructure on the overall properties. The microstructural parameters controlling the macroscopic properties are on one hand the morphology of the microstructure and on the other hand the constitutive behaviour of each individual component. The correlation between the microstructure and the macroscopic properties is addressed by homogenisation methods. To this end, the concept of a representative volume element (RVE) is introduced, which may be viewed as a heterogeneous structure under prescribed boundary conditions which correspond to the uniform local continuum fields.

By using the homogenisation methods of periodic media, the macroscopic admissible domain is founded from the resolution of a shakedown analysis problem on a representative volume element accounting particularly for debonding effects between two phases. By means of the finite element method and the von Mises yield condition, shakedown analysis is reduced to a problem of mathematical programming with constraints which is solved by a non-linear optimisation algorithm. In future, frictional sliding and more complex problems, like non-periodic patterns, have to be included in the theoretical and numerical scheme.

Chapitre 4

Application aux problèmes industriels

Application to engineering problems

Collaborations liées à ce chapitre :

- Prof. Le Thi Hoai An, Université de Metz
- M. S. Mouhtamid, RWTH Aachen
- Prof. Pham Dinh Tao ; Dr. F. Akoa, INSA-Rouen
- Dr. J.B. Tritsch, USTL
- M. K. Wirtz ; M. H. Lang, Framatome GmbH

Table of contents

1. Introduction

The aim of this chapter is to develop an algorithm for the determination of lower bounds in limit and shakedown analysis for large-scale three-dimensional problems. Direct Method in shakedown and limit analysis leads, as it has been developed in chapters 1, 2 and 3, to a problem of mathematical programming, which requires large computer memory if other than one or two-dimensional structures are studied. Furthermore, for non-linear yield conditions (e.g. von Mises-type criteria), the solution of the respective non-linear optimisation problem often requires highly iterative procedures and is therefore very time-consuming. This results from the fact, that the non-linear programming approaches use often solution schemes based on purely mathematical considerations and disregarding simplifying physical or technological features. To overcome this problem, a new algorithm has been developed and implemented for solving large-scale non-linear optimisation problems [5, 69]. It is based on the interior point method combined with the method of difference of convex functions (DC) [133]. To generate the data for IPDCA, the lower bound direct method has been implemented into the commercial code ANSYS. Some applications show the advantage of this algorithm in comparison with standard code like LANCELOT (**L**arge **A**nd **N**onlinear **C**onstrained **E**xtended **L**agrangian **O**ptimization **T**echniques) [29]. As alternative to numerical optimisation algorithms, a geometrical hyper-sphere algorithm can be used to solve large-scale problems. This algorithm consist in finding the residual stresses state by determining the centre of the smallest hyper-sphere circumscribing the stress loading path in the deviatoric stress-tensor space [175].

2. Equivalent convex program

To overcome the problem of prohibitive time-consumption for numerical calculations, a new, specially problem-adapted optimisation algorithm has been developed (IPDCA: **I**nterior-**P**oint-**D**ifference-of-**C**onvex-Functions-**A**lgorithm). It is based on the interior point method combined with the method of difference of convex functions (DC) [133] (for details, see [3, 4]). To simplify the formulation of this algorithm, we restrict ourself to the particular case of limit analysis. To this end we rewrite the problem (eqn. (1.39-42) as follows:

$$(\mathcal{P})\begin{cases} \max\ \alpha \\ \text{s.t.} \\ \sum_{i=1}^{NG} C_i\, \overset{\circ}{\sigma}_i^{(\mathrm{r})} = 0 \\ (\sigma_{1i}-\sigma_{2i})^2+(\sigma_{2i}-\sigma_{3i})^2+(\sigma_{3i}-\sigma_{1i})^2+6(\sigma_{4i}^2+\sigma_{5i}^2+\sigma_{6i}^2) \le 2\sigma_{\mathrm{Y}i}^2 \\ \sigma_i - \alpha\,\sigma_i^{(\mathrm{c})} - \overset{\circ}{\sigma}_i^{(\mathrm{r})} = 0 \\ i = 1, \ldots, NG. \end{cases} \tag{4.1}$$

where $\alpha \in \mathbb{R}$, $\sigma_i^{(\mathrm{c})} \in \mathbb{R}^6$ and $C_i \in \mathcal{M}_{(3NK,\ 6)}(\mathbb{R})$ (the vector space of (3NK) × 6 real matrices) are given, $\sigma_i \in \mathbb{R}^6$ and $\sigma_i^{(\mathrm{c})} = (\sigma_{1i}^{(\mathrm{c})}, \ldots, \sigma_{6i}^{(\mathrm{c})})$ for $i = 1, \ldots, NG$. The problem has $12NG + 1$ variables and $3NK + 7NG$ constraints. In practice $NG \ge NK$ and the values of NK are about several thousands. It then leads to large-scale convex problem.

Before applying IPDCA to the problem (4.1), we introduce some transformations which lead to a simpler equivalent convex problem with significantly less variables and constraints. Let $T \in \mathcal{M}_{(6,\ 6)}(\mathbb{R}^6)$ be the following non-singular matrix whose inverse T^{-1} is easily computed by

$$T = \begin{pmatrix} 1/2 & 1/2 & 1/2 & & & & \\ -1/2 & 1/2 & 1/2 & & & & \\ -1/2 & -1/2 & 1/2 & & & & \\ & & & 1/\sqrt{6} & & & \\ & & & & 1/\sqrt{6} & & \\ & & & & & 1/\sqrt{6} & \end{pmatrix} \tag{4.2}$$

and

$$T^{-1} = \begin{pmatrix} 1 & -1 & & & & & \\ & 1 & -1 & & & & \\ 1 & & 1 & & & & \\ & & & \sqrt{6} & & & \\ & & & & \sqrt{6} & & \\ & & & & & \sqrt{6} & \end{pmatrix} \tag{4.3}$$

Set $v = T^{-1}u$ and then $u = T\,v$. Making u (resp. v) play the role of σ_i (resp. u_i in $(\mathcal{P})$), the second constraints in $(\mathcal{P})$ becomes

$$u_{1i}^2 + u_{2i}^2 + (u_{1i}^2 + u_{2i}^2)^2 + u_{4i}^2 + u_{5i}^2 + u_{6i}^2 \leq 2\,\sigma_{Yi}^2 \tag{4.4}$$

Since $\sigma_i = T\,u_i$, the third constraint in $(\mathcal{P})$ takes the form

$$\sigma_i^{(r)} - T\,u_i + \alpha\sigma_i^{(c)} = 0 \tag{4.5}$$

We have

$$T\,u_i = \sum_{q=1}^{6} T^q\,u_{qi} = \sum_{\substack{q=1 \\ q\neq 3}}^{6} T^q\,u_{qi} + T^3\,u_{3i}, \tag{4.6}$$

where T^q denotes the i-th column of the matrix T. On the other hand, it follows from (4.5) and (4.6) that

$$\begin{aligned} C_i\,\sigma_i^{(r)} &= C_i\,Tu_i - \alpha C_i\,\sigma_i^{(c)} \\ &= C_i\left(\sum_{\substack{q=1 \\ q\neq 3}}^{6} T^q\,u_{qi} + T^3\,u_{3i}\right) - \alpha C_i\,\sigma_i^{(c)}. \end{aligned} \tag{4.7}$$

Consider now the new variables $\overline{u}_i$ in $\mathbb{R}^5$

$$\overline{u}_i = (\overline{u}_{1i} = u_{1i},\ \overline{u}_{2i} = u_{2i},\ \overline{u}_{3i} = u_{4i},\ \overline{u}_{4i} = u_{5i},\ \overline{u}_{5i} = u_{6i},) \tag{4.8}$$

and the matrix

$$A_i = \left((C_i\,T)^1 \quad (C_i\,T)^2 \quad (C_i\,T)^4 \quad (C_i\,T)^5 \quad (C_i\,T)^6\right) \in \mathcal{M}_{(3NK,\,5)}\,(\mathbb{R}). \tag{4.9}$$

We can write

$$\sum_{\substack{q=1 \\ q\neq 3}}^{6} (C_i\,T)^q\,u_{qi} = A_i\,\overline{u}_i. \tag{4.10}$$

Let x be the vector in $\mathbb{R}^{NG}$ whose components x_i are defined by

$$x_i = u_{3i} \quad \text{for } i = 1, ..., NG. \tag{4.11}$$

It follows that

$$C_i T u_i \ = A_i \bar{u}_i + (C_i T)^3 x_i. \tag{4.12}$$

In the sequel B is the matrix

$$B = \left((C_1 T)^3 \quad (C_2 T)^3 \quad (C_3 T)^3 \quad \dots \quad (C_{NG} T)^3 \right) \in \mathcal{M}_{(3NK,\,5)}(\mathbb{R}). \tag{4.13}$$

and we set

$$w = \sum_{i=1}^{NG} C_i \, \sigma_i^{(c)}. \tag{4.14}$$

Then, the problem $(\mathcal{P})$ is equivalently transformed into the following

$$(\mathcal{P}) \begin{cases} \max \alpha \\ \text{s.t.} \\ \sum_{i=1}^{NG} A_i \bar{u}_i + Bx - \alpha w = 0 \\ u_{1i}^2 + u_{2i}^2 + (u_{1i}^2 + u_{2i}^2)^2 + u_{4i}^2 + u_{5i}^2 + u_{6i}^2 \le 2 \, \sigma_{Yi}^2 \\ i = 1, \dots, NG. \end{cases} \tag{4.15}$$

We transform now the above convex quadratic constraints into Euclidean ball constraints. For this we first consider the convex quadratic form

$$f(u) = \frac{1}{2} < Q \, \bar{u}; \, \bar{u} > = u_1^2 + u_2^2 + (u_1 + u_2)^2 + u_4^2 + u_5^2 + u_6^2 \tag{4.16}$$

where $\overline{u} = (u_1 + u_2 + u_4 + u_5 + u_6)$ and the matrix Q is given by

$$Q = \begin{pmatrix} 4 & 2 & & & & \\ 2 & 4 & & & & \\ & & 2 & & & \\ & & & 2 & & \\ & & & & 2 & \\ & & & & & 2 \end{pmatrix}. \tag{4.17}$$

The Cholesky factorisation LL^T of the matrix $\frac{1}{2}Q$ is computed by

$$L = \begin{pmatrix} \sqrt{2} & & & & & \\ \frac{1}{\sqrt{2}} & \frac{\sqrt{3}}{\sqrt{2}} & & & & \\ & & 1 & & & \\ & & & 1 & & \\ & & & & 1 & \\ & & & & & 1 \end{pmatrix}. \tag{4.18}$$

Hence

$$\begin{aligned} \frac{1}{2} < Q\,\overline{u};\, \overline{u} > &= < LL^T \overline{u};\, \overline{u} > \\ &= < L^T \overline{u};\, L^T \overline{u} > . \end{aligned} \tag{4.19}$$

The transformed problem takes then the form

$$(\mathcal{PM}) \begin{cases} \max\ \alpha \\ \text{s.t.} \\ \sum_{i=1}^{NG} A_i \overline{u}_i + Bx - \alpha w = 0 \\ \| L^T \overline{u}_i \|^2 \le 2\ \sigma_{Yi}^2 \\ i = 1, \ldots, NG. \end{cases} \tag{4.20}$$

Finally, by using the new change of variables $u_i = L^T \bar{u}_i$ and keeping the same notations A_i and u_i for $A_i L^{-T}$ and $\frac{u_i}{\sqrt{2}\sigma_Y}$ respectively (i.e. $A_i = A_i L^{-T}$ and $u_i = \frac{u_i}{\sqrt{2}\sigma_Y}$) for notation simplicity, the problem $(\mathcal{PM})$ gets the following form

$$(\mathcal{PM}) \begin{cases} \max \alpha \\ \text{s.t.} \\ \sum_{i=1}^{NG} A_i \bar{u}_i + Bx - \alpha w = 0 \\ \| u_i \|^2 \le 1 \\ i = 1, \ldots, NG. \end{cases} \tag{4.21}$$

This convex problem has $6NG + 1$ variables and $3NK + NG$ constraints. In the following section, we will describe IPDCA to solve the convex problem $(\mathcal{PM})$.

3. The IPDCA algorithm

The algorithm of IPDCA can be formulated as follows [3, 4]:

Find a Karush-Kuhn-Tucker(KKT) point of the following non-linear programming problem:

$$(\mathcal{P}_{\mathcal{EI}}) \begin{cases} \min f(x) \\ \text{s.t.} \\ A x - b = 0 \\ c(x) \ge 0 \\ x \in \mathbb{R}^n \end{cases} \tag{4.22}$$

where f and $c : \mathbb{R}^n \to \mathbb{R}^{m_I}$ are two twice continuous differentiable functions and c is supposed to be concave. $A \in \mathbb{R}^{m_E \times n}$ a surjective matrix and $b \in \mathbb{R}^{m_E}$ a vector. The first step in the chosen interior-point approach is to add slack variables w to each of the inequality constraints in $(\mathcal{P}_{\mathcal{EI}})$ and to add linear constraints in order to handle free variable x. The problem $(\mathcal{P}_{\mathcal{EI}})$ is then transformed to

$$(\mathcal{P}) \begin{cases} \min\ f(x) \\ \text{s.t.} \\ A\,x - b = 0 \\ c(x) - w = 0 \\ x - y\ + z = 0 \\ w \geq 0, y \geq 0, z \geq 0 \end{cases} \tag{4.23}$$

The second step is to consider the problem with the barrier objective function

$$(\mathcal{P}_\mu) \begin{cases} \min\ \bar{f}_\mu(w, x, y, z) \\ \text{s.t.} \\ A\,x - b = 0 \\ c(x) - w = 0 \\ x - y\ + z = 0 \\ w > 0, y > 0, z > 0 \end{cases} \tag{4.24}$$

with

$$\bar{f}_\mu(w, x, y, z) = f(x) - \mu \sum_{i=1}^{m_I} \log(w_i) - \mu \sum_{j=1}^{n} \log(y_j) - \mu \sum_{j=1}^{n} \log(z_j). \tag{4.25}$$

IPDCA requires a DC decomposition of $f = g - h$, where g and h are two convex functions. By linearising the concave component of the objective function, IPDCA solves approximately the problem,

$$(\mathcal{DC}_k) \begin{cases} \min\ \bar{g}_k(x) \\ \text{s.t.} \\ A\,x - b = 0 \\ c(x) - w = 0 \\ x - y\ + z = 0 \\ w \geq 0, y \geq 0, z \geq 0 \end{cases} \tag{4.26}$$

where

$$\bar{g}_k(x) = g(x) - \nabla^{\mathrm{T}} h(x_k)\, x.$$

The problem is then transformed to a sequence of problems with the logarithmic barrier function

$$(\mathcal{DC}_\mu)\begin{cases} \min g_\mu(w, x, y, z) - \nabla^{\mathrm{T}} h(x_k)\, x \\ \text{s.t.} \\ A\,x - b = 0 \\ c(x) - w = 0 \\ x - y + z = 0 \end{cases} \tag{4.27}$$

with

$$g_\mu(w, x, y, z) = g(x) - \mu \sum_{i=1}^{m_I} \log(w_i) - \mu \sum_{j=1}^{n} \log(y_j) - \mu \sum_{j=1}^{n} \log(z_j) \tag{4.28}$$

$$h_\mu(w, x, y, z) = h(x).$$

4. Comparison between IPDCA and LANCELOT

To show the efficiency, the robustness and the large superiority of IPDCA with respect to standard code like LANCELOT [29], numerical simulations have been investigated on a perforated sheet with different number of variables. The data for IPDCA have been performed by using the commercial code ANSYS, where the lower bound direct method has been implemented. The comparison between the two algorithms is presented in the Table 4.1.

Dimension		*CPU Times*		*Optimum value*	
n	*m*	*IPDCA*	*LANCELOT*	*IPDCA*	*LANCELOT*
38401	25046	1356 s	86400 s	2.4	2.4
57601	36552	1828 s	—	5.1	—
192001	125200	2d0h33min	—	5.5	—

Table 4.1. Comparison between IPDCA and LANCELOT.

Here, *n* is the number of variables and *m* the number of constraints. The computational results show that the running-time of IPDCA [5, 69] is more faster than the standard code LANCELOT [29].

5. Conclusions

As concluding results of this chapter a lower bound direct method for the direct safety and reliability analysis of engineering structures has been established. The developed lower-bound Direct Method provides design tools for the increase of safety, life-time, and reliability of structures. The method needs less information about expected loading and about the details of material behaviour. Therefore the analysis becomes quicker and cheaper. It is an important advantage that the analysis can be performed with incomplete technological information, because:

- It could already be performed early in the design stage. This helps reduce costs and time to market.
- It can also be performed if detailed information is not available in principle (unknown future or unknown history) or if it is too expensive to generate.

In addition to the existing design codes the developed design tools will help the researchers and industrials to solve limit shakedown problems for large-scale problems (more than 100.000 degrees of freedoms). The method is still under development to include more sophistically material laws considered in the previous chapters.

Références

[1] Ainsworth, R.A.: Application of bounds for creeping structures subjected to load variations above the shakedown limit. *Int. J. Solids Struct.*, 13: 981-993, 1977.

[2] Ainsworth, R.A.: A note on bounding solutions for creeping structures subjected to load variations above the shakedown limit. *Int. J. Solids Struct.*, 15: 981-986, 1979.

[3] Akoa, F.; Le Thi Hoai An; Pham Dinh Tao: An interior point algorithm with DC regularisation for nonconvex quadratic programming. In: Le Thi Hoai An; Pham Dinh Tao, Eds., Modelling, Computation and Optimization in Information Systems and Management Sciences. Hermes Science Publishing, London, pp. 87-96, 2004.

[4] Akoa, F.: *Approches de points intérieurs et de la programmation DC en optimisation non convexe: codes et simulations numériques industrielles*. Doctor Thesis, Institut National des Sciences Appliquées de Rouen, 2005.

[5] Akoa, F.; Hachemi, A.; Le Thi Hoai An; Mouhtamid, S.; Pham Dinh Tao: Application of lower bound direct method to engineering structures. *Special Issue of J. Global Optim.* (Accepted).

[6] Aunay, S.: *Architecture de logiciel de modélisation et traitement distribués*. Doctor Thesis, Université Technologique de Compiègne, 1990.

[7] Basar, Y.; Krätzig, W.B.: *Mechanik der Flächentragwerke*. Braunschweig: Vieweg, 1985.

[8] Bathe, K.J.; Wilson, E.L.; Iding, R.H.: *NONSAP: a structural analysis program for static and dynamic response of nonlinear systems*. Report No. UGSESM 74-3, University of California, Berkeley, 1974.

[9] Bazant, P.Z; Prat, P.C.: Microplane model for brittle plastic material. *J. Eng. Mech.*, 114: 1672-1702, 1988.

[10] Belouchrani, M.A.: *Contribution to the shakedown analysis of inelastic cracked structures*. Doctor Thesis, Université des Sciences et Technologies de Lille, 1997.

[11] Belouchrani, M.A.; Weichert, D.: An extension of the static shakedown theorem to inelastic cracked structures. *Int. J. Mech. Sci.*, 41: 163-177, 1999.

[12] Belouchrani, M.A.; Weichert, D.; Hachemi, A.: Fatigue threshold computation by shakedown theory. *Mech. Res. Comm.*, 27, 3: 287-293, 2000.

[13] Bieniek, M.P.; Funaro, J.R.: *Elastic-plastic theory of shells and plates*. Report No. DNA 3954 T, New York: Weidlinger Associates, 1976.

[14] Bleich, H.: Über die Bemessung statisch unbestimmter Stahlwerke unter der Berücksichtigung des elastisch-plastischen verhaltens des Baustoffes. *Bauingenieur*, 13: 261-267, 1932.

[15] Bodovillé, G.; de Saxcé, G.: Plasticity with non-linear kinematic hardening: modelling and shakedown analysis by the bipotential approach. *Eur. J. Mech. A/Solids*, 20: 99-112, 2001.

[16] Boulbibane, M.: *Application de la théorie d'adaptation aux milieux élastoplastiques non-standards: cas des géomatériaux*. Doctor Thesis, Université des Sciences et Technologies de Lille, 1995.

[17] Boulbibane, M.; Weichert, D.; Application of shakedown theory to soils with non associated flow rules. *Mech. Res. Comm.*, 24: 513-519, 1997.

[18] Bousshine, L.; Chaaba, A. de Saxcé, G.: Softening in stress-strain curve for Drucker-Prager non-associated plasticity. *Int. J. Plasticity*, 17: 21-46, 2000.

[19] Carrère, N.; Kruch, S.; Vassel, A.; Chaboche, J.-L.: Damage mechanisms in unidirectional SiC/Ti composites under transverse creep loading: Experiments and modeling. *Int. J. Damage Mech.*, 11: 41-63, 2002.

[20] Carvelli, V.; Maier, G.; Taliercio, A.: Limit analysis of periodic composites by a kinematic approach. In *Proc. European Conf. on Composite Materials ECCM-8*, Naples, pp. 389-396, 1998.

[21] Carvelli, V.; Maier, G.; Taliercio, A.: Shakedown analysis of periodic heterogeneous materials by a kinematic approach. *Mech. Eng.*, 50: 229-240, 1999.

[22] Carvelli, V.; Maier; G. Taliercio; A.: Kinematic limit analysis of periodic heterogeneous media, *Comput. Model. Eng. Sci.*, 1: 229-240, 2000.

[23] Casey, J.: Approximate kinematical relations in plasticity. *Int. J. Solids Struct.*, 21: 671-682, 1985.

[24] Cazzani, A.; Contro, R. Corradi, L.: On the evaluation of the shakedown boundary for temperature-dependent elastic properties. *Eur. J. Mech. A/Solids*, 11: 539-550, 1992.

[25] Chwala, U.S.; Biron, A.: *Limit analysis of shells of revolution of arbitrary shape under pressure*. Rapport No. 1775, Labo. Rech. Essai Mat., Ecole Polytechnique de Montréal, 1969.

[26] Cocchetti, G. Maier, G.: Static shakedown theorems in piecewise linearized poroplasticity. *Arch. Appl. Mech.*, 68: 651-661, 1998.

[27] Cocchetti, G. Maier, G.: Shakedown analysis in poroplasticity by linear programming. *Int. J. Num. Meth. Engng.*, 47: 141-168, 2000.

[28] Cocks, A.C.F.; Leckie, F.A.: Deformation bounds for cyclically loaded shell structures operating under creep condition. *ASME, J. Appl. Mech.*, 55, 509-516, 1988.

[29] Conn, A.R.; Gould, N.I.M.; Toint, Ph.L.: *LANCELOT: A fortran package for large-scale nonlinear optimization (Release A)*. Springer-Verlag, Berlin, 1992.

[30] Corigliano, A.; Maier, G.; Pycko, S.: Dynamic shakedown analysis and bounds for elastoplastic structures with nonassociative, internal variable constitutive laws. *Int. J. Solids Struct.*, 32: 3145-3166, 1995.

[31] Corigliano, A.; Maier, G.; Pycko, S.: Kinematic criteria of dynamic shakedown extended to nonassociative constitutive laws with saturation hardening. *Rendic. Acc. Naz. dei Lincei*, Scienze, 6: 55-64, 1995.

[32] Creager, M.: Master Thesis, Lehigh University, 1966.

[33] Débordes, O.; Nayroles, B.: Sur la théorie et le calcul à l'adaptation des structures élastoplastiques. *J. Mécanique*,15: 1-53, 1976.

[34] Débordes, O.; Licht, C.; Marigo, J. J.; Mialon, P.; Michel, J.-C.; Suquet, P.: Calcul des charges limites de structures fortement hétérogènes. Actes du 3ème Colloque Tendances Actuelles en Calcul de Structures, Pluralis, Bastia, pp. 55-71, 1985.

[35] Débordes, O.: Homogenization computations in the elastic or plastic collapse range ; applications to unidirectional composites and perforated sheets. Forth Int. Symp. Innovative Num. Meth. in Engng., Computational Mechanics Publications, Springer-Verlag, Atlanta, pp. 453-458, 1986.

[36] de Saxcé., G.; Bousshine, L.: The limit analysis theorems for the implicit standard materials: application to the unilateral contact with dry friction and the non associated flow rules in soils and rocks. *Int. J. Mech. Sci.*, 40, 387-398, 1998.

[37] Döbert, C.; Mahnken, R.; Stein, E.: Numerical simulation of interface debonding with a combined damage/friction constitutive model. *Comput. Mech.*, 25: 456-467, 2000.

[38] Dorosz, S.: An upper bound to maximum residual deflections of elastic-plastic structures at shakedown. *Bull. Acad. Polon. Sci. Ser. Sci. Tech.*, 24: 167-174, 1976.

[39] Dorosz, S.: Influence of cyclic creep on the upper bound of shakedown of inelastic deflections. I In: Mròz, Z. et al., Eds, *Inelastic Behaviour of Structures under Variable Loads*, Kluwer Academic Publishers, Dordrecht, pp. 169–181, 1995.

[40] Drucker, D.C.: On the postulate of stability of material in the mechanics of continua. *J. Mécanique*, 3: 235-249, 1964.

[41] Druyanov, B. Roman, I.: On adaptation (shakedown) of a class of damaged elastic plastic bodies to cyclic loading. *Eur. J. Mech. A/Solids*, 17: 71-78, 1998.

[42] Druyanov, B. Roman, I.: Conditions for adaptation of damaged elastic-plastic bodies to cyclic loading. *Fatigue Fract. Engng. Mater. Struct.*, 21: 631-640, 1998.

[43] Duszek, M.K.; Sawczuk, A.: Stable and unstable states of rigid-plastic frames at the yield-point load. *J. Struct. Mech.*, 4: 33-77, 1976.

[44] Duszek, M.K.: *Problems of geometrically non-linear theory of plasticity*. Mitt. Inst. Mechanik, 21, Ruhr-Univ, Bochum, 1988.

[45] Dvorak, G.J.; Lagoudas, D.C.; Huang, C.M.: Fatigue damage and shakedown in metal matrix composite laminates. *Mech. Composite Mat. Struct*., 1: 171-202, 1994.

[46] Feng, X.Q; Yu, S.W.: An upper bound on damage factor at shakedown. *Int. J. Damage Mech.*, 3: 277-287, 1994.

[47] Feng, X.Q; Yu, S.W.: Damage and shakedown analysis of structures with strain-hardening. *Int. J. Plasticity*, 11: 237-249, 1995.

[48] Feng, X.Q.; Gross, D.: A global/local shakedown analysis method of elastoplastic cracked structures. *Eng. Fract. Mech.*, 63: 179-192, 1999.

[49] Friaâ, A.; Frémond, M.: Les méthodes statique et cinématique en calcul à la rupture et en analyse limite. *J. Méc. Théo. Appl.* 1: 881-905, 1982.

[50] Gao, D.Y.: Extended bounding theorems for nonlinear limit analysis. *Int. J. Solids Struct.*, 27: 523-531, 1991.

[51] Gao, D.Y.: Limit analysis of plastic shells subjected to large deformations. *Eur. J. Mech. A/Solids*, 14: 459-472, 1995.

[52] Giambanco, F.; Palizzolo, L.: Optimal bounds on plastic deformations for bodies constituted of temperature-dependent elastic hardening material. *J. Appl. Mech.*, 64: 1-9, 1997.

[53] Giese, H.: *On the application of shakedown-theory in soil mechanics*. IfM-Report, Ruhr-Universität, Bochum, 1988.

[54] Gokhfeld, D.A.; Cherniavsky, O.F.: *Limit analysis of structures at thermal cycling*. Sijthoff-Noordhoff, Leyden, 1980.

[55] Green, A.E.; Naghdi, P.M.: A general theory of elastic-plastic continuum. *Arch. Rat. Mech. Analys.*, 18: 251-281, 1965.

[56] Gross-Weege, J.: Zum Einspielverhalten von Flächentragwerken. IfM-Report, No. 58, Ruhr-Universität, Bochum, 1988.

[57] Gross-Weege, J.: A unified formulation of statical shakedown criteria for geometrically nonlinear problems. *Int. J. Plasticity*, 6: 433-447, 1990.

[58] Gross-Weege, J.; Weichert, D.: Elastic-plastic shells under variable mechanical and thermal loads. *Int. J. Mech. Sci.*, 34: 863-880, 1992.

[59] Gross-Weege, J. Weichert, D.: Shakedown of shells undergoing moderate rotations. In: Mròz, Z. et al., Eds, Inelastic Behaviour of Structures under Variable Loads, Kluwer Academic Publishers, Dordrecht, pp. 263–277, 1995.

[60] Griffith, A.A.: The theory of rupture. Proc. 1st Int. Cong. Appl. Mech., Delft, pp. 55-63, 1924.

[61] Grüning, M.: *Die Tragfähigkeit statisch unbestimmter Tragwerke aus Stahl bei beliebig häufig wiederholter Belastung*. Springer Verlag, Berlin, 1926.

[62] Guennouni, T.; Le Tallec, P.: Calcul à la rupture, régularisation de Norton-Hoff et Lagrangien augmenté. *J. Méc. Théo. Appl.* 2: 75-99 , 1982.

[63] Gvozdev, A.A.: *Raschet konstruktsij nesushchej sposobnosti po metodu predel'nogo ravnoves'ya*. Strojizdat, Moskva, 1949.

[64] Hachemi, A. Weichert, D.: An extension of the static shakedown theorem to a certain class of inelastic materials with damage. *Arch. Mech.*, 44: 491-498, 1992.

[65] Hachemi, A.: *Contribution à l'analyse de l'adaptation des structures inélastiques avec prise en compte de l'endommagement*. Doctor Thesis, Université des Sciences et Technologies de Lille, 1994.

[66] Hachemi, A. Weichert, D.: Application of shakedown theory to damaging inelastic material under mechanical and thermal loads. *Int. J. Mech. Sci.*, 39: 1067-1076, 1997.

[67] Hachemi, A.; Weichert, D.: Numerical shakedown analysis of damaged structures. *Comput. Methods Appl. Mech. Engrg.*, 160: 57-70, 1998.

[68] Hachemi, A.; Magoariec, H.; Débordes, O; Weichert, D.: Application of shakedown theory to layered composites. CD-Rom of the 2nd European Conference on Computational Mechanics, Cracow, Poland, June 26-29, 2001.

[69] Hachemi, A.; Le Thi Hoai An; Mouhtamid, S.; Pham Dinh Tao: Large-scale nonlinear programming and lower bound direct method in engineering applications. In: Le Thi Hoai An; Pham Dinh Tao, Eds., Modelling, Computation and Optimization in Information Systems and Management Sciences. Hermes Science Publishing, London, pp. 299-310, 2004.

[70] Hachemi, A.; Weichert, D.: On the problem of interfacial damage in fibre-reinforced composites under variable loads. *Mech. Res. Comm.*, 32: 15-23, 2005.

[71] Hachemi, A.; S. Mouhtamid; Weichert, D.: Progress in shakedown analysis with applications to composites. *Arch. Appl. Mech* (To appear).

[72] Halphen, B.; Quoc Son, N.: Sur les matériaux standards généralisés. *J. Mécanique,* 14: 39-63, 1975.

[73] Hill, R.: *The mathematical theory of plasticity*. Oxford, 1950.

[74] Hill, R.: Elastic properties of reinforced solids: some theoretical principles. *J. Mech. Phys. Solids*, 11: 357-372, 1963.

[75] Hjiaj, M.; Bodovillé, G.; de Saxcé, G.: Matériaux viscoplastiques et lois de normalité implicites. *C. R. Acad. Sci. Paris*, *Série IIb*, 328: 519-524, 2000.

[76] Hodge, P.G.: *Shake-down of elasto-plastic structures*. Reinhold Pub, 1954.

[77] Hodge, P.J.: *Limit analysis of rotationnally symmetric plates and shells*. Prentice-Hall, New-York, 1963.

[78] Huang, Y., Stein, E.: An analytical method for shakedown problems with linear kinematic hardening materials. *Int. J. Solids. Struct.*, 31: 2433-2444, 1994.

[79] Huang, Y.; Stein, E.: Shakedown of a cracked body consisting of kinematic hardening material. *Eng. Fract. Mech.*, 54: 107-112, 1996.

[80] Ilyuschin, A.A.: *Plasticity*. Paris: Eyrolles, 1956.

[81] Ismar, H.; Schröter, F.; Streicher, F.: The effect of interfacial properties on the mechanical behavior of layered aluminum matrix composites. *Tech. Mech.*, 20: 329-338, 2000.

[82] Ju, J.W.: On energy-based coupled elastoplastic damage theories: Constitutive modeling and computational aspects. *Int. J. Solids Struct.* 25:803-833, 1989.

[83] Kachanov, L.M.: Time of the rupture process under creep conditions. *Izv. Akad. Nauk, S.S.R., Otd. Tech. Nauk* 8: 26-31, 1958.

[84] Kamenjarzh, J.A.; Weichert, D.: On kinematic upper bounds for the safety factor in shakedown theory. *Int. J. Plasticity*, 8: 827-837, 1992.

[85] Kamenjarzh, J.A.; Merzljakov, A.: On kinematic method in shakedown theory; I. Duality of extremum problems; II. Modified kinematic method. *Int. J. Plasticity*, 10: 363-392, 1994.

[86] Kamenjarzh, J.A.: *Limit analysis of solids and structures*. CRC Press, London, 1996.

[87] Kleiber, M.; König, J.A.: Incremental shakedown analysis in case of thermal effects. *Int. J. Num. Meth. Engng.*, 20: 1567-1573, 1984.

[88] König, J.A.: Shakedown theory of plates. Arch. Mech. Stos., 5: 623-637, 1969.

[89] König, J.A.: A shakedown theorem for temperature dependent elastic moduli. *Bul. Ac. Pol. Sci., Ser. Sci. Tech.*, 17: 161-165, 1969.

[90] König, J.A. Maier, G.: Adaptation of rigid-work-hardening discrete structures subjected to load temperature cycles and second-order geometric effects. *Comput. Methods Appl. Mech. Engrg.*, 8: 37-50, 1976.

[91] König, J.A.; Kleiber, M.: On a new method of shakedown analysis. Bull. Acad. Polon. Sci., Sér. Sci., 26: 165-171, 1978.

[92] König, J.A.: On the incremental collapse criterion accounting for the temperature dependence of the yield-point stress. *Arch. Mech. Stos*. 31: 317-325, 1979.

[93] König, J.A.: Shakedown criteria in the case of loading and temperature variations. *J. Mech. Théor. Appl*., 21: 99-108, 1982.

[94] König, J.A.: Stability of the incremental collapse. In: Polizzotto, C.; Sawczuk, A., Eds., Inelastic Structures under Variable Loads, Palermo, COGRAS, pp. 329–334, 1984.

[95] König, J.A.: *Shakedown of elastic-plastic structures*. Elsevier, Amsterdam, 1987.

[96] König, J.A.; Siemaszko, A.: Strainhardening effects in shakedown processes. *Ing. Arch.*, 58: 58-66, 1988.

[97] Koiter, W.T.: A new general theorem on shake-down of elastic-plastic structures. *Proc. Koninkl. Ned. Akad. Wet.*, 59: 24-34, 1956.

[98] Koiter, W.T.: General theorems for elastic-plastic solids. In Sneddon, I.N.; Hill, R., eds. *Progress in Solid Mechanics*. Amsterdam, North-Holland, pp. 165-221, 1960.

[99] Kreja, I.; Schmidt, R.; Teyeb, O.; Weichert, D.: Geometrically nonlinear analysis of inelastic damaged shells. Proceeding of World Congress of Nolinear Analysis, Tampa, Florida 19-26, 1992.

[100] Leckie, F.A.; Martin, J.B.: Deformation bounds for bodies in state of creep. *ASME, J. Appl. Mech.* 34: 411-417, 1967.

[101] Leckie, F.A.: Limit and shakedown loads in the creep range. In Proc. *Thermal stress and Thermal Fatigue*, London, pp. 368-373,1971.

[102] Lee, E.H.: Elasto-plastic deformation at finite strains. *J. Appl. Mech.*, 36:1-6, 1969.

[103] Lemaitre, J.: A continuous damage mechanics model for ductile fracture. *J. Engng. Mat. Tech.* 107: 83-89, 1985.

[104] Lemaitre, J.; Chaboche, J.L. *Mécanique des matériaux solides*. Paris: Dunod, 1985.

[105] Lemaitre, J.: Formulation unifiée des lois d'évolution d'endommagement. *C. R. Acad. Sci.* 305:1125-1130, 1987.

[106] Lissenden, C.J.; Herakovich, C.T.: Numerical modelling of damage development and viscoplasticity in metal matrix composites. *Comput. Methods Appl. Mech. Engrg*, 126: 289-303, 1995.

[107] Litewka, A.; Sawczuk, A.; Stanislawska, J.: Simulation of oriented continuous damage evolution, *J. Méc. Théo. Appl.*, 3: 675-688, 1984.

[108] Magoariec, H.; Bourgeois, S.; Débordes, O.; Hachemi, A.; Weichert, D.: A numerical approach of shakedown analysis coupled with periodic homogenization for 3D elastic-plastic media. CD-Rom of the Fifth World Congress on Computational Mechanics, Eds.: H.A. Mang, F.G. Rammerstorfer, J. Eberhardsteiner, Vienna, Austria, July 7-12, 2002.

[109] Magoariec, H.: *Adaptation élastoplastique et homogénéisation périodique*. Doctor Thesis, Université Aix-Marseille II, 2003.

[110] Magoariec, H.; Bourgeois, S.; Débordes, O.: Elastic-plastic shakedown of 3D periodic heterogeneous media: a numerical approach. *Int. J. Plasticity*, 20: 1655-1675, 2004.

[111] Maier, G.: Shakedown theory in perfect elastoplasticity with associated and nonassociated flow-laws: a finite element, linear programming approach. *Meccanica*, 4: 250-260, 1969.

[112] Maier, G.: A shakedown matrix theory allowing for workhardening and second-order geometric effects. In: Sawczuk, A., Ed., *Foundations in Plasticity,* Vol. 1, Noordhoff, Leyden, pp. 417-433, 1973.

[113] Maier, G.: Upper bounds on deformations of elastic-workhardening structures in the presence of dynamic and second-order effects. *J. Struct. Mech.*, 2: 265-280, 1973.

[114] Maier, G.; Novati, G.: A shakedown and bounding theory allowing for nonlinear hardening and second-order geometric effects with reference to discrete structural models. In: Kleiber, M.; König, J.A., Eds., A. Sawczuk Memorial Volume, *Inelastic Solids and Structures*, Pineridge, Swansea, pp. 451-471, 1990.

[115] Maier, G.; Comi, C.; Corigliano, A.; Perego, U.; Hübel, H.: *Bounds and estimates on inelastic deformations: a study of their practical usefulness*. Europ. Commission, Directorate General. for Science, Research. and Development, Activity Group 2: 'Structural Analysis', EUR 16555 EN, Brussels, 1995.

[116] Maier, G.; Carvelli, V.; Cocchetti, G.: On direct methods for shakedown and limit analysis. *Eur. J. Mech. A/Solids*, 19: 79-100, 2000.

[117] Maier, G.; Pastor, J.; Ponter, A.R.S.; Weichert, D.: *Direct methods of limit and shakedown analysis*. In: De Borst, R.; Mang, H. A., Eds., Numerical and Computational Methods, Chapter 12, Vol. 3. In: Milne, I.; Ritchie, R. O.; Karihaloo, B., Eds., Comprehensive Structural Integrity, Elsevier-Pergamon, Amsterdam, 2003.

[118] Mandel, J.: Adaptation d'une structure plastique écrouissable et approximations. *Mech. Res. Comm.* 3: 483-488, 1976.

[119] Mandel, J.; Zarka, J.; Halphen, B.: Adaptation d'une structure élastoplastique à écrouissage cinématique. *Mech. Res. Comm.*, 4: 309-314, 1977.

[120] Marigo, J.J.; Mialon P.; Michel, J.C.; Suquet P.: Plasticité et homogénéisation: un exemple de prévision des charges limites d'une structure hétérogène périodique, *J. Méc. Théo. Appl.*, 6: 47-75, 1987.

[121] Melan, E.: Theorie statisch unbestimmter Systeme aus ideal-plastischem Baustoff. *Sitber. Akad. Wiss., Wien, Abt. IIA*, 145: 195-218, 1936.

[122] Melan, E.: Zur Plastizität des räumlichen Kontinuums. *Ing. Arch.*, 9: 116-126, 1938.

[123] Morelle, P. ; Nguyen Dang Hung : Etude numérique de l'adaptation plastique des plaques et coques de révolution par les éléments finis d'équilibre. *J. Méc. Théo. Appl.*, 2: 567-599, 1983.

[124] Morelle, P.: Numerical shakedown analysis of axisymmetric sandwich shells: An upper bound formulation. *Int. J. Num. Meth. Engrg.*, 23: 2071-2088, 1986.

[125] Morelle, P.: *Analyse duale de l'adaptation plastique des structures par la méthode des éléments finis et la programmation mathématique*. Doctor Thesis, Université de Liège, 1989.

[126] Mróz, Z.; Weichert, D.; Dorosz, S.: *Inelastic behaviour of structures under variable loads*. Kluwer Academic Publishers, Dordrecht, 1995.

[127] Nayroles, B.; Weichert, D.: La notion de sanctuaire d'élasticité et l'adaptation des structures. *C. R. Acad. Sci.* 316: 1493-1498, 1993.

[128] Neal, B.G.: Plastic collapse and shake-down theorems for structures of strain-hardening material. *J. Aero. Sci.*, 17: 297-306, 1950.

[129] Neuber, H.: Über die Berücksichtigug der Spannungskonzentration bei Festigkeitsberechnungen. *Konstruktion*, 20: 245-251, 1968.

[130] Nguyen Dang Hung; Trapletti, M.; Rensart, D.: Bornes quasi-inférieurs et bornes supérieurs de la pression de ruine des coques de révolution par la méthode des éléments finis et par la programmation non-linéaire. *Int. J. Non-Linear Mech.*, 13: 79-102, 1978.

[131] Palmer, A.C.: A limit theorem for materials with non-associated flow laws. *J. Mécanique*, 5: 217-222, 1966.

[132] Perzyna, P.: Constitutive modelling of dissipative solids for postcritical behaviour and fracture. ASME, J. Eng. Mat. Techn., 106: 410-419, 1984.

[133] Pham Dinh Tao; Le Thi Hoai An: D.C. Optimization algorithm for solving the trust region problem. *SIAM J. Optimization*, 8: 476-505, 1998.

[134] Polizzotto, C.: Bounding principles for elastic-plastic-creeping solids loaded below and above the shakedown limit. *Meccanica*, 17: 143-148, 1982.

[135] Polizzotto; C. Sawczuk, A.: *Inelastic structures under variable loads*. Proc. Euromech Colloquium 174, COGRAS, Palermo, 1983.

[136] Polizzotto, C.: Deformation bounds for elastic-plastic solids within and out of the range of creep. *Nucl. Engng. Design*, 83, 293-301, 1984.

[137] Polizzotto, C.; Borino, G.; Caddemi, S.; Fuschi, P.: Shakedown problems for material models with internal variables. *Eur. J. Mech. A/Solids*, 10: 621-639, 1991.

[138] Polizzotto, C.; Borino, G.: Shakedown and steady-state responses of elastic-plastic solids in large displacements. *Int. J. Solids Struct.*, 33: 3415-3437, 1996.

[139] Polizzotto, C.; Borino, G.; Fuschi, P.: An extended shakedown theory for elastic-plastic-damage material models. *Eur. J. Mech. A/Solids*, 15: 825-858, 1996.

[140] Polizzotto, C.; Borino, G.; Fuschi, P.: Weak forms of shakedown for elastic-plastic structures exhibiting ductile damage. *Meccanica*, 36:49-66, 2001.

[141] Ponter, A.R.S.: On the relationship between plastic shakedown and the repeated loading of creeping structures. *ASME, J. Appl. Mech.*, 38: 437-440, 1971.

[142] Ponter, A.R.S.: A general shakedown theorem for elastic-plastic bodies with workhardening. Third SMiRT Conference, London, paper L5/2, 1972.

[143] Ponter, A.R.S.: Deformation, displacement and work bounds for structures in a state of creep and subject to variable loading. *ASME, J. Appl. Mech.*, 39: 953-959, 1972.

[144] Ponter, A.R.S.; Williams, J.J.: Work bounds and associated deformation of cyclically loaded creeping structures. *ASME, J. Appl. Mech.*, 40: 921-927, 1973.

[145] Ponter, A.R.S.; Karadeniz, S.: An extended shakedown theory for structures that suffer cyclic thermal loading – Part I, II. *ASME, J. Appl. Mech.*, 52: 877-889, 1985.

[146] Ponter, A.R.S.; Leckie, F.A.: Bounding properties of metal-matrix composites subjected to cyclic thermal loading. *J. Mech. Phys. Solids*, 46: 697-717, 1998.

[147] Ponter, A.R.S.; Leckie, F.A.: On the behaviour of metal-matrix composites subjected to cyclic thermal loading. *J. Mech. Phys. Solids*, 46: 2183-2199, 1998.

[148] Prager, W.: Shakedown in elastic-plastic media subjected to cycles of load and temperature. Symposium Plasticità nella Scienza delle Construzioni, Bologna, 239-244, 1956.

[149] Pycko, S.; König, J.A.: Steady plastic cycles on reference configuration in the presence of second-order geometric effects. *Eur. J. Mech. A/Solids*, 10: 563-574, 1991.

[150] Pycko, S.; Maier, G.: Shakedown theorems for some classes of nonassociative hardening elastic-plastic material models. *Int. J. Plasticity*, 11: 367-395, 1995.

[151] Quoc Son, N.: Méthode énergétique en mécanique de la rupture. *J. Mécanique* 19: 363-386, 1980.

[152] Radenkovic, D.: Théorèmes limites pour un matériau Coulomb à dilatation non standardisée. *C. R. Acad. Sci.*, 252: 4103-4104, 1961.

[153] Radhakrishna, V.M.: In Beevers, C.J., ed., Fatigue '84, Proc. 2nd Int. Conf. on *Fatigue and Fatigue Thresholds*, Birmingham, september 3-7, *Engineering and Materials Advisory Services*, Warley, 1984.

[154] Saczuk, J.; Stumpf, H.: On statical shakedown theorems for non-linear problems. IfM-Report, No 74, Ruhr-Universität, Bochum, 1990.

[155] Save, M.A.; Massonnet, C.E.; de Saxcé, G.: *Plastic limit analysis of plates, shells and disks*. In: Achenbach, J.D. et al., Eds., North-Holland Series in Applied Mathematics and Mechanics, Vol. 43, Elsevier, 1997.

[156] Sawczuk, A.: On plastic shell theories at large strains and displacements. *Int. J. Mech. Sci.*, 24: 231-244, 1982.

[157] Schwabe, F.: *Einspieluntersuchungen von Verbundwerkstoffen mit periodischer Mikrostruktur*. Doctor Thesis, RWTH Aachen, 2000.

[158] Shichun, W.; Hua, L.: A kinetic equation for ductile damage at large plastique strain. *J. Mat. Proc. Tech.* 21:295-302, 1990.

[159] Siemaszko, A.; König, J.A.: An analysis of stability of incremental collapse of skeletal structures. *J. Struct. Mech.*, 13: 301-321, 1985.

[160] Siemaszko, A.: Inadaptation analysis with hardening and damage. *Eur. J. Mech. A/Solids*, 12: 237-248, 1993.

[161] Stein, E.; Zhang, G.; König, J.A.: Shakedown with nonlinear strain hardening including structural computations using finite element method. *Int. J. Plasticity*, 8: 1-31, 1992.

[162] Stein, E.; Huang, Y.: An analytical method for shakedown problems with linear kinematic hardening materials. *Int. J. Solids Struct.*, 31: 2433-2444, 1994.

[163] Stumpf, H.: Theoretical and computational aspects in the shakedown analysis of finite elastoplasticity. *Int. J. Plasticity*, 9: 583-602, 1993.

[164] Suquet, P.: *Plasticité et homogénéisation*. Doctor Thesis, Université Pierre et Marie Curie, Paris 6, 1982.

[165] Suquet, P.: Analyse limite et homogénéisation. C.R. Acad. Sci., 296: 1355-1358, 1983.

[166] Symonds, P. S.: Shakedown in continuous media. *Trans. ASME, Appl. Mech.*, 18: 85-89, 1951.

[167] Taliercio, A.: Lower and upper bounds to the macroscopic strength domain of a fiber-reinforced composite material. *Int. J. Plasticity*, 8: 741-762, 1992.

[168] Tarn, J.Q.; Dvorak, G.J.; Rao, M.S.M.: Shakedown of unidirectional composites. *Int. J. Solids Struct.*, 11: 751-764, 1975.

[169] Taylor, D.: In : In Beevers, C.J., ed., Fatigue '84, Proc. 2nd Int. Conf. on *Fatigue and Fatigue Thresholds*, Birmingham, september 3-7, *Engineering and Materials Advisory Services*, Warley, 1984.

[170] Temin-Gendron, P.; Laurent-Gengoux, P.: Calculation of limit loads for composite materials via equilibrium finite elements. *Comput. Struct.*, 45: 947-957, 1992.

[171] Tirosh, J.: The dual shakedown conditions for dilute fibrous composites. *J. Mech. Phys. Solids*, 46: 167-185, 1998.

[172] Tritsch, J.B.: *Analyse d'adaptation des structures élasto-plastiques avec prise en compte des effets géométriques*. Doctor Thesis, Université des Sciences et Technologies de Lille, 1993.

[173] Tritsch, J.B.; Weichert, D.: Shakedown of elastic-plastic structures at finite deformations - A comparative study of static shakedown theorems. *ZAMM*, 73: T309-312, 1993.

[174] Tritsch, J.B.; Weichert, D.: Case studies on the influence of geometric effects on the shakedown of structures. In: Mròz, Z. et al., Eds, Inelastic Behaviour of Structures under Variable Loads, Kluwer Academic Publishers, Dordrecht, pp. 309–320, 1995.

[175] Tritsch, J.B.; Hachemi, A.: On shakedown analysis using hyper-sphere algorithm. 5th Euromech Solid Mechanics Conference (ESMC-2003), Thessaloniki, August 17-22, 2003.

[176] Voldoire, F.: Limit analysis by the Norton-Hoff-Friaâ regularising method. Internal-Lisa report, 1999.

[177] Wasen, J.; Hamberg, K.; Karlsson, B.: The influence of grain size and fracture surface geometry on the near-threshold fatigue crack growth in ferritic steels. *Mat. Sci. Engng.*, 102: 217-226, 1988.

[178] Weichert, D.: On the influence of geometrical nonlinearities on the shakedown of elastic-plastic structures. *Int. J. Plasticity*, 2: 135-148, 1986.

[179] Weichert, D.; Gross-Weege, J.: The numerical assessment of elastic-plastic sheets under variable mechanical and thermal loads using a simplified two-surface yield condition. *Int. J. Mech. Sci.* 30: 757-767, 1988.

[180] Weichert, D.: Shakedown of shell-like structures allowing for certain geometrical nonlinearities. *Arch. Mech.*, 41: 61-71, 1989.

[181] Weichert, D.: Combined shakedown- and crack propagation-analysis of elastic-plastic structures. Khan, A.S.; Tokuda, M., Eds., Proc. Plasticiy'89, 2nd Int. Symp. Plasticity and Its Current Applications, Pergamon Press, pp. 531-534, 1989.

[182] Weichert, D. Hachemi, A.: Influence of geometrical nonlinearities on the shakedown of damaged structures. *Int. J. Plasticity*, 9: 891-907, 1998.

[183] Weichert, D.; Hachemi, A.; Schwabe, F.: Shakedown analysis of composites. *Mech. Res. Comm.*, 26: 309-318, 1999.

[184] Weichert, D.; Hachemi, A.; Schwabe, F.: Application of shakedown analysis to the plastic design of composites. *Arch. Appl. Mech.*, 69: 623-633, 1999.

[185] Weichert, D.; Maier, G.: *Inelastic analysis of structures under variable repeated loads*. Kluwer Academic Publishers, Dordrecht, 2000.

[186] Weichert, D.; Maier, G.: *Inelastic behaviour of structures under variable repeated loads: Direct Analysis Methods*. CISM Courses and Lectures No. 432, International Centre for Mechanical Sciences, Springer Wien/New-York, 2002.

[187] Weichert, D.; Hachemi, A.: Shakedown- and limit analysis of periodic composites. *J. Theo. Appl. Mech.*, 40: 273-289, 2002.

[188] Zahl, D.B.; Schmauder, S.: Transverse strength of continuous fiber metal matrix composites, *Comput. Mat. Sci.*, 3: 293-299, 1994.

[189] Zarka, J.; Casier, J.: Elastic-plastic response of a structures to cyclic loading: practical rules. In Nemat-Nasser, S., Ed., Mechanics Today, Vol. 6., pp. 93-198, Pergamon, Oxford, 1981.

[190] Życzkowski, M.: *Combined loadings in the theory of plasticity.* PWN-Polish Scientific Publishers, Warsaw, 1981.